From the Centre for Integrated Physiology and Molecular Medicine (CIPMM)
Saarland University
Jun.-Prof. Dr. rer. nat. Sandra Rother

Development of biomimetic glycosaminoglycan-gelatine hydrogel systems for the controlled delivery of pro- and anti-angiogenic factors

Dissertation for the degree of Doctor of Medicine (Dr. med.)
Faculty of Medicine
SAARLAND UNIVERSITY
2025

Submitted by: Fabian Junker
Born 23rd of November 2000
In St. Wendel, Germany

Day of MD Graduation (Tag der Promotion): 23.06.2025

Dean (Dekan):	Univ.-Prof. Dr. med. dent. Matthias Hannig
Reviewer (Berichterstattende):	Jun.-Prof. Dr. rer. nat. Sandra Rother
	Prof. Dr. med. Matthias W. Laschke

Table of Contents

List of Abbreviations

A	Area
ADAM	Disintegrin and Metalloproteinase
ADAMTS	Disintegrin and Metalloproteinase with Thrombospondin motifs
aECM	Artificial extracellular matrix
BSA	Bovine serum albumin
Brij35	Polyoxyethylen(23)laurylether
Ca.	Circa
CS	Chondroitin sulphate
d	Tip displacement
Da	Dalton
DMAB	p-Dimethylaminobenzaldehyde
DMEM	Dulbecco's modified Eagle's medium, high glucose, pyruvate
DMMB	1, 9-Dimethyl-methylene blue zinc chloride double salt
PBS	Dulbecco's phosphate buffered saline
DR	Diabetic retinopathy
DS	Dermatan sulphate
ECM	Extracellular matrix
e.g.	Example given
F	Force
FCS	Fetal bovine serum
g	Gram
GAG	Glycosaminoglycan(s)
GelMA	Methacrylated gelatine
GlcA	d-Glucuronic acid
GlcNAc	n-Acetyl-d-glucosamine
he	Height
h	Hour(s)
HA	Hyaluronan
HA-MAC	Methacrylated hyaluronic acid
HEPES	4-(2-hydroxyethyl)-1-piperazineethanesulfonic acid

HIF	Hypoxia inducible factor
HRP	Horse radish peroxidase
HS	Heparan sulphate
IA	Intrasusceptive angiogenesis
IC_{50}	Half maximal inhibitory concentration
KS	Keratan sulphate
LAP	Lithium phenyl-2, 4, 6-trimethylbenzoylphosphinate
m_0	Mass at 0 hours
m_t	Mass at specific time point
MMP	Matrix metalloproteinase
MMP-2	Matrix metalloproteinase 2
MMP-9	Matrix metalloproteinase 9
NNGH	*N*-Isobutyl-*N*-(4-methoxyphenylsulfonyl)glycyl hydroxamic acid
Notch	Neurogenic locus notch homolog protein
O	Oxygen atom
PAD	Peripheral arterial disease
PG	Proteoglycans
RGD	Arginine-glycine-aspartic acid sequence
rpm	Rounds per minute
RT	Room temperature
SA	Sprouting angiogenesis
SEM	Scanning electron microscopy
sGAG	Sulphated glycosaminoglycan(s)
sHA	Sulphated hyaluronan
sHA1-AC	Sulphated and acrylated hyaluronan
SR	Swelling ratio
TGF-β	Transforming growth factor β
TIMP	Tissue inhibitor of matrix metalloproteinase
TIMP-3	Tissue inhibitor of matrix metalloproteinase 3
U	Unit (enzymatic activity)
UV	Ultraviolet light
u.p. water	Ultrapure water
VEC	Vascular endothelial cell(s)

VEGF-A	Vascular endothelial growth factor A
VEGF-C	Vascular endothelial growth factor C
$VEGF_{121}$	Vascular endothelial growth factor 121
$VEGF_{165}$	Vascular endothelial growth factor 165
$VEGF_{165a/b}$	Vascular endothelial growth factor 165 subtype a/b
VEGFR	Vascular endothelial growth factor receptor
VEGFR-1	Vascular endothelial growth factor receptor 1
VEGFR-2	Vascular endothelial growth factor receptor 2
VEGFR-3	Vascular endothelial growth factor receptor 3
w/v	Weight/volume
w/w	Weight/weight

List of Figures

List of Tables

I. Abstract

The demographic change in western countries leads to an increasing number of chronic wounds which require adequate health care as age and age-associated diseases, including diabetes, are major risk factors for their development. Chronic wounds are in a state of persistent inflammation which inhibits the proliferation and angiogenesis necessary for physiological wound healing. A promising approach to improve angiogenesis in chronic wounds is the application of bioactive wound dressings mimicking the extracellular matrix and releasing pro-angiogenic factors into the surrounding tissue. Hydrogels based on collagen and derivatives of naturally occurring glycosaminoglycans, including sulphated hyaluronan (sHA), showed promising results for the delivery of pro-angiogenic factors as well as limiting their rapid degradation *in vivo*. Furthermore, tissue inhibitor of matrix metalloproteinase 3 (TIMP-3) could limit the degradation of vascular endothelial growth factor A (VEGF-A) without significant inhibition of angiogenesis. However, the current collagen-based hydrogels are limited because of the chemical heterogeneity of collagen resulting in heterogenous hydrogel properties, whereas gelatine offers an alternative with homogenous chemical properties as well as the potential use in bioprinting. This thesis developed a biomimetic glycosaminoglycan-gelatine hydrogel system and examined it for its mechanical properties and for the controlled release of the pro-angiogenic factor VEGF-A and the inhibitor of matrix degradation TIMP-3. Hydrogels based on 10% methacrylated gelatine (GelMA) showed promising results regarding their mechanical stability and therefore were chosen to conduct further experiments. Compared to GelMA and GelMA/hyaluronan (HA) hydrogels, GelMA/sHA hydrogels showed an improved hydrogel stiffness and swelling which are necessary for a drug-delivery system. All hydrogel types were able to bind and release both VEGF-A and TIMP-3. Initially, all hydrogels bound similar amounts of VEGF-A and/or TIMP-3 but only GelMA/sHA hydrogels showed a constant release of VEGF-A and/or TIMP-3 for 21 days whereas both GelMA and GelMA/HA hydrogels rapidly released large amounts of VEGF-A and/or TIMP-3. The released VEGF-A and TIMP-3 was examined for its remaining bioactivity. VEGF-A released from GelMA/sHA hydrogels showed an increased VEGF receptor stimulation on KDR/NF AT-RE HEK293 cells compared to VEGF-A released from GelMA and GelMA/HA hydrogels. Similar results were found for TIMP-3 after release from GelMA/sHA hydrogels as it still showed inhibitory potential towards two major enzymes in extracellular matrix remodelling, collagenase and matrix metalloproteinase 9. In summary, the present thesis shows the potential of GelMA/sHA hydrogels for the controlled delivery of bioactive VEGF-A and TIMP-3 over a prolonged period. This highlights the promising potential of GelMA/sHA hydrogels as off-the-shelf bioactive wound dressings in future.

II. Zusammenfassung

Der demographische Wandel in westlichen Ländern führt zu einer Zunahme der Zahl chronischer Wunden. Diese benötigen eine angepasste Gesundheitsversorgung, da besonders das Alter sowie altersassoziierte Erkrankungen, z. B. Diabetes mellitus, Risikofaktoren für die Entstehung von chronischen Wunden sind. Chronische Wunden befinden sich in einem Zustand der dauerhaften Entzündung, die die für die physiologische Wundheilung notwendige Proliferation und Angiogenese inhibiert. Ein vielversprechender Ansatz zur Verbesserung der Angiogenese in chronischen Wunden ist die Verwendung von bioaktiven Wundauflagen, die die extrazelluläre Matrix nachahmen. Hydrogele, die auf Kollagen und Glykosaminoglykanderivaten, wie zum Beispiel sulfatiertes Hyaluron (sHA), basieren, zeigten vielversprechende Ergebnisse für die Freisetzung von pro-angiogenen Faktoren. Des Weiteren können bioaktive Wundauflagen pro-angiogene Faktoren in das umliegende Gewebe abgeben und den schnellen *in vivo*-Abbau dieser begrenzen. Weiterhin könnte der Gewebsinhibitor der Metalloproteinasen 3 (TIMP-3) den Abbau von vaskulärem endothelialem Wachstumsfaktor A (VEGF-A) einschränken ohne signifikante Inhibition der Angiogenese. Allerdings sind die aktuellen, Kollagen-basierten Hydrogele durch die heterogenen chemischen Eigenschaften des Kollagens und den daraus resultierenden heterogenen Hydrogeleigenschaften eingeschränkt. Als Alternative bietet Gelatine homogene chemische Eigenschaften und die mögliche Nutzung im Rahmen des Bioprintings. In dieser Arbeit wurde ein biomimetisches Glykosaminoglykan-Gelatine Hydrogel entwickelt und dessen mechanische Eigenschaften sowie die kontrollierte Freisetzung von dem pro-angiogenen VEGF-A und dem Inhibitor des Matrixabbaus TIMP-3 untersucht. Hydrogele basierend auf 10% methacrylierter Gelatine (GelMA) zeigten vielversprechende Ergebnisse hinsichtlich ihrer machanischen Stabilität, sodass mit diesen weitere Experimente durchgeführt wurden. GelMA/sHA Hydrogele zeigten verbesserte Steifheit und Schwellung verglichen mit GelMA und GelMA/Hyaluron (HA) Hydrogelen. Dabei handelt es sich um notwendige Eigenschaften für sog. „drug-delivery“-Systeme. Alle Hydrogelarten waren in der Lage VEGF-A sowie TIMP-3 zu binden und freizusetzen. Initial banden alle Hydrogele ähnliche Mengen an VEGF-A und/oder TIMP-3, aber nur GelMA/sHA Hydrogele zeigten eine konstante Freisetzung von VEGF-A und/oder TIMP-3 über 21 Tage, wohingegen die Freisetzung aus GelMA und GelMA/HA Hydrogelen schnell große Mengen an VEGF-A und/oder TIMP-3 freisetzten. Die verbleibende biologische Aktivität von freigesetztem VEGF-A und TIMP-3 wurde untersucht. VEGF-A zeigte nach seiner Freisetzung aus GelMA/sHA Hydrogelen, im Vergleich zu GelMA und GelMA/HA Hydrogelen, eine verstärkte Aktivierung des VEGF-Rezeptors von KDR/NF AT-RE HEK293 Zellen. Ähnliche Ergebnisse fanden sich für TIMP-3 nach der Freisetzung aus GelMA/sHA Hydrogelen. TIMP-3 zeigte weiterhin eine inhibierende Wirkung gegenüber zwei wichtigen Enzymen des Remodellings der extrazellulären Matrix, Kollagenase und

Matrixmetalloprotease 9. Zusammenfassend zeigt die vorliegende Arbeit das Potential von GelMA/sHA Hydrogelen zur kontrollierten Freisetzung von bioaktivem VEGF-A und TIMP-3 über längere Zeit. GelMA/sHA Hydrogele haben das Potential zukünftig als bioaktive „off-the-shelf“-Wundauflagen angewandt zu werden.

1. Introduction and theoretical background

1.1. Introduction

1.1.1. Relevance of angiogenesis in chronic wounds

The pooled prevalence of chronic wounds is estimated at 2.21 per 1000. However, specific data regarding the prevalence of chronic wounds is incoherent because of different classifications and reporting systems in literature [78]. When it comes to Germany, 785000 patients within the general population suffered from chronic wounds in 2012. Within three years, an increase of 50% in treatment-relevant chronic wounds was found [47]. More current data suggests that, between 2012 and 2018, 7.8% of all German nursing home residents suffered from chronic wounds [100]. By comparison, a study of routine-linked health data of the Welsh National Health Service revealed a chronic wound prevalence of 6% amounting to costs of £ 328.8 million equalling 5.5% of the costs in Welsh health care [94].

Especially the aging population has an increased risk of chronic wounds requiring adequate health care. The spectrum of risk factors for impaired wound healing is broad and includes factors such as age, disease, e.g., diabetes mellitus, infection, hypoxia and medication, e.g., glucocorticoids and chemotherapy [41]. The risk factors for chronic wounds often are accompanied by each other. Age, wound infection and diabetes are independent risk factors and therefore the risk of a *circulus vitiosus* is increased [32,41,56].

Wound healing in general consists of a set of four steps: I) haemostasis, II) inflammation, III) proliferation, including angiogenesis and extracellular matrix (ECM) production, and IV) remodelling. Wounds with impaired healing are often “trapped” in a state of pathological inflammation and therefore do not enter the phase of proliferation and angiogenesis [41]. Current treatment options for chronic wounds include debridement, infection control, creating a moist environment and regular monitoring of the wound size [11,148].

Bioactive wound dressings which stimulate angiogenesis and ECM formation e.g., by using adipose-derived mesenchymal stem cells, seem to be promising alternatives for the treatment of impaired wound healing [43]. Proliferation of endothelial cells can be increased if treated together with sulphated hyaluronan (sHA) and vascular endothelial growth factor A (VEGF-A). Glycosaminoglycans (GAG) are polysaccharides, consisting of repetitive disaccharide units. They are ubiquitous within the human body and they are key regulators of several physiological or pathological condition e.g., angiogenesis, wound healing and tumorigenesis [53]. Previously, collagen-based hydrogels containing sulphated glycosaminoglycans (sGAG) have been shown to have two advantages: I) they can mediate VEGF-A release which promotes the

formation of endothelial tubes and II) sGAG can increase VEGF-A availability and endothelial proliferation which is a crucial step in the formation of new blood vessels and therefore offers the opportunity for a targeted therapy [87,111].

However, *Rother et al.* used a collagen-based hydrogel. Collagen-based hydrogels are limited in their use by a low mechanical stability, fast degradation and limited possibilities for bioprinting [111,125].

Therapeutic strategies that effectively stimulate angiogenesis have the potential to significantly improve wound healing outcomes. Innovative biomaterials such as methacrylated gelatine (GelMA)-based hydrogels are emerging as promising tools in this context. GelMA hydrogels are biocompatible, non-toxic and non-immunogenic, suitable for bioprinting and customizable for controlled growth factor release, making them ideal candidates for promoting angiogenesis in chronic wound therapy. Furthermore, the mechanical properties of GelMA hydrogels can be modified to imitate the ECM [155]. Additionally, the incorporation of sulphated glycosaminoglycans (sGAG) into hydrogels has been shown to regulate key modulators of angiogenesis, such as vascular endothelial growth factor (VEGF) and tissue inhibitor of metalloproteinases 3 (TIMP-3). By influencing the bioavailability of VEGF and mitigating the inhibitory effects of TIMP-3 on angiogenesis, sGAG-modified hydrogels offer a dual advantage in supporting both tissue regeneration and vascular growth [5,99,108,115].

Against this background, this thesis aims to explore the development of biomaterials that integrate GelMA hydrogels with sGAG to create a scaffold that enhances wound healing. Such an approach not only holds promise for overcoming the pathologic inflammatory phase but also fosters physiologic tissue regeneration, providing a novel therapeutic avenue for patients suffering from chronic wounds.

1.1.2. Objective of my work

Angiogenesis is an omnipresent subject in the field of medicine and medical research. The increased risk for impaired wound healing due to an aging population and the mismatch between availability and need of donor organs, and therefore the necessity of tissue engineering, makes it even a more important subject [41,76]. Hyaluronan (HA) is a GAG ubiquitous in the ECM and therefore in all tissues and plays an important role for cell and tissue functionality [12]. sHA mimics physiological ECM functions and therefore it is suitable for the use in an artificial ECM (aECM) [111]. The unique biochemical properties of GelMA make it ideal for the use as a scaffold for cells. These biomaterials can be combined to an aECM. The goal of this thesis is to develop a biomimetic functional hydrogel system that allows the defined release of pro- and anti-angiogenic factors. In future, this might be useful to stimulate wound healing as well as angiogenesis during medical treatment. Figure 1.1 shows the possible

application of a GelMA-based and sulphated, acrylated hyaluronan (sHA1-AC)-functionalized hydrogel as a drug-delivery system to promote wound healing and angiogenesis.

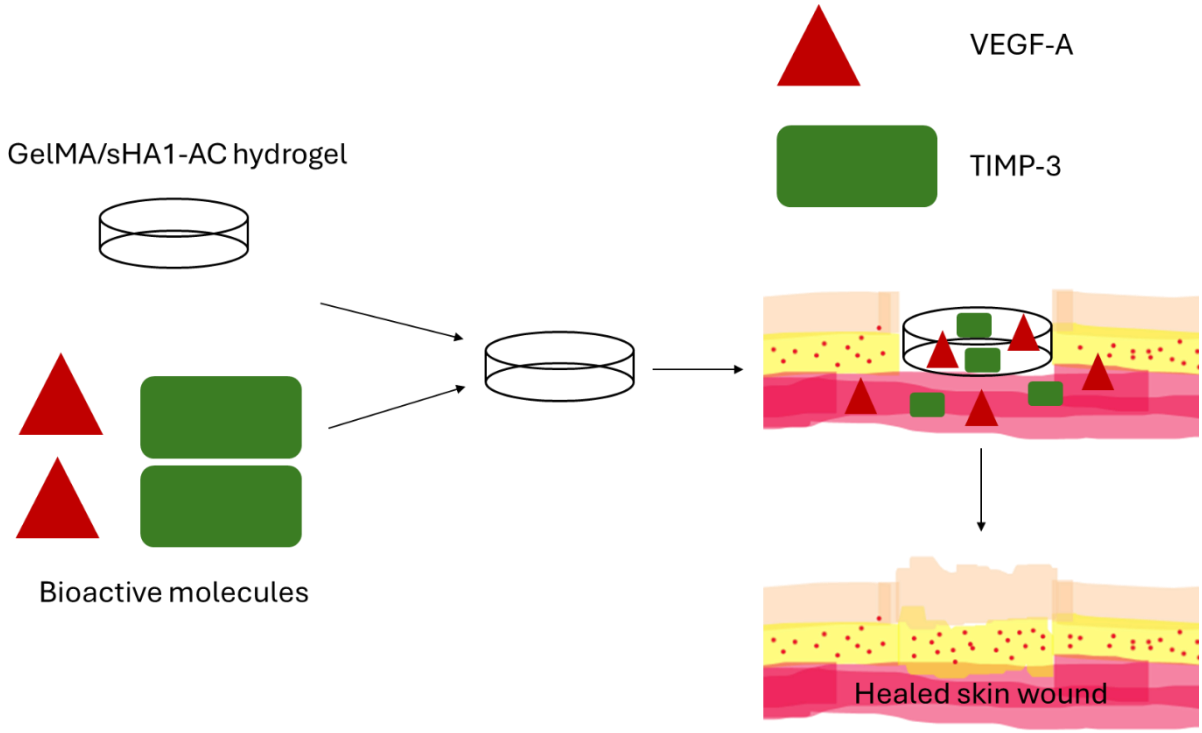

Figure 1.1 Possible approach to facilitate wound healing using a GelMA-based GAG-functionalized hydrogel. The hydrogel can be used for the delivery of VEGF-A and TIMP-3 as bioactive molecules for improved wound healing and angiogenesis.

1.1.3. Hypothesis

To reach the goal of this thesis, the following three hypothesis were tested for the hydrogel system:

I. GelMA-based hydrogels can be functionalized with photocrosslinkable HA derivatives.
II. sHA1-AC-functionalized hydrogels show improved mechanical properties and stability over an extended period compared to GelMA-based hydrogels without GAG-functionalisation.
III. sHA1-AC functionalized hydrogels can facilitate a controlled release of bioactive VEGF-A and/or TIMP-3 over an extended period of time.

1.2. Theoretical background

1.2.1. Angiogenesis: from cell to vessel

1.2.1.1. Structure of blood vessels

All blood vessels have the same basic properties, yet they must adapt to their specific function. For example, the main purpose of the coronary arteries is to deliver oxygen to cardiac muscle cells, whereas the vessels of the nephron serve the purpose of ultrafiltration. However, the histological organization is similar. The structures of the vessel wall are named *tunic*, Latin meaning “membrane or related structure covering or lining a body part or organ”. The *tunics* are named from the lumen to the periphery (Table 1.1 and Figure 1.2) [96]:

Table 1.1 Different layers of blood vessels and their specific morphology.

Tunica	Morphology	References
Tunica intima	Single endothelial cell layer on basal membrane, connective tissue, *membrana elastica interna*, pericytes	[96,135]
Tunica media	Smooth muscle cells, elastic fibres, *membrana elastica externa*	[96,135]
Tunica adventitia	Connective tissue, neurons, *vasa vasorum*	[96,135]

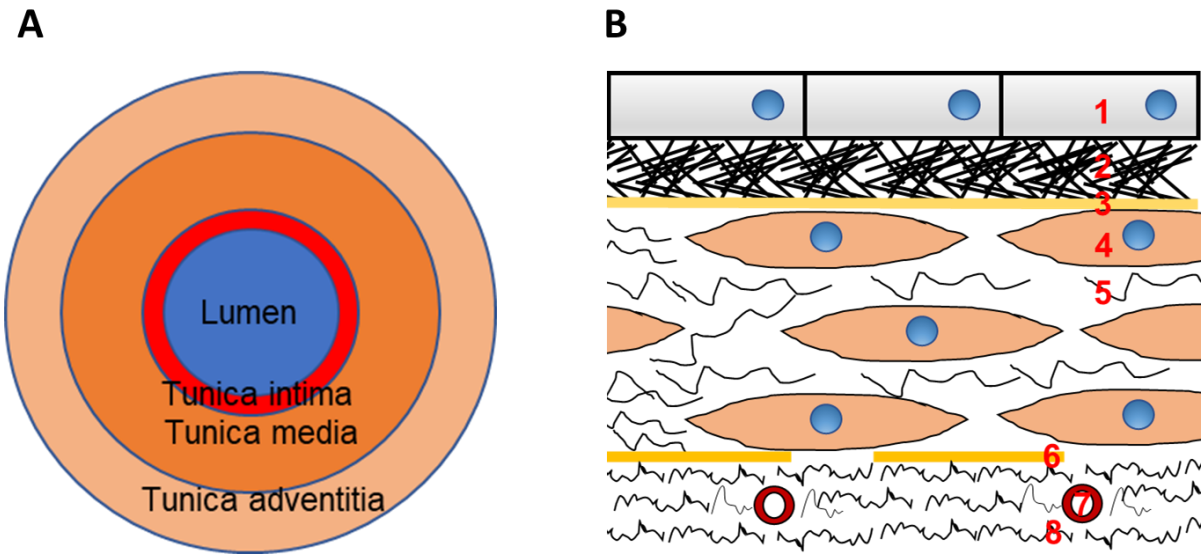

Figure 1.2 Histology of blood vessels. A: Simplified schematic of a vessel wall depicting lumen, tunica intima, tunica media and tunica adventitia. B: Schematic of the histological wall structure. 1: endothelial cells, 2 and 8: connective tissue, 3: Membrana elastica interna, 4: smooth muscle cells, 5: elastic fibres, 6: Membrana elastica externa, 7: Vas vasorum. Adapted and modified after [135].

1.2.1.2. Physiology of blood vessels

Blood vessels play an important role in the human body. Their role is to “guide” the blood through the cardiovascular system and enable an exchange between blood and cells. Therefore, blood vessels and blood cells transport necessary metabolites such as oxygen to the cells but they are also necessary for the elimination of cellular products such as carbon dioxide. This shows the importance of blood vessels for normal cellular function and homeostasis [96]. Blood vessels are important for housekeeping functions of the organism. The vascular endothelium plays an integral role in haemostasis regulation. Healthy endothelium hinders coagulation whereas an endothelial defect promotes it [1]. This is partly due to effect of endothelial nitrogen oxide which plays an important role not only in haemostasis but in the regulation of blood flow and pressure as well as in the regulation of angiogenesis and inflammation [28].

1.2.1.3. Definition of angiogenesis

Angiogenesis can be defined as the development of new blood vessels out of an existing vascular structure (Figure 1.3). It is an important process for tissue formation e.g., embryonic development, and repair as well as physiological remodelling to accommodate new conditions. But its role is not limited to physiological processes, angiogenesis plays an important role in pathological conditions such as tumour development and atherosclerosis [91]. In contrast, vasculogenesis means the *in situ* formation of capillaries out of progenitor cells, the so-called angioblasts [134]. It should be mentioned that angiogenesis is very rare under physiological conditions, except for example in skeletal muscle and the endometrium, but increases under pathophysiological conditions e.g., after physical trauma [93].

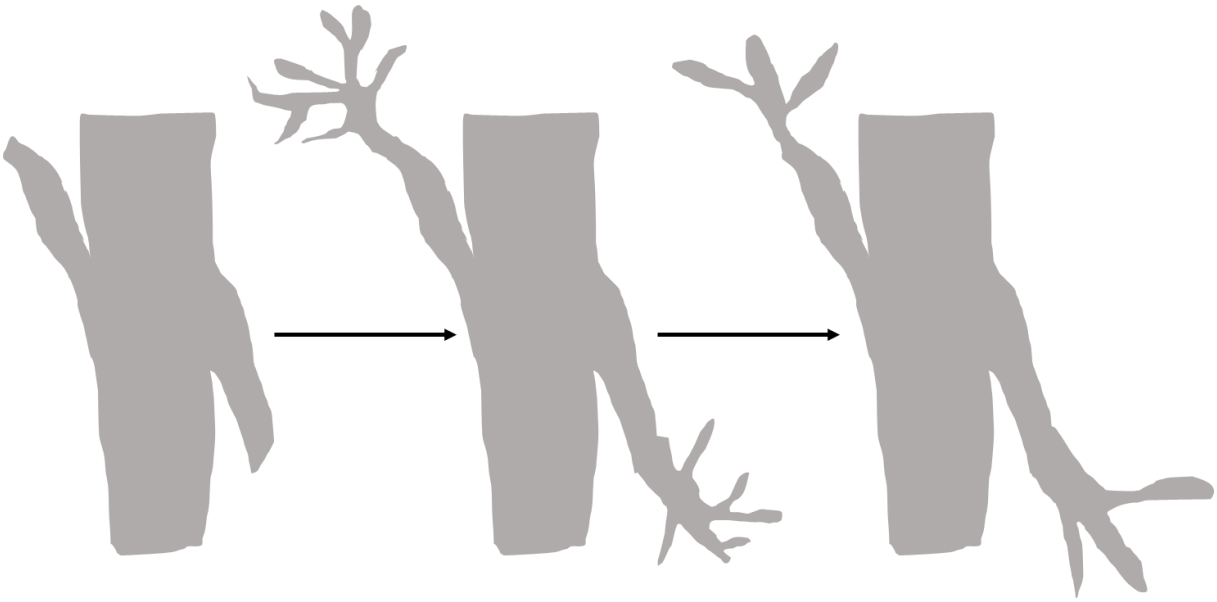

Figure 1.3 Schematic of physiologic angiogenesis. A pre-existing vessel starts to sprout new vessels after exposure to an angiogenic stimuli. The sprouting is followed by a maturation which leads to the formation of a working vascular network.

1.2.1.4. Physiology of angiogenesis

There are two mechanisms for angiogenesis: one is the sprouting of endothelial cells (SA) and the other is the intussusceptive angiogenesis (IA). Sprouting refers to the proliferation of vascular endothelial cells into the surrounding tissue whereas intussusceptive angiogenesis means the division of one blood vessel into two different blood vessels caused by a tissue pillar [134]. In angiogenic sprouting the vascular endothelial cells (VEC) show a growth into the ECM which means proliferation is directed outward. IA could be referred to as an inward growth of the endothelial cells (EC) into the vessel lumen. Both processes are relevant for the development of a functional vascular network and therefore play a role in physiological and pathological angiogenesis. The main differences between both types, except for the direction of the vascular growth, are the following:

1) Dependence on blood flow: IA is dependent on blood flow, SA on the other hand is not.
2) VEC proliferation: SA is associated with an increase in VEC proliferation whereas IA “thins” the endothelial cell layer out.
3) Metabolic costs: the metabolic efficiency is better in IA than in SA.
4) Duration: SA has a duration of a few days, but IA can remodel the vascular system within few minutes or hours.
5) Perfusion: after SA there is a perfusion-free interval until the new formed capillary is integrated in the vascular network whereas with IA there is no such interval.
6) Both processes are important for vessel proliferation but IA`s plays an important role for vessel remodelling as well.

This shows that both types of vessel formation are complementary to one another. However, in general, angiogenesis is associated with the sprouting of endothelial cells [24]. Sprouting angiogenesis consists of several steps: it starts with an increase in the number of EC and their migration. Following this step, the VEC form a tube, the precursor of the developing vessel, which is followed by VEC discrimination and ripening. The regulation of angiogenesis involves a broad spectrum of growth factors and other molecules which have their own respective signalling pathways [113]. An overview of the involved signalling pathways will be given later (**1.2.1.5.**).

On the cellular level, pro-angiogenic signals lead to the development of a so-called tip cell with filopodia for signal-sensing. These tip cells guide the sprouting vessel to the site of factor production. The tip cell is followed by stalk cells that proliferate and as a result form the vascular tube. After vessel perfusion, these stalk cells will become phalanx cells and differentiate to cells of the vascular endothelial layer (Figure 1.4). Stalk and tip cells are not pre-determined. Instead, it is a plastic process in which tip cells can become stalk cells and the other way around. This flux ensures that the “fittest” endothelial cell guides the stalk cells to their target site [93]. Important for the formation of a tip cell is a complex interaction between vascular endothelial growth factor receptor 1 (VEGFR-1) and vascular endothelial growth factor receptor 2 (VEGFR-2), neurogenic locus notch homolog protein (notch) and other receptors. Vascular endothelial growth factor A (VEGF-A) stimulation enables the tip cell to form filopodia. The increased expression and conformational changes of notch and a handful of other receptors hinders neighbouring cells to become tip cells. On the other hand, tip cells express vascular endothelial growth factor receptor 3 (VEGFR-3) for vascular endothelial growth factor C (VEGF-C) binding. This interaction of growth factor and receptor seems to be essential to the solidity of angiogenic sprouts. Stalk cells express higher quantities of the non-angiogenic VEGFR-1 which binds VEGF-A without initiating the signalling process. Therefore, the normal pro-angiogenic effect of VEGF-A on these cells is diminished. This complex regulation shows that tip cell formation as well as sprouting angiogenesis underlies a firm physiological control mechanism. However, the exact regulation of endothelial tip cell formation still needs to be determined [27].

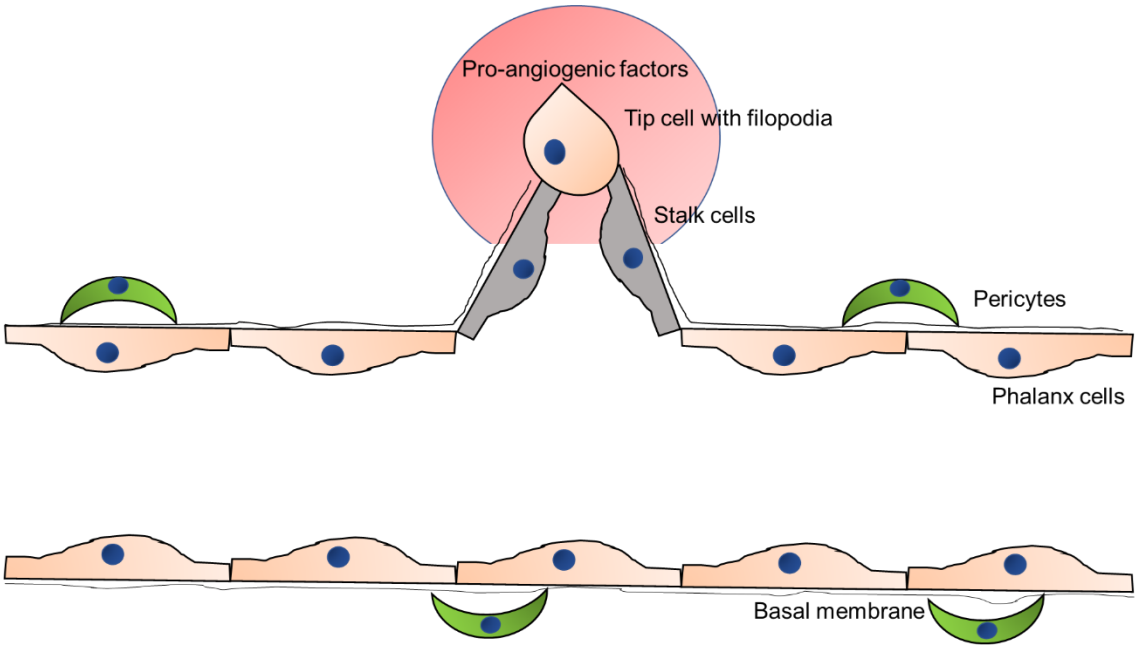

Figure 1.4 Sprouting angiogenesis as a schematic. A tip cell with filopodia follows the pro-angiogenic factors into the ECM and is followed by the so-called stalk cells. After the formation of a new vessel the tip and stalk cells differentiate to phalanx cells which coat the vessels lumen. Modified and adapted from [104].

1.2.1.5. Regulation of angiogenesis

A key regulator of angiogenesis is VEGF-A. The vascular endothelial growth factor (VEGF) family consists of five subtypes A to E. For vascular angiogenesis, VEGF-A is the most important growth factor. The VEGF-A family consists of several isoforms such as $VEGF_{165}$ and $VEGF_{121}$. These isoforms are the result of alternative splicing. $VEGF_{165}$ is the most common isoform and the one with the greatest physiological relevance. $VEGF_{165}$ has just one heparin-binding site, which leads to $VEGF_{165}$ being partly bound to the ECM and being partly soluble [5]. $VEGF_{165}$ can be divided into the pro-angiogenic isoform $VEGF_{165a}$ and the anti-angiogenic isoform $VEGF_{165b}$ and both isoforms have heparin-binding domains with different structures. As a result, $VEGF_{165a}$ binds to sHA whereas the anti-angiogenic isoform does not [69,111]. *Rother at al.* showed that VEGF-A has an increased binding strength towards sHA than naturally occurring GAG such as chondroitin sulphate (CS) and HA [111].

$VEGF_{165}$ does not only play an important role in angiogenesis, but it also acts as a growth factor for other cell types such as lymphocytes or hematopoietic stem cells and is associated with embryonic implantation and the female reproductive cycle [42]. There is evidence supporting the hypothesis that endogenous VEGF may be necessary for endothelial cell viability, this seems to apply to other cells such as stem and tumour cells. The underlying signalling pathways are yet to be fully understood [27].

Signalling requires the binding of VEGF to its receptor VEGFR with its three subtypes 1 to 3. VEGFR-1 and VEGFR-2 are mainly expressed on endothelial cells and VEGF-A binds to both types. VEGFR-2 has a lower affinity to VEGF-A than VEGFR-1 but nonetheless it is the main receptor for VEGF-A. The primary function of VEGFR-1 is to bind VEGF-A and thereby reducing the bioavailability of VEGF-A and inhibiting angiogenesis. The affinity of VEGF-A towards VEGFR-2 is increased if heparin is bound to the heparin-binding domain of VEGF-A. The activation of VEGFR-2 as main signal receptor for angiogenesis regulates EC mitosis and permeability. After activation VEGFR-2 is internalized. This is important for the regulation of the signalling pathway as well for the regulation of the cell's response to VEGF as one part of VEGFR-2 seems to be cycling and another one seems to be stable on the cells surface. One of the major impact factors on angiogenesis is hypoxia and its impact is mainly regulated via hypoxia inducible factor (HIF) but not exclusively. Factors such as epidermal growth factor and platelet-derived growth factor play a role as well. These factors regulate the expression of the VEGF gene and are therefore inevitably necessary for the VEGF/VEGFR signalling pathway. Activation of VEGFR-2 leads to the regulation of different kinases (e.g., phosphoinositide 3-kinase and mammalian Target of Rapamycin) which in turn regulate the different steps of angiogenesis. The pathway is controlled by a negative feedback-loop via notch-signalling pathway. An increase in notch-signals in nearby cells leads to a decrease in VEGFR-2 expression [5,27,30,42].

Another inhibitory regulator of angiogenesis is TIMP-3. TIMP-3 inhibits angiogenesis through hindering the chemotactic properties of VEGF towards VEC. The VEGF-mediated chemotaxis of VEC is important for a functional angiogenesis [4]. TIMP-3 differs from other TIMPs by its lack of solubility as it is firmly bound to GAG within the ECM [115,153]. However, TIMP-3 not just inhibits the interaction of VEGF-A and VEGFR-2 by competing for the same binding site as VEGF-A, it decreases the amount of secreted matrix metalloprotease 2 and 9 (MMP-2, MMP-9), mediated by VEGF, as well [21,124]. Like VEGF-A interacts with sGAG derivatives, TIMP-3 was shown to be influenced sGAG as well. A complex of sGAG/TIMP-3 decreases TIMP-3 ability to bind to VEGFR-2. This inhibitory effect of sGAG on TIMP-3 needs a much smaller amount of sGAG than the same mechanism with VEGF. Therefore, sGAG inhibit the binding of TIMP-3 to VEGFR-2 more effectively than VEGF. The interaction is influenced by the sGAG degree of sulfation and its concentration. sGAG do not decrease the inhibitory effect of TIMP-3 towards matrix metalloproteinases (MMP) [108].

Furthermore, it was found that *von Willebrandt*-factor deficient mice had an increased vascularisation, especially in the ear and brain. Therefore, the evidence suggests that *von Willebrandt*-factor inhibits angiogenesis but only to a small extend and its relevance in embryonic development seems to be minor. Such inhibition of angiogenesis due to *von*

Willebrandt-factor is caused by an impact on VEGFR-2 signalling but the exact pathway remains unknown [102].

Angiogenesis is influenced by the catecholamines adrenaline, noradrenaline and dopamine. The effect of dopamine on angiogenesis depends on the respective receptor. Whereas dopamine D2 receptor inhibits angiogenesis, its counterpart the dopamine D1 receptor promotes angiogenesis. This should be kept in mind because catecholamines play an important role in physiologic as well as pathophysiologic conditions such as chronic wounds associated with stress [15].

Yet another pro-angiogenic factor that is associated with VEGF is nitric oxide (NO). VEGF regulates the activation and phosphorylation of endothelial NO synthase[39,147]. This leads to the production of endothelial NO which on the other hand induces angiogenesis [39].

The regulation of angiogenesis is complex and involves a variety of different systems of the human body. An overview of the different signalling pathways is given in Figure 1.5.

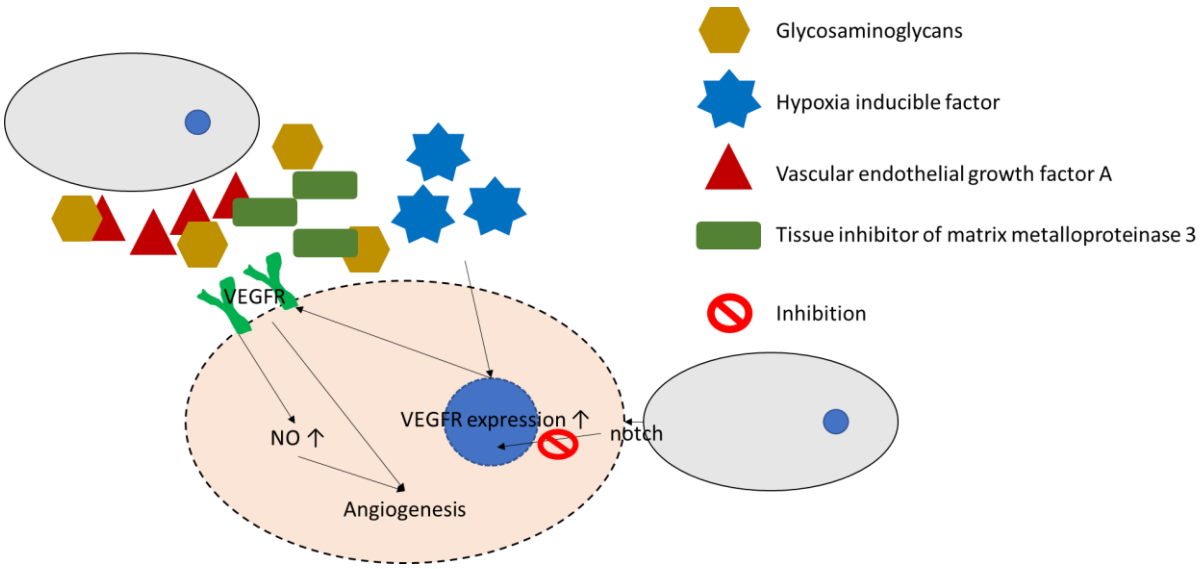

Figure 1.5 Overview of the major signalling pathways involved in angiogenesis. The interaction of VEGF, GAG and VEGFR is shown which leads to an increase of angiogenesis, as well as the pro-angiogenic NO. Depicted as well is the inhibitory interaction of TIMP-3 and VEGF and its modulation via GAG. VEGFR expression is regulated via HIF and notch-signals.

1.2.1.6. Disruption of physiologic angiogenesis

The normal function of the endothelium is necessary for angiogenesis. If the endothelium is dysfunctional, it inevitable affects normal angiogenesis, e.g. in peripheral arterial disease (PAD). This leads to an increase in peripheral ischaemia and to a decrease in microcirculation [44,106]. Not only does endothelial dysfunction impair angiogenesis in PAD but also the increased secretion of the antiangiogenic isoform $VEGF_{165b}$. Interestingly, $VEGF_{165b}$ is

associated with metabolic dysfunction and its secretion is activated by obesity via protein Wnt5a/Jun N-terminal kinase pathway, this could be a reason why VEGF-A treatment in PAD is not efficient [44,55].

A decrease in angiogenesis is one of the reasons for impairment in chronic wounds. In chronic venous ulcers the degradation of VEGF-A by proteases, such as plasmin, and an increased concentration of VEGFR-1 as neutralizing agent for VEGF-A could lead to the described impairment in wound healing [26,61,138]. In chronic diabetic wounds yet another mechanism is responsible for the healing impairment: a dysfunction of wound macrophages, as major "production site" for angiogenic factors, at the wound site and therefore a deficiency of VEGF-A and other pro-angiogenic factors is responsible for the decrease in angiogenesis [84,92,120].

Another example for the disruption of angiogenesis in a pathophysiologic condition is diabetic retinopathy (DR). In DR a retinal hypoxia or ischaemia caused by capillary occlusions leads to an increase of HIF-1. An increase of HIF-1 leads to an enhanced VEGF-A expression. VEGF-A is associated with VEC mitosis and the formation of new, in this case dysfunctional, vessels. The sum of VEGF-A related functions leads to a progress of the DR [145]. A similar mechanism is associated with angiogenesis in gliomas and in the pathophysiological liver changes occurring in portal hypertension [19,31].

1.2.2. Extracellular matrix

1.2.2.1. Definition

The ECM is a cell-free 3D scaffold that is composed out of a variety of macromolecules. These are mainly glycoproteins like collagen and elastin as well as proteoglycans and GAG [129]. The difference between glycoproteins and proteoglycans is that proteoglycans (PG) consist of a protein core to which at least one long chain of GAG is attached, whereas glycoproteins are only posttranslational modified with glycan side groups bound to different amino acids [38,144]. However, the ECM does not just provide structure, it interacts with the cells as well, as is shown in Figure 1.6. The ECM is involved in cellular homeostasis and regulation e.g., cellular growth and differentiation. Yet it is not an unchanging construct but undergoes a constant enzymatic degradation and re-building. The ECM is more than just a "house" for cells but an interacting "social network" for cells that plays an important role in physiological and pathophysiological conditions [129].

For example, genetic defects of different collagen types can lead to Ehlers-Danlos syndrome or, as an example for a disease not related to a specific gene, osteoarthritis. In osteoarthritis, the external circumstances (e.g., intra-articular blood) lead to a decrease in the synthesis of proteoglycans and collagen as well as to an increase in degeneration. In a state of chronic inflammation, such as osteoarthritis, the regeneration is compromised due to the state of

chronic inflammation. Another example for a disease associated with the ECM is fibrosis. Fibrosis results from a dysfunctional tissue repair e.g., wound healing. An increased differentiation towards myofibroblasts and their deregulation leads to the synthesis of a dysfunctional and stiff ECM e.g., scars, pulmonary fibrosis and liver fibrosis [130].

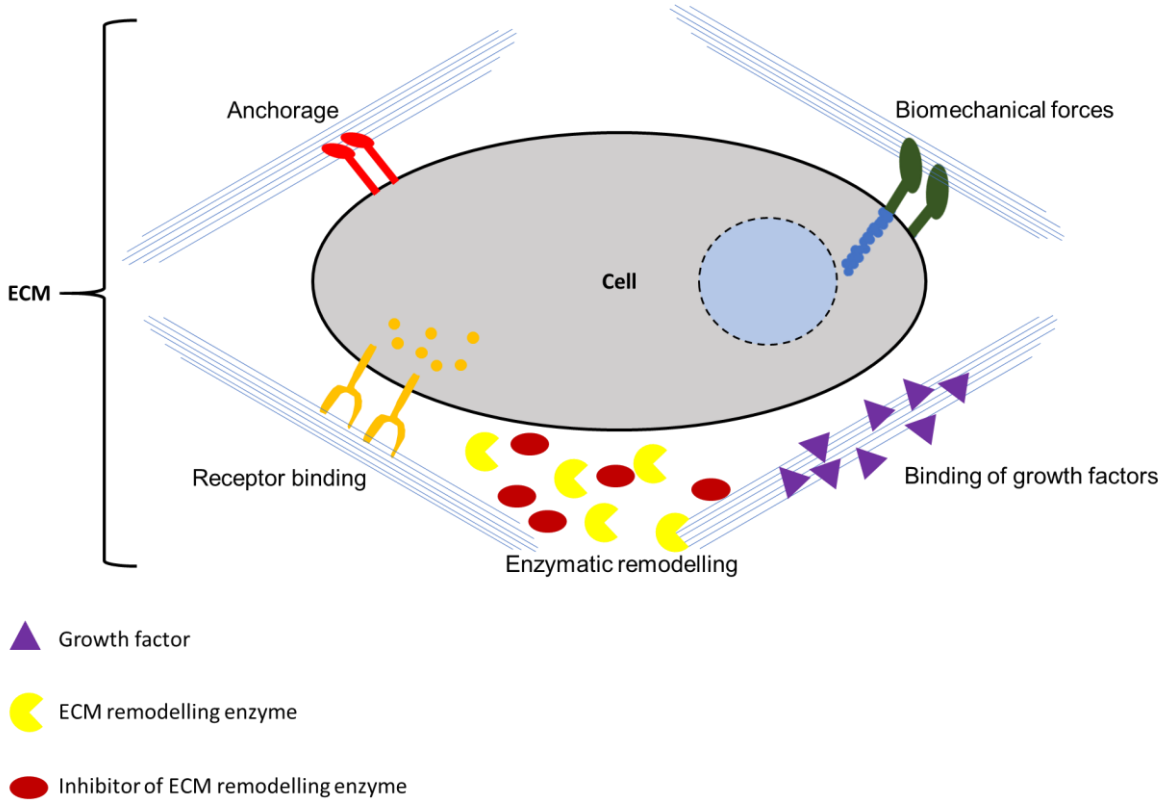

Figure 1.6 The cell's integration into the ECM. The major interactions between cell and ECM are shown: the anchorage the ECM provides for cells, the binding of different cellular receptors to the ECM, the ECM importance for biomechanical stability of the tissue, its capability to bind growth factors. The constant remodelling of the ECM is depicted as well.

1.2.2.2. Composition

The composition of the ECM depends on the tissue and its specific function. The ECM is very heterogenous. However, the basic elements are always similar. The components of the ECM are water, proteins, and polysaccharides. The specific molecules and their concentrations vary largely because of its close interaction with cells. The ECM reflects the momentary physiologic condition of the tissue. There are two main types of macromolecules in the ECM: fibrous proteins and PG. Collagen, elastin, fibronectin and laminin are the most important fibrous proteins of the ECM whereas the PG composition is tissue-specific (Figure 1.7). For example, in renal glomerular other PG are important in comparison to endothelial tissue. The reason for this is that PG often modulate the specific properties of the ECM like buffering, hydration, mechanical properties, e.g. stiffness, or the binding of growth factors to the ECM. The major

fibrous protein of the ECM is collagen with up to 30% of the total protein mass of an animal. Collagen is important for physical as well as biochemical properties of the ECM as it provides strength and offers cells a place to attach to, regulates cellular movement and tissue development [34]. Although there are 29 different collagen proteins, only collagen type I, type III and type V forms fibrils with collagen type I being the predominant form in the skin under physiological conditions. This changes when the skin is injured. During wound healing, collagen type III becomes more dominant which can lead to scars [37]. It is noteworthy that collagen type III is increased in diabetic wounds [161]. Collagen for fibre synthesis is secreted and modified by fibroblasts, and, after several steps of synthesis, the collagen is assembled to create collagen fibres [34,37]. These fibres contain a variety of different subtypes of collagen but within one tissue, there is one dominant isoform of collagen at a time. Collagen interacts with elastin, an elastic fibre that is important in tissues that undergo physical stress repeatedly. The third of these proteins is fibronectin, which interacts with collagen as well and plays an important role for the structural organization of the ECM. However, fibronectin is not only of structural importance, but it is also a key player in cellular attachment to the ECM as well as in the pleiotropic regulation of the cells that adhere to it [34]. The key proteinases for ECM remodelling are MMP. Their activity is increased during states of tissue inflammation or damage. Other proteinases involved in the remodelling of the ECM are adamalysins which have a variety of functions including the processing of pro-collagens. Both MMP and adamalysins are inhibited by TIMP-3 [9].

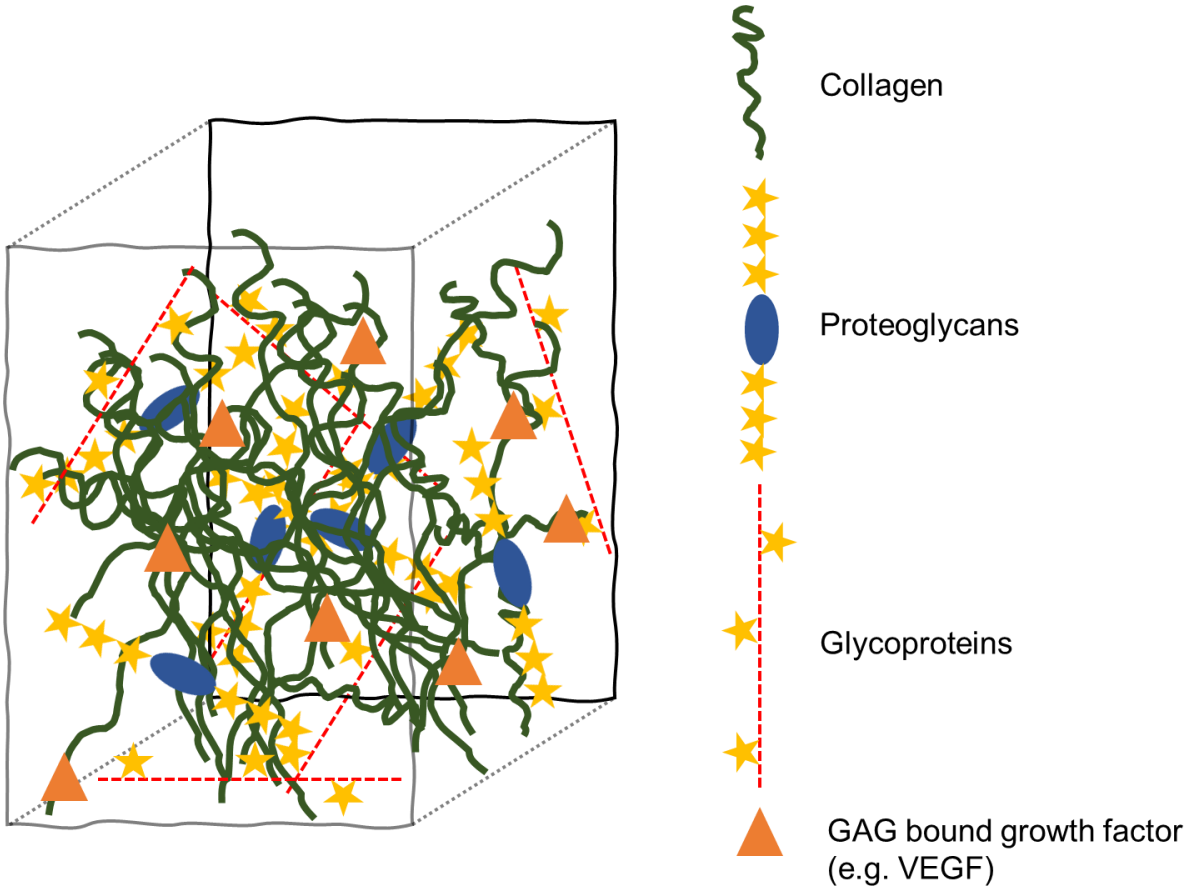

Figure 1.7 Schematic overview of the composition of the ECM. The ECM mainly consist of PG, collagen and glycoproteins. To the proteinous components of the ECM different GAG are bound to which different growth factors can bind, e.g. VEGF-A [5]. Modified after [34].

1.2.2.3. Glycosaminoglycans

There are six naturally occurring GAG in the ECM: dermatan sulphate (DS), keratan sulphate (KS), heparan sulphate (HS), heparin, CS and HA. GAG consist of repetitive, unbranched disaccharide units which carry a negative charge and differ in their degree of sulfation and in their disaccharide units. Every GAG except for HA is produced in the Golgi apparatus and the endoplasmic reticulum [53].

Only HA, the simplest GAG, is produced in the cell membrane and secreted without further modifications. In comparison, all other GAG are sulphated and bound to a protein core as PG [53]. The responsible enzymes for HA synthesis are HA synthases which are subtypes of glycosyltransferases. The enzymes are inserted into the plasma membrane and catalyse the synthesis of HA out of uridine diphosphate-activated monosaccharides. Of the three known isoforms, HA synthase 2 is the essential isoform. The HA synthase isoforms differ in their activity and tissue expression. Yet it remains unknown how exactly hyaluronan synthase choses its substrate, introduces regio- and stereospecific glycosyl transfers or how it controls the secretion and chain length of HA [77].

The different GAG chains differ in length, place, and degree of sulfation. Overall, cells can produce a wide variety of proteoglycans. Glycosaminoglycans are involved in the regulation of many signalling pathways, this is caused by their interactions with different proteins e.g., they can bind growth factors like VEGF and transforming growth factor β (TGF-β) or further regulators of ECM homeostasis such as TIMP-3 [53,153]. Whereas heparin and heparan sulphate play an important role in homeostasis and development, chondroitin sulphate and dermatan sulphate are important for neurons and chondrocytes. Like heparin, HS, DS and CS play an important role in tumour growth and metastasis. Keratan sulphate seems to be of major importance for vesicle formation. Nevertheless, it is involved in other processes such as embryonic development, wound healing and collagen fibre organization [53].

HA is one of the most biologically active compounds in the human body, it plays an important role in several physiological processes, such as wound healing and tissue development and regeneration. However, HA is not only associated with physiological processes, but it is also involved in pathological processes such as cancer and inflammation. Essential cellular processes rely on HA: for example, mitosis and cell migration are regulated by an increasing concentration of HA. Nearly one third of the entire HA is being degraded and replaced every day, which is essential for the HA homeostasis in the ECM. Furthermore, HA homeostasis is necessary to control the regulatory functions of HA [53]. HA's influence on tissue hoemostasis depends on the molecular weight of its chain. For example, it was discovered that fragments of HA (< 500-700 kDa) increase inflammatory reactions and promote angiogenesis. This is opposed to the effect of high-molecular weight HA (> 1 MDa) which promotes anti-angiogenic, immune suppressive and anti-inflammatory pathways. It also leads to increased wound healing [36,53]. For the regulatory effects of HA special receptors are required which lead to an intra-cellular signalling cascade. All HA binding proteins can be referred to as hyaladherins. The hyaladherins are a heterogenous group, which involves PG and receptors e.g., Cluster of Differentiation 44 that trigger a specific signalling cascade or regulate HA synthesis and degradation [53].

From a chemical point of view, HA is a natural occurring linear, non-sulphated and negatively charged polysaccharide. HA consists of repeating monosaccharide units: *D*-glucuronic acid and *N*-acetyl-*D*-glucosamine. These monosaccharides are bound via β-1,3 or β-1,4 glycosidic bonds. In the human body, HA is found as a hydrophilic sodium salt. The most studied HA derivatives for biomaterial applications have a molecular weight between 5 kDa and 3000 kDa. Other important properties of HA are its non-immunogenetic and non-toxic character and its biocompatibility as well as its biodegradability [8]. Figure 1.8 shows a part of the polysaccharide chain of HA depicted as described in the Symbol Nomenclature for Glycans [137].

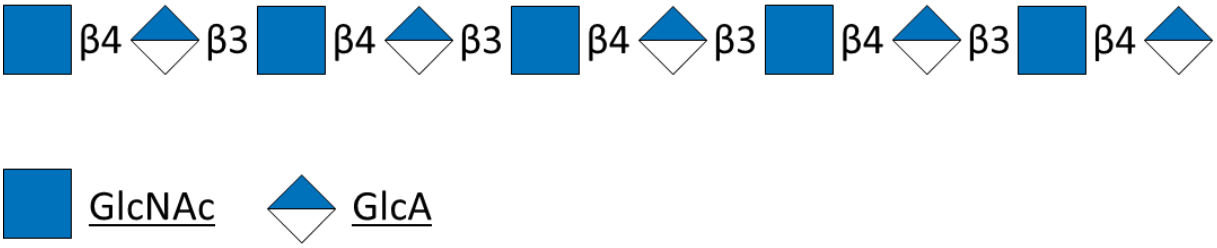

Figure 1.8 Composition of hyaluronan. It consists of *N*-acetyl-*D*-glucosamine (GlcNAc) and *D*-glucuronic acid (GlcA). The figure only represents a small part of the large HA molecule [137].

1.2.2.4. Glycosaminoglycan derivatives

By design, natural occurring GAG show a sample-dependent variation of composition. Furthermore, their availability for research purposes is limited. HA and CS offer as native GAG a variety of opportunities for chemical modifications. Modified HA and biotechnologically synthesized CS are therefore viable alternatives to natural GAG because their structure resembles the structure of natural GAG yet they are reproducible in regard to molecular weight and sulphation. Natural, bacteria-derived HA can be degraded to low-molecular weight HA via thermal degradation. It is possible to introduce sulphate groups to HA and CS using a sulphation agent with a SO_3 functional group. The degree of sulphation can be varied using different sulphation agents or a different ration of GAG and SO_3. It is even possible to introduce regiospecific sulphate groups to HA [48,116].

As mentioned above, VEGF-A and TIMP-3 (**1.2.1.**) both interact with natural occurring GAG. For both VEGF-A and TIMP-3 it was shown that they interact with sHA, a sulphated HA derivative, similar to their interaction with natural sGAG [107–109]. Furthermore, acrylated derivatives of HA as well as sHA were found to be suitable for the synthesis of aECM [109,118,131].

As a derivative of hyaluronan sHA1-AC may be used for hydrogels. It is sulphated on the C_6 primary hydroxyl group of the *N*-acetyl-*D*-glucosamine monosaccharide unit (Figure 1.9) [109,111]. In this case, not only a sulphate group is introduced but an acrylate group as well. The acrylate group makes crosslinks with other acrylate groups or with thiol groups possible [121]. The possibility of modifying the sulphation pattern of sGAG derivatives is important because the binding of GAG derivatives to VEGF-A and TIMP-3 not only depends on the carbohydrate backbone but on the degree and pattern of sulphation as well [12,50,111]. Moreover, sHA can lead to an increased amount of HA in the ECM and therefore has an influence on the important functions of native HA [12,117].

The binding of VEGF-A to sGAG offers the opportunity for engineering a gradual and more controlled release of the respective growth factor. Therefore, sHA as part of an aECM offers a

valuable opportunity to design a biomaterial which can mediate angiogenesis due to its regulation of VEGF-A and TIMP-3 [108,111].

However, growth factor binding is not the only interesting property of sHA. In addition, *Möller et al*. showed that a highly sulphated variant of sHA has antiviral properties, especially concerning the Severe Acute Respiratory Distress Corona Virus 2 [85].

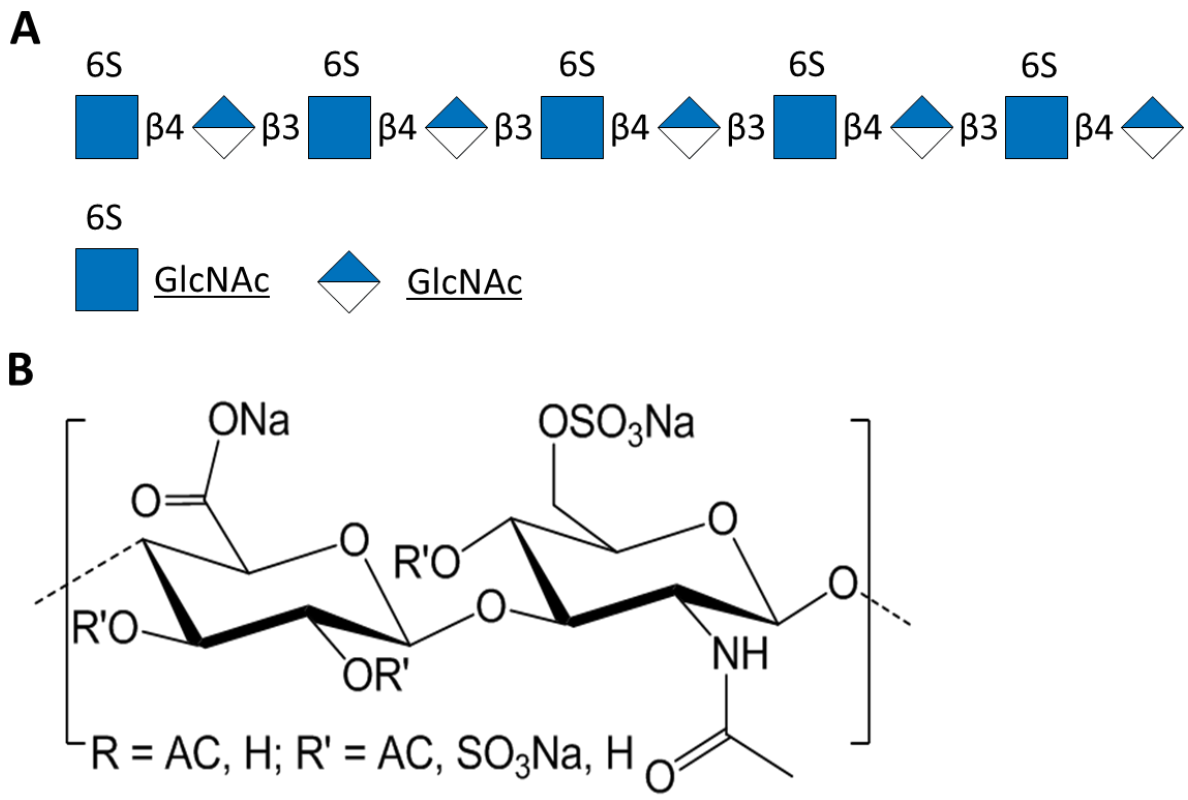

Figure 1.9 Composition of sulphated hyaluronan. A: sHA consists of *N*-acetyl-*D*-glucosamine (GlcNAc) and *D*-glucuronic acid (GlcA). They are bound using alternating β3 and β4 glycosidic bonds The primary hydroxyl group of the C6 of GlcNAc is sulphated, represented as 6S [111,137]. B: Chemical structure of a sHA1-AC monomer is shown. Here, the primary hydroxyl groups are sulphated while a crosslinkable acrylate goup is introduced at the secondary hydroxyl groups (AC) [69].

1.2.2.5. Gelatine-based artificial extracellular matrices

Biopolymers commonly used as aECM such as Matrigel™, collagen or fibrin have their own individual disadvantages. In the case of Matrigel™, its clinical use is limited because it is derived from Engelbreth-Holm-Swarm mouse sarcomas leading to a heterogeneous composition and a lack of tunability [2]. The use of collagen and fibrin is limited due to their fast degradation and poor mechanical properties [119].

Gelatine is the product of collagen hydrolysis. Collagen is the major ECM protein in most tissues, and it offers suitable conditions for cell attachment and remodelling due to target

sequences for MMP. Further disadvantages of collagen are its heterogeneity regarding its structure, its solubility and antigenicity [155].

These disadvantages can be reduced if GelMA is used. An advantage of GelMA is the variety of chemical reactions that can be used to engineer GelMA hydrogels, this allows the creation of fine-tuned hydrogels specific to the applicational need. Hydrogel configuration and modification have an influence on cellular behaviour. Despite the methacrylamide groups of GelMA, the major biologic motifs of collagen for cell attachment with amino acid sequences like arginine-glycine-aspartic acid (RGD), which define its biological properties, are intact. Furthermore, GelMA-based hydrogels have been tested for a variety of possible applications in different fields of research [155].

However, there are unresolved issues with GelMA when it comes to its mechanical properties. GelMA's mechanical properties such as rheology, gelation and stability depend on factors such as temperature, photo-crosslinking kinetics and degree of substitution. Furthermore, hydrogels which are only based on GelMA have limited compatibility with certain cell lines e.g., chondrocytes [40,82]. Furthermore, GelMA hydrogels are limited by the decrease of crosslinking on hydrophobic surfaces. However, this decrease in crosslinking only affects the immediate surface of the hydrogel and it is only relevant for very thin hydrogel preparations [72].

GelMA degradation products are gelatine peptides which naturally occur in the ECM; therefore, they are non-toxic. Another advantage of GelMA being a modified gelatine derivative is that it can be synthesised inexpensively through hydrolysis at high temperatures out of collagen [50].

For gelatine modification, the amine side-groups of gelatine react with methacrylic anhydride. Residual methacrylic anhydride is removed via dialysis and GelMA is lyophilized creating a foam. The resulting foam can be dissolved in biocompatible solutions such as phosphate buffered saline (PBS) or cell culture medium. The result is a biocompatible photocrosslinkable polymer for tissue engineering applications (Figure 1.10.A). GelMA solutions are stable for several weeks, if stored correctly [50]. The cellular behaviour as well as mechanical properties of GelMA hydrogels are influenced by its degree of methacrylation. Lower degrees of methacrylation were found to allow the formation of an increased vessel diameter and density [18].

A common photoinitiator for GelMA crosslinking is lithium phenyl-2,4,6-trimethylbenzoylphosphinate (LAP, Figure 1.10.B) [50]. LAP shows no relevant cytotoxicity at low concentrations, which can be further reduced if the cell's exposure to non-crosslinked LAP is very short. The reaction of GelMA and LAP with a LAP concentration of 1% or less showed no significant reduction in short term cell viability [89,152]. LAP is easier to dissolve in water

and its gelation rate is increased in comparison to Irgacure 2959. LAP works at wavelengths around 400 nm and a short time of UV irradiation can activate crosslinking (Figure 1.10.C) [152]. GelMA can be combined with other materials to engineer its properties. Furthermore, it is possible to use GelMA as a bio ink [50].

In literature, there are several examples for GelMA-based drug-delivery systems. One system uses a GelMA-based hydrogel to encapsule exosomes for the therapy of osteoarthritis. Another system for the treatment of osteoarthritis was used to deliver the anti-inflammatory drug diclofenac [45,141]. Another application from the field of orthopaedics was to use GelMA to deliver small interfering ribonucleic acid [14]. For the successful delivery of antibiotics such as vancomycin and anthracyclines such as doxorubicin a GelMA-based drug-delivery system was developed [52,79]. Another example for a successful GelMA-based system was the use of microneedles to deliver drugs as an alternative to conventional transdermal application [71]. When it comes to drug-delivery in a broader sense, a GelMA-based system was successful in delivering encapsulated cells to their destination tissue [54].

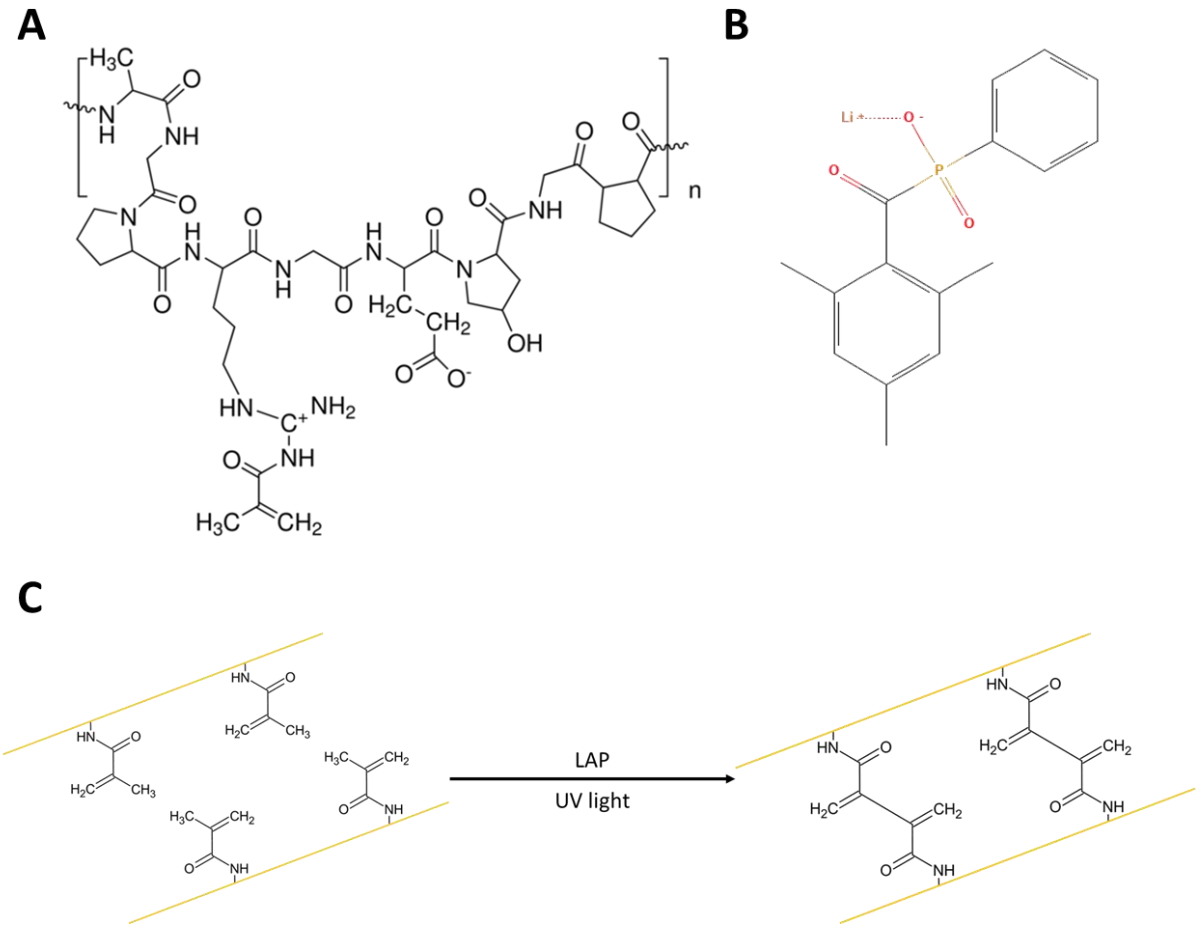

Figure 1.10 GelMA polymerisation. A: Chemical structure of GelMA. GelMA consists of repetitive monomers. The methacrylate group is important for crosslinking. B: Molecular structure of LAP [162]. C: Schematic of GelMA crosslinking depending on LAP and UV irradiation. The methacrylate groups are shown as structure formula whereas the residual protein of GelMA is depicted as yellow lines. UV

irradiation in combination with LAP leads to a chemical crosslinking between methacrylate groups and results in covalently bound GelMA strands.

1.2.3. Influences of the ECM on bioactive proteins

1.2.3.1. Influence of the ECM on growth factor signalling

Growth factors are soluble proteins which induce specific biologic functions of the cell after binding to specific growth factor receptors on the cell's surface. These include a broad spectrum of processes such as apoptosis, mitosis and cellular differentiation. Growth factor binding to specific cellular receptors leads to complex cellular responses, depending on a variety of factors such as the exact type of cellular receptor, the transduction pathways and the number of cells which are in contact with the specific growth factor. Furthermore, extracellular factors can influence the cellular response to a specific growth factor such as the factor binding to the ECM, ECM regeneration, spatial alignment of ECM and cells, the concentration of growth factors on site and the location of the cells in the human body [62]. A prominent example is VEGF-A which binds with its heparin-binding domain to sGAG e.g., the ubiquitous heparin, leading to VEGF-A being partly bound to the ECM [5,81]. Especially one enzyme of the ECM, heparinase, can regulate the expression of growth factors e.g., VEGF and TGF-β through gene regulation. As MMP expression is regulated by TGF- β, heparinase influences MMP expression as well [80,81,158].

Some growth factors can bind to different HS PG e.g., VEGF-A and form a kind of pool, which can lead to the creation of growth factor gradients. However, other proteins in the ECM can bind inactive growth factors complexes and lead to their activation. For example, TGF-β forms a complex with a protein called latency-associated peptide. The inactive complex of both proteins can bind to ECM proteins such as fibronectin, which in turn leads to the activation of TGF-β through different mechanisms [49].

Especially MMP, which can be found int the ECM, have a profound impact on growth factor signalling. MMP can release, activate or disinhibit growth factors or process them in a different manner. This can lead to active growth factors or inactive and degraded growth factors depending on the different types of growth factor and their interaction with ECM proteins [33]. Growth factors act paracrine, and their actions are dependent on their usually short half-life as well as on their diffusion capabilities. For example, if injected intravenous VEGF-A has a half-life of 30 min, which would make multiple high-dose injections necessary. However, high doses of VEGF-A could be harmful leading to systemic increase in vascular formation with a risk of neovascularization of dormant malignancies [62]. The diffusion capability of growth factors is governed by the ECMs capability to bind these factors. If growth factors cannot bind to the ECM, their ability to diffuse is increased. Therefore, the therapeutic applications of recombinant

mediator proteins are currently very limited. Novel approaches like tuneable hydrogel systems are required to control the growth factor release and the mode of application [62].

1.2.3.2. Role of TIMP-3 in the ECM

Like VEGF-A, TIMP-3 plays an important role in angiogenesis. However, unlike VEGF a higher percentage of TIMP-3 is bound to the ECM [5,115]. Responsible for the binding of TIMP-3 to the ECM are *C*- (Arg-163, Lys-165) and *N*-terminal (Lys-26, Lys-27, Lys-30, Lys-76) binding motifs which interact with extracellular sGAG like heparin, HS and CS [63,154]. Changes to the positively charged amino acid binding motifs result in a soluble isoform of TIMP-3 [63].Therefore, it is possible to deliver TIMP-3 for treatment using GAG hydrogels which release TIMP-3 after gradual degradation [98].

MMP are the main enzymes involved in ECM remodelling. They degrade for example PG and glycoproteins and are either soluble or anchored in the cell membrane [9,74]. One important subtype of MMP is MMP-9 which can degrade denatured collagen (gelatine) and therefore is also called a gelatinase [13]. Therefore, successful inhibition of MMP-9 is necessary to prevent rapid degradation of a GelMA-based hydrogel. Furthermore, increased MMP-9 activity leads the destruction of the ECM in diabetic foot ulcers through an increase in inflammation and a decrease in angiogenic potential. Additionally, wound infections and increased wound severity lead to an increase in active MMP-9 [17].

However, TIMP inhibit MMP through binding. The TIMP family consist of four different inhibitors, which carry all the same two domains of 125 *N*-terminal and 65 *C*-terminal amino acid residues. These domains are necessary for binding and inhibition of the MMP. The ratio TIMP:MMP is 1:1 and their interaction results in a complex that can be recognized by scavenger receptors, which results in an intake of the complex by macrophages. TIMP can inhibit nearly all MMP but their affinity varies slightly. However, it is possible that the TIMP family can inhibit other proteinase families as well such as Disintegrin and Metalloproteinase (ADAM) and Disintegrin and Metalloproteinase with Thrombospondin motifs (ADAMTS) [74] ADAM and ADAMTS have a variety of functions including ECM degradation. Furthermore, they can release the ectodomain of cytokines, growth factors and receptors and therefore are not limited to only one function [9,13,74]. TIMP-3 is the main inhibitor of ADAM and ADAMTS [9]. TIMP-3's influence on angiogenesis has been discussed in a previous chapter (**1.2.1.5.**).

2. Materials

2.1. Chemicals without GAG

Table 2.1 General chemicals used for experiments.

Chemical	**Vendor**
Sigmacote	Sigma-Aldrich, Taufkirchen, Germany
Potassium hydroxide	Grüssing, Filsum, Germany
Ethanol	Chemsolute Th Geyer, Renningen, Germany
Methacrylic gelatine	Sigma-Aldrich, Taufkirchen, Germany
Dulbecco's phosphate buffered saline	ThermoFisher Scientific, Schwerte, Germany
Dulbecco's Phosphate Buffered Saline, without calcium chloride and magnesium chloride	Sigma-Aldrich, Taufkirchen, Germany
Ultrapure water	ThermoFisher Scientific, Schwerte, Germany
Lithium phenyl-2,4,6-trimethylbenzoylphosphinate	Sigma-Aldrich, Taufkirchen, Germany
Papain	Sigma-Aldrich, Taufkirchen, Germany
1,9-Dimethyl-Methylene Blue zinc chloride double salt	Sigma-Aldrich, Taufkirchen, Germany
Pierce BCA Protein Assay Kit	ThermoFisher Scientific, Schwerte, Germany
Acetylacetone	Carl Roth, Karlsruhe, Germany
p-Dimethylaminobenzaldehyde	Sigma-Aldrich, Taufkirchen, Germany
Hydrochloric acid	Bernd Kraft, now AnalytiChem, Duisburg, Germany
Direct Red	Sigma-Aldrich, Taufkirchen, Germany
Picric acid	Sigma-Aldrich, Taufkirchen, Germany
Toluidine Blue	Carl Roth, Karlsruhe, Germany
Sodium chloride	Grüssing, Filsum, Germany
Sodium hydroxide	Grüssing, Filsum, Germany
Bovine Serum Albumin	Sigma-Aldrich, Taufkirchen, Germany
Silica Gel orange/green, 2-5 mm, with indicator, pearls	Carl Roth, Karlsruhe, Germany

Carbon SCD030	Balzers Union, Balzers, Liechtenstein
Tween20	Carl Roth, Karlsruhe, Germany
Sulphuric acid	Carl Roth, Karlsruhe, Germany
Pierce TMB Substrate Kit	ThermoFisher Scientific, Schwerte, Germany
Glycin	Merck, Darmstadt, Germany
Sodium carbonate	Merck, Darmstadt, Germany
Acetic acid	Carl Roth, Karlsruhe, Germany
Collagen I, rat tail	ThermoFisher Scientific, Schwerte, Germany
Dulbecco's Modified Eagle`s Medium, high glucose, pyruvate	ThermoFisher Scientific, Schwerte, Germany
Collagenase from Clostridium histolyticum, sterile-filtered, Type I-S	Sigma-Aldrich, Taufkirchen, Germany
Disodium hydrogen phosphate	Sigma-Aldrich, Taufkirchen, Germany
Potassium dihydrogen phosphate	Sigma-Aldrich, Taufkirchen, Germany
Invitrogen ambion Ethylenediaminetetraacetic acid (EDTA) (0.5M), pH 8.0	ThermoFisher Scientific, Schwerte, Germany

2.2. Glycosaminoglycans

Table 2.2 Glycosaminoglycans used for this thesis.

GAG	**Abbreviation**	**Vendor**
Methacrylate hyaluronic acid	HA-MAC	Sigma-Aldrich, Taufkirchen, Germany
Sulphated and acrylated hyaluronan RK1810	sHA1-AC	Innovent e.V., Jena, Germany
sHA1-AC RK1824R		

2.2.1. Properties of the used glycosaminoglycans

The different glycosaminoglycans used in this study have each different chemical properties. Therefore, the molecular weight (MW) and the degree of substitution are listed in Table 2.3.

Table 2.3 Chemical properties of GAG used for the experiments including molecular weight and degree of substitution.

Abbreviation	**MW [kDa]**	**Degreee of substitution**
HA-MAC	20000-30000	20-50% methacrylate
sHA1-AC RK1810	15832	Degree of sulfation: 1.2 (C6'), degree of acrylation: 0.2
sHA1-AC RK1824R	14291	Degree of sulfation: 1.3 (C6'), degree of acrylation: 0.2

2.3. Bioactive proteins

Table 2.4 Bioactive proteins used in the experiments with catalogue and batch number.

Protein	**Abbreviation**	**Catalogue number**	**Batch number**	**Vendor**
Recombinant Human vascular endothelial growth factor 165 (VEGF-A)	VEGF-A	293-VE-050/CF	II6522011	R&D Systems, Minneapolis, USA
Recombinant Human tissue inhibitor of matrix metalloproteinase 3 (TIMP-3)	TIMP-3	973-TM-010	ETB1622021	R&D Systems, Minneapolis, USA

2.4. Assay kits

Table 2.5 Assay kits with catalogue and batch number.

Kit	Catalogue number	Batch number	Vendor
Human VEGF DuoSet ELISA, 15 plate	DY293B	P306591	R&D Systems, Minneapolis, USA
Human TIMP-3 DuoSet ELISA, 15 plate	DY973	P362950	R&D Systems, Minneapolis, USA
Matrix Metalloproteinase-9 (MMP-9) Fluorometric Drug Discovery Kit	BML-AK411	43LE40	Enzo Life Sciences, Lörrach, Germany
VEGF Bioassay	GA2001	See components	Promega Corporation, Madison, USA
Bio-Glo Luciferase Assay System	G720A	0000608090	
DMEM with 4.5 g/l Glucose, L-Glutamine, Sodium Pyruvate	J236A	0000540692	
Bio-Glo Luciferase Assay Buffer	G719A	0000588764	
KDR/NF AT-RE HEK293 cells	GA109A	0000536147	
Fetal Bovine Serum	J121A	/	

2.5. Consumables

Table 2.6 Consumables used to conduct the experiments.

Consumable	Vendor
Microtest Plate 96 Well,F; sterile	Sarstedt, Nümbrecht, Germany

Fisherbrand SureOne (10, 20, 300, 1000µl)	ThermoFisher Scientific, Schwerte, Germany
5ml Plastibrand	BRAND SCIENTIFIC, Wertheim, Germany
Combitips Plus (5ml, 10ml)	Eppendorf, Hamburg, Germany
Micro tube 1.5ml/2.0ml	Sarstedt, Nümbrecht, Germany
Falcon (15ml, 50ml)	Corning Science, New York, USA
Cover slips	Carl Roth, Karlsruhe, Germany
Cover glasses	R. Langenbrinck, Emmendingen, Germany
SuperFrost Plus Microscope Slides	R. Langenbrinck, Emmendingen, Germany
Conductive carbon adhesive tabs	Plano GmbH, Wetzlar, Germany
Zellkulturtestplatte 48	TPP Techno Plastic Products, Trasadingen, Switzerland
ELISA plate, High binding, F	Sarstedt, Nümbrecht, Germany

2.6. Instruments

Table 2.7 Instruments used for non-cell culture experiments.

Instrument	**Vendor**
Spark 20M plate reader	Tecan Group, Männedorf, Switzerland
TS basic	CellMedia, Elsteraue, Germany
Speed Vac Plus SC 110 A	ThermoFisher Scientific, Schwerte, Germany
Vortex-Genie 2	Scientific Industries, Bohemia, USA
Water-Jacketed Incubator 3250	Forma Scientific, Marietta USA
HeraTherm Oven	ThermoScientific, Schwerte, Germany
ALS 120-4	Kern & Sohn, Balingen, Germany
UV/LED Nail lamp WT60	CET Product Service, Ludwigsburg, Germany
HandyStep S	BRAND SCIENTIFIC, Wertheim, Germany
VaCo	ZIRBUS technology, Bad Grund, Germany
3 mm REF 49301	Kai Europe, Solingen, Germany
Clip & Close, set of 3 pieces (3.7 l, 2.3 l, 1.0 l)	EMSA, Emsdetten, Germany
FEI XL 30 ESEM FEG scanning electron microscope (SEM)	FEI, Hillsboro, OR, USA
Orbital shaker Typ KL 2	Edmund Bühler GmbH, Hechingen, Germany
Barstead GenPure Pro	Werner Reinstwassertechnik, Leverkusen, Germany
Digital-Mess-Schieber	Carl Roth, Karlsruhe, Germany

MicroTester	CellScale, Waterloo, Canada
Sony Cyber-shot digital still camera	Sony Europe, Berlin, Germany

2.7. Cells and cell culture

2.7.1. Cell culture medium

Table 2.8 Cell culture medium used for cell-culture experiments.

Medium/Serum	**Abbreviation**	**Vendor**
Dulbecco's Modified Eagle`s Medium, high glucose, pyruvate	DMEM	ThermoFisher Scientific, Schwerte, Germany

2.7.2. Cell culture consumables

Table 2.9 The cell culture consumables used to conduct the cell culture experiments.

Consumable	**Vendor**
Fisherbrand SureOne (10, 20, 300, 1000µl)	ThermoFisher Scientific, Schwerte, Germany
Micro tube 1.5ml/2.0ml	Sarstedt, Nümbrecht, Germany
Falcon (15ml, 50ml)	Corning Science, New York, USA
Sarstedt Serological Pipette 2.5, 5, 10, 25 ml	Sarstedt, Nümbrecht, Germany
Dulbecco's phosphate buffered saline	ThermoFisher Scientific, Schwerte, Germany
96 Well Optical Btm Pit Polymer Base White w/Lid Cell Culture Sterile PS	ThermoFisher Scientific, Schwerte, Germany

2.7.3. Cell culture appliances

Table 2.10 Cell culture instruments used to conduct cell culture experiments.

Instrument	**Vendor**
CO_2 incubator 9040-0131	Binder, Tuttlingen, Germany
JOUAN CR3i multifunction Centrifuge	ThermoFisher Scientific, Schwerte, Germany
Nikon Eclipse TS100	Nikon Instruments, Melville, USA
HERA safe cell culture bench	Kendro, Langenselbold, Germany
EXATHERM P5 electronic	JULABO, Seelbach, Germany

2.8. Computer programmes

Table 2.11 Computer programmes used for data analysis and figure creation.

Programmes	**Source**
GraphPad Prism 8	GraphPad Software, San Diego, USA
Microsoft Excel	Microsoft Corporation, Redmond, USA
Microsoft PowerPoint	

3. Methods

3.1. Hydrogel preparation

3.1.1. Siliconization of moulds

To reproducibly create equal sized hydrogels moulds are required. The use of round, siliconized, cover glasses was chosen as an easy and reproducible way to create equally shaped hydrogels. Sigmacote, a siliconizing agent, was used for siliconization. Before the siliconization, the glass surface was cleaned. The cleansing was carried out as described below (Table 3.1).

Table 3.1 Steps for cleaning of glass surface

1	H_2O bidist.	120s
2	0.1M KOH	120s
3	H_2O bidist.	120s
4	99% ethanol	120s
5	H_2O bidist.	120s

Each time the cover glasses were gently stirred. After the cleansing the cover glasses were dried for 3 hours at 60°C. For siliconization, the dried glasses were emersed into Sigmacote while being gently stirred for 60 s. Afterwards, the siliconized glasses were separated on a clean surface and then dried at 60°C for 3 h using a dry oven. The glasses were prepared in advance and stored in Petri dishes until use. The following types of glass (Table 3.2.) where used.

Table 3.2 Dimensions of glass slides used for hydrogel synthesis

Product name	Shape	Measurement
Cover slips	Round	Diameter 12 mm, thickness 0.13-0.16 mm
Cover glasses	Rectangular	24x60 mm, thickness 0.13-0.16 mm
SuperFrost Plus Microscope Slides	Rectangular	25x75mm, thickness 1.0 mm

3.1.2. Hydrogel preparation

3.1.2.1. Preparation GelMA-based hydrogels without GAG

The hydrogel preparation used 10% (w/v) of GelMA in PBS. To create 1 ml of a 10% GelMA solution 100 mg GelMA was dissolved in 1000 µl PBS at 37°C for at least 60 min. For GelMA

hydrogels, 190 µl of a 10% GelMA solution was mixed with 10 µl of PBS and 15 µl 1% (w/v) LAP solution in u.p. water for photo initiation of cross-linking. Until usage, the gel solution was protected from light with an aluminium foil cover around the tubes or falcons. The amount of gel solution is adequate for four hydrogels of each 50 µl. The hydrogels were prepared by pipetting 50 µl GelMA solution on siliconized microscope slides or rectangular cover glasses and putting round siliconized cover slips over the drops of solution. Afterwards, the hydrogels were cross-linked using UV light with a wavelength of 365 nm. The duration of UV exposure was limited to 60 s serving the purpose of avoiding cell and protein damage due to the UV light. Similarly, 20% GelMA hydrogels using 20% (w/v) GelMA solution (200 mg GelMA in 1 ml PBS) and 2.5% GelMA hydrogels using 2.5% (w/V) GelMA solution (25 mg GelMA in 1 ml PBS) were synthesized.

3.1.2.2. Preparation of GAG-functionalized GelMA-based hydrogels

The basic hydrogel configuration for gels containing GAG derivatives is the same as for hydrogels without GAG. All solutions were freshly prepared and were protected from light until usage. The preparation was conducted as described below:

(A) GelMA/HA-MAC gels: First, a 20% (w/v) HA-MAC solution was prepared by dissolving 200 mg HA-MAC in 1 ml of PBS at room temperature (RT) for 60 min. Afterwards, the GelMA/HA-MAC polymer mixture was prepared using 190 µl 10% GelMA solution (dissolved in PBS), 10 µl 20% HA-MAC solution and 15 µl 1% LAP.

(B) GelMA/sHA1-AC gels: A 20% (w/v) sHA1-AC-1 solution was prepared through the dissolving of 20 mg sHA1-AC in 100 µl PBS at RT for 60 min. For a GelMA/sHA1-AC polymer mixture, 190 µl 10% GelMA solution, 10 µl 20% sHA1-AC solution and 15 µl 1% LAP were mixed.

3.1.2.3. Gel production for growth factor binding and release study

GelMA, GelMA/HA-MAC and GelMA/sHA1-AC gels with a diameter of 3 mm were used for release studies with VEGF-A and TIMP-3. Here, gels prepared as described above, were freeze-dried between two siliconized cover slips (3.1.2.). A 3 mm biopsy punch was used for the creation of equal gels from the freeze-dried hydrogels.

3.2. Lyophilization and storage of hydrogels

3.2.1. Lyophilization

For some experiments it was necessary to freeze-dry the hydrogels. The hydrogels were stored at -20°C. After pre-freezing at -20°C the gels were freeze-dried as followed: the

temperature was lowered to -90°C and the systemic pressure was lowered to 0.08 mbar (8 Pa) using a lyophilization unit.

3.2.2. Storage

If the hydrogels needed to be prepared in advance or if they were stored for later analysis a method of conservation was necessary. If the hydrogels remained native (meaning hydrated), they were stored at -20°C. If the hydrogels were lyophilized in advance, they were stored in separate Falcons. These Falcons were stored in an air-tight box of which the bottom was covered in dry-pearls to avoid hygroscopic influence on the hydrogels. The dry-pearls were dehydrated as described following: they were dried at 120°C for 90 min using a dry-oven. After the 90 min, they were cooled down to RT (duration about 60 min) before the bottom of the air-tight box was covered with them.

3.3. Visualisation of hydrogel components

3.3.1. Sirius Red

Sirius Red is a dye for collagen staining and was used to stain for GelMA as a collagen derivative [73,136].

For the Sirius Red staining solution Direct Red dye was used as well as a saturated 1.3% solution of picric acid in water. 100 ml of solution was prepared using 100 mg of Direct Red and 100 ml of picric acid. For staining, 1 ml of solution was added to each gel. Following this step, the gels were incubated for 30 min at RT on a shaker protected from light. After incubation the gels were washed using 0.01 M HCl. The washing procedure was repeated until no staining solution was visible.

3.3.2. Toluidine Blue

Toluidine Blue was used to stain for sGAG [140]. For staining a solution of Toluidine Blue in 37% HCl and NaCl was used. Preparation of 100 ml staining solution: 1.666 ml 6 M HCl, 200 mg NaCl and 40 ml Toluidine Blue were mixed. The gels were stained using 1 ml of Toluidine Blue solution for each hydrogel and an incubation period of 4 h at RT using a shaker. After that the stained gels were washed using distilled water until the water was macroscopical free of staining solution.

3.3.3. Scanning electron microscopy

Scanning electron microscopy (SEM) was used to assess the microscopic surface of the hydrogels. The following types of hydrogels were scanned: GelMA, GelMA/HA-MAC and GelMA/sHA1-AC.

All gels were prepared as described previously. For SEM imaging the hydrogels were lyophilized as described above (**3.2.1.**). Following the procedure, the freeze-dried hydrogels were transferred to conductive carbon adhesive tabs. To reach conductivity, which is required for SEM, the hydrogels were sputtered with carbon. For analysis the samples were placed in a SEM under conditions of high vacuum at an acceleration voltage of 5 kV in secondary electrons mode.

The SEM images were taken by PD Dr. rer. nat. Wolfgang Metzger (Department of Trauma, Hand and Reconstructive Surgery, Saarland University).

3.4. Hydrogel characterization

3.4.1. GAG binding capacity of hydrogels

For analysing the chemical stability and release properties of the gels, the release of GAG and GelMA was measured over time. Each hydrogel was incubated in 1000 µl of PBS for 672 h at 37°C. At specific time points during the 672 h the supernatants were collected and stored at -20°C for further analysis. Samples were collected after 1 h, 24 h, 168 h, 336 h, 504 h and 672 h. To each gel 1000 µl PBS was added after sample collection and the incubation was resumed. At the end point every hydrogel was degraded using a 1 mg/ml papain solution over night at 60°C. After sample collection the samples for GAG analysis were concentrated using a SpeedVac, whereas the samples for GelMA determination were used unconcentrated. Following the restriction of the samples, the samples were dissolved using 150 µl or 200 µl u.p. water. This served the purpose to create a higher sample concentration and to increase the accuracy of measurements. Samples were analysed using appropriate assays, in this case DMMB assay, Pierce BCA assay and Hexosamine assay (**3.5.**).

3.4.2. Evaluation of hydrogel swelling

For this experiment siliconized 96 well-plates were used as a mould to obtain hydrogels (volume: 50 µl) of a different format which were required for the necessary measurements. The 96 well-plates were prepared as described in **3.1.1.**. The following hydrogel types were prepared as described before: GelMA, GelMA/HA-MAC and GelMA/sHA1-AC.

After crosslinking, the hydrogels were pre-frozen at -20°C and on the following day lyophilized (**3.2.1.**) in the mould as described. After freeze-drying the diameter and height of each gel was taken with a calliper and the hydrogels were weight. Following the initial measurements, the lyophilized gels were each re-hydrated in 1000 µl of PBS and incubated at 37°C. The measurement procedure was repeated after 1 h, 24 h after 96 h.

The swelling ratio as described by *Chang et al.* was used to characterize hydrogel swelling (for abbreviations see Table 3.3.) [16]:

$$SR = \frac{m_t - m_0}{m_0}$$

Table 3.3 Formula abbreviations for calculating the swelling ratio.

Abbreviation	Meaning
SR	Swelling ratio
m_t	Mass at specific time point
m_0	Mass of hydrogels at time point 0 h

3.4.3. Evaluation of hydrogel stiffness

GelMA, GelMA/HA-MAC and GelMA/sHA1-AC hydrogels with a volume of each 240 µl were prepared as described previously, using a siliconized 96 well-plate. After preparation, the hydrogels were lyophilized for transportation and storage. The measurements of the Young's modulus for each hydrogel were performed by Dr.-Ing. Poh Soo Lee (TU Dresden, Institute for Materials Science, Max-Bergmann Centre for Biomaterials).

The samples were rehydrated in tubes with a volume of 1 ml PBS each. For the rehydration process, the samples were placed on a shaker (100 rpm) for four hours at 27°C.

For mechanical testing, the samples were placed in a PBS bath at 26°C.

A cantilever with a diameter of 1.016 mm was used with the aim of achieving a deflection ratio between 0.55 and 0.7.

The cantilever used for this experiment consists of a round tungsten beam (diameter 1.016 mm, length 60 mm) with a Young's modulus of 411000 MPa and a quadratic stainless-steel plate (4 mm x 4 mm) (Figure 3.1).

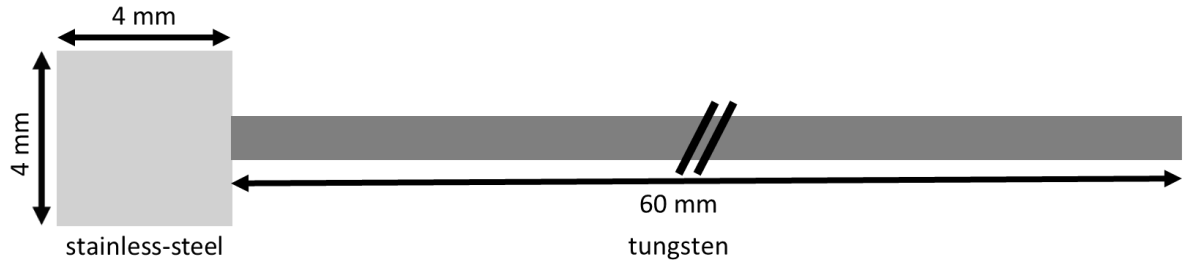

Figure 3.1 Sketch of a cantilever. The cantilever consists of a 4 mm x 4 mm stainless-steel plate and a 60 mm long, round tungsten beam.

The following compression loading programme was used for the experiment: type z-compression, ramp; amplitude 50%; cycles 2.

The data was used to calculate Stress [Pa] and Strain [Arbitrary Units] (see Table 3.4 for abbreviations used in the formulas).

$$Stress = \frac{F}{A}$$

$$Strain = \frac{d}{he}$$

Table 3.4 Formula abbreviations for calculating hydrogel stiffness.

Abbreviation	Meaning
F	Force
A	Area
d	Tip displacement
he	Height of hydrogels

These calculated values were used to calculate the Young's modulus:

$$Young's\ modulus = \frac{Stress}{Strain}$$

Only the first slope is considered, in this case up to a Strain of 0.15 and only the first measurement was used to calculate the Young's modulus.

3.5. Quantification of hydrogel components

For the quantification of GAG release, GAG residuals in gel and gel degradation different photometric assays were used. For analysis DMMB assay, Pierce BCA assay and Hexosamine assay were used as described below. All assays used for the quantification of hydrogel components are listed below (Table 3.5).

Table 3.5 Assays for analysis of hydrogel components.

GAG	Purpose	Assay
HA-MAC	Quantifying of release	Hexosamine
GelMA	Measuring gel degradation	BCA
sHA1-AC	Quantifying release	DMMB

3.5.1. DMMB assay

The 1,9-Dimethyl-Methylene Blue (DMMB) assay was used to quantify the release of sHA1-AC (**3.6.1.**). 1 l of DMMB reagent was prepared using 16 mg DMMB zinc chloride double salt

which was diluted in 1 l of distilled water containing 95 ml of 0.1 M acetic acid, 3.04 g glycine and 1.6 g of NaCl. The protocol was modified from *Coulson-Thomas et al.* [20]. 20 µl of each sample was pipetted in a 96 well-plate and to each sample 200 µl of DMMB reagent was added. Then the absorbance at 595 nm was measured using a plate reader, measuring the free DMMB. Every microplate contained a set of sHA1-AC standard dilutions. The standard dilutions were prepared using sHA1-AC and PBS as dissolving agent. The sHA1-AC standard dilutions were 0 µg/ml, 0.5 µg/ml, 1.0 µg/ml, 2.5 µg/ml, 5.0 µg/ml, 10.0 µg/ml, 12.5 µg/ml, 25.0 µg/ml and 50.0 µg/ml. The linear regression was determined using GraphPad Prism.

3.5.2. BCA assay

For the quantification of GelMA (**3.4.1.**) a Pierce BCA Protein Assay Kit was used. 25 µl per sample was pipetted into a 96 well-plate and 200 µl of BCA working reagent was added to each well. The working reagent was prepared as following: (standards + unknowns) x replicates x 200 µl = total volume, ratio reagent A:B = 50:1. Following this step, the samples were incubated at 37°C for 30 min and then the absorbance was measured at 562 nm using a plate reader. The standard GelMA dilutions were prepared using GelMA and PBS as a dissolving agent. They were stored at -20°C until use. As standard concentration 0 µg/ml, 5 µg/ml, 25 µg/ml, 125 µg/ml, 250 µg/ml, 500 µg/ml, 750 µg/ml, 1000 µg/ml, 1500 µg/ml and 2000 µg/ml GelMA were used. Beforehand, standard GelMA solutions were compared to the recommended standard BSA dilutions (BSA is part of the kit) with two replicates each. The linear regression was determined using GraphPad Prism.

3.5.3. Hexosamine assay

The Hexosamine assay was used to quantify the released HA-MAC (**3.4.1.**) and it consists of three steps which are described in the following section:

I) Sample hydrolysis: 100 µl of each sample was diluted with 100 µl PBS each in a tube. Following the dilutions 200 µl of 12 M HCl was added to every sample dilution. The next step was to incubate the samples for 6 h at 98°C and 300 rpm using a thermo mixer.

II) Drying and neutralisation: Following step I) the samples were cooled (on ice) and the lids of the sample tubes were opened. The samples were placed in a desiccator which was filled prior to this step with NaOH pellets. The sample-filled desiccator was incubated at 37°C for 5-7 days until all samples were sufficiently dried.

III) Photometric measurement: on the day of measurement acetylacetone-reagent and Ehrlich-reagent were freshly prepared:

- Acetylacetone-reagent: to a 4% acetylacetone dilution sodium carbonate and bi-distilled water was added. For 10 ml 1.324 g Na_2CO_3 and 400 µl acetylacetone were

mixed in a 10 ml-volumetric flask and bi-distilled water was added up to the 10 ml mark.

- Ehrlich-reagent: the reagent was prepared using p-dimethylaminobenzaldehyde (DMAB), 6M HCl and 95% ethanol. For 10 ml 0.266 g DMAB was mixed with 5 ml 6 M HCl and 5 ml 95% ethanol.

After the preparation of the different reagents, 125 µl bi-distilled water was added to each of the dried samples. Following the rehydration, 250 µl of acetylacetone-reagent was added to each sample and the samples were mixed. Next the samples were incubated for one hour at 98°C and 300 rpm using a thermo mixer. After the previous step, 1.25 ml 95% ethanol was pipetted in a number (equal to sample number) of 2 ml tubes and 300 µl of cooled sample preparation was added to each tube (one sample per tube). The next step was to pipet 250 µl Ehrlich-reagent to each sample, stir the samples and incubate them at RT for 1 h. Following the incubation period 200 µl of each sample was pipetted in a 96 well-plate and the absorption at 540 nm was measured using a Spark 20M plate reader.

A standard dilution scheme was prepared containing the following HA-MAC dilutions: 0 µg/ml, 1.0 µg/ml, 2.5 µg/ml, 5.0 µg/ml, 10.0 µg/ml, 20.0 µg/ml, 40.0 µg/ml, 50.0 µg/ml, 100.0 µg/ml. The standard dilutions were prepared like the samples with one exception: of each standard dilution an undiluted volume of 200 µl was used in step I) and not a diluted sample volume of 100 µl sample plus 100 µl PBS. The sample was diluted to reduce the needed volume and to make other assays possible.

3.6. VEGF-A and TIMP-3 release and binding capacity of hydrogels

3.6.1. Experimental setup

The binding and release profiles of GelMA, GelMA/HA-MAC and GelMA/sHA1-AC for VEGF-A and TIMP-3 as well as a combination of VEGF-A and TIMP-3 were determined. The solution of VEGF-A, TIMP-3 and VEGF-A + TIMP-3 were prepared as following:

I) VEGF-A (500 ng/ml): 1800 µl 1 µg/ml VEGF-A-solution in 1% BSA/PBS + 1800 µl 1% BSA/DPBS

II) TIMP-3 (57.397 ng/ml): 1800 µl 114.794ng/ml TIMP-3-solution in 1% BSA/PBS + 1800 µl 1% BSA/PBS

III) VEGF-A (500 ng/ml) + TIMP-3 (57.397 ng/ml): 1800 µl 1 µg/ml VEGF-A-solution in 1% BSA/PBS + 1800 µl 114.794ng/ml TIMP-3-solution in 1% BSA/PBS

To each gel, 400 µl of either VEGF-A, TIMP-3 or VEGF-A + TIMP-3 solution was added. This step was followed by an overnight incubation at 37°C. After the incubation period the medium was taken out, collected and stored at -20°C. This was used to determine the amount of

absorbed protein per gel at time point 0 h. Afterwards, 400 µl 1% BSA/PBS was added to each gel for growth factor binding and the gels were incubated at 37°C. At the following time points the medium of every hydrogel was changed, collected and stored at -20°C to measure the proteins: 1 h, 24 h, 168 h, 336 h and 504 h.

3.6.2. VEGF-A-ELISA

A specific VEGF-A sandwich ELISA was used to quantify the amount of non-gel bound VEGF-A in solution. The 1 µg/ml VEGF-A capture antibody solution was prepared in PBS on ice. The wells of an ELISA-plate were coated by adding 100 µl of VEGF-A capture antibody solution per well and incubating the plate overnight at RT. The following day, the residual solution of each well was aspirated and a total of three wash steps followed:

I) 400 µl PBS + 0.05% Tween20 (preparation for 100 ml: 50 µl Tween20 + 99.95 µl PBS) was added to each coated well.

II) Each well was aspirated and step I) was repeated.

After three wash steps the plate was cleared of residual fluid. The next step was to add 300 µl of a 1% BSA in PBS solution (preparation for 10 ml: 100 mg BSA + 10 ml PBS) to each well for blocking. This was incubated for 1 h at RT. After the incubation period, the washing step previously described was repeated. Next 100 µl of adequately diluted sample solution and VEGF-A standard protein (both in 1% BSA in PBS) solution were added to the respective wells. The VEGF-A standard protein solution of 120 ng/ml VEGF-A was prepared with 1% BSA in PBS. The following dilutions of the 120 ng/ml VEGF-A standard protein solution were used: 0 pg/ml, 31.3 pg/ml, 62.5 pg/ml, 125 pg/ml, 250 pg/ml, 500 pg/ml, 1000 pg/ml, 2000 pg/ml. The samples and standard dilutions were allowed to bind to the capture antibody for 90-120 min at RT. Following the incubation, the wash steps were repeated. After that the VEGF-A detection antibody was prepared as a 100 ng/ml solution in PBS and 100 µl of the solution was added to each well. Then, the plate was incubated for 90-120 min at RT. This was again followed by the wash procedure. Following the wash procedure, Streptavidin-Horse radish peroxidase (HRP) solution was prepared as a 1:40 dilution in 1% BSA/PBS (initial concentration not specified by the manufacturer). 100 µl of Streptavidin-HRP were added to each well. This was incubated in the dark at RT for 20 min. Then again, the ELISA-plate was washed as described and to each well 100 µl of substrate solution consisting of hydrogen peroxide and tetramethylbenzidine (prepared as stated in the instructions, 1:1). This was incubated in the dark until the colour was sufficiently developed. The time was taken, and the reaction was stopped using 50 µl per well 1 M sulphuric acid. The plate's absorbance was measured using a plate reader at 450 nm and 570 nm for optical imperfection correction of the used plate.

3.6.3. TIMP-3-ELISA

The TIMP-3-ELISA measurements were performed by M.Sc. Charlotte Berhorst according to the manufacturer's instructions for Human TIMP-3 DuoSet ELISA.

A TIMP-3 specific sandwich ELISA was used to quantify the amount of non-gel bound TIMP-3 in solution. The 2 µg/ml TIMP-3 capture antibody solution was prepared in PBS on ice. The wells of an ELISA-plate were coated by adding 100 µl of TIMP-3 capture antibody solution per well and incubating the plate overnight at RT. On the following day, the residual solution of each well was aspirated and a three wash steps followed:

I) 400 µl PBS + 0.05% Tween20 (preparation for 100 ml: 50 µl Tween20 + 99.95 µl PBS) was added to each coated well.
II) Each well was aspirated and step I) was repeated.

After three wash steps the plate was cleared of residual fluid. The next step was to add 300 µl of a 1% BSA in PBS solution (preparation for 10 ml: 100 mg BSA + 10 ml PBS) to each well for blocking and incubating the plate for 1 h at RT. After the incubation period, the washing step previously described was repeated. Next 100 µl of adequately diluted sample solution and TIMP-3 standard protein (both in 1% BSA in PBS) solution were added to the respective wells. The TIMP-3 standard protein solution of 130 ng/ml TIMP-3 was prepared with 1% BSA in PBS. The following dilutions of the 130 ng/ml TIMP-3 standard protein solution were used: 0 pg/ml, 62,5 pg/ml, 125 pg/ml, 250 pg/ml, 500 pg/ml, 1000 pg/ml, 2000 pg/ml, 4000 pg/ml. The samples and standard dilutions were allowed to bind to the capture antibody for 120 min at RT. After the incubation period, the wash steps were repeated. In a next step, the TIMP-3 detection antibody was prepared as a 2 µg/ml solution in PBS and 100 µl of the solution was added to each well. Then, the plate was incubated for 120 min at RT. This was again followed by the wash procedure. Following the wash procedure, Streptavidin-HRP solution was prepared as a 1:40 dilution in 1% BSA/PBS (initial concentration not specified by the manufacturer). 100 µl were added to each well. This was incubated in the dark at RT for 20 min. Then again, the ELISA-plate was washed as described and to each well 100 µl of substrate solution consisting of hydrogen peroxide and tetramethylbenzidine (prepared as stated in the instructions, 1:1). This was incubated in the dark until the colour was sufficiently developed. The time was taken, and the reaction was stopped using 50 µl per well 1 M sulphuric acid. The plate’s absorbance was measured using a plate reader at 450 nm and 570 nm for optical imperfection correction of the used plate.

3.7. Evaluation of VEGF-A and TIMP-3 bioactivity

3.7.1. VEGF-A bioactivity

To determine the bioactivity of released VEGF-A, a commercial assay using luminescent KDR/NF AT-RE HEK293 cells were used. KDR/NF AT-RE HEK293 cells express VEGFR-2 which interacts with VEGF-A and activates a luciferase. The increase in luciferase activity is directly dependent on the increase in VEGF-A concentration [143,149].

With the data gained from the VEGF-A release experiment (**3.6.**), the average of VEGF-A per hydrogel was extrapolated as well as the expected release. In a next step, the experimental setup was adjusted to accommodate for a VEGF-A release within the VEGF-A bioassay's detection range (extrapolated from user manual, between 0.1 ng/ml – 100 ng/ml VEGF-A). TIMP-3 concentration was calculated to be equimolar to the used VEGF-A concentrations. Lyophilized, punched GelMA, GelMA/HA-MAC, GelMA/sHA1-AC hydrogels (**3.2.1.**) were loaded with each 200 µl of the following concentrations of bioactive proteins.

1) 455 ng/ml VEGF-A (in DMEM)
2) 260.7 ng/ml TIMP-3 (in DMEM)
3) 455 ng/ml VEGF-A + 260.7 ng/ml TIMP-3 (in DMEM)

Next, the hydrogels were incubated overnight at 37°C. After the incubation, supernatants were removed and 200 µl of DMEM was added to each tube.

The sample collection was repeated after 24, 72 and 168 h. Samples were stored at -20°C until the time of the VEGF-A bioassay.

The following steps were conducted under sterile conditions. The VEGF-A bioassay was performed by Jun.-Prof. Dr. rer. nat. Sandra Rother.

In a first step, the reagents (Bio-Glo reagent and 2% (v/v) FCS/DMEM) for the VEGF-A bioassay were prepared according to the manufacturer's instructions.

The following standards were prepared:

1) VEGF-A: 0 ng/ml, 0.781 ng/ml, 1.563 ng/ml, 3.125 ng/ml, 6.25 ng/ml, 12.5 ng/ml, 25 ng/ml, 50 ng/ml, 100 ng/ml.
2) TIMP-3 (only): 100 ng/ml and 6.25 ng/ml.
3) TIMP-3 + 60 ng/ml VEGF-A: 0 ng/ml, 0.781 ng/ml, 1.563 ng/ml, 3.125 ng/ml, 6.25 ng/ml, 12.5 ng/ml, 25 ng/ml, 50 ng/ml, 100 ng/ml of TIMP-3.

Two white 96 well-plates were prepared with the KDR/NF AT-RE HEK293 cells as instructed by the manufacturer. Dilution of 0.4 ml of provided cell suspension in 4.6 ml of medium

(2% FCS/DMEM) leading to a concentration of 40000 cells per 25 µl and therefore equalling 40000 cells per well.

The samples were added to the cells in the following manner I) VEGF-A and VEGF-A + TIMP-3: 25 µl cell suspension + 50 µl sample and II) TIMP-3: 25 µl cell suspension + 25 µl sample + 25 µl 60 ng/ml VEGF-A

Control 1) 25 µl cell suspension + 50 µl medium (+ 2% FCS) and control 2) 25 µl cell suspension + 25 µl medium (+ 2% FCS) + 25 µl medium (without 2% FCS)

For calibration 25 µl cell suspension + 25 µl 20 ng/ml VEGF-A + 25 µl medium per well was used.

Following the preparation, the cells were incubated at 37°C, 5% CO_2 for 5 h and 45 min.

The following steps were performed under non-sterile conditions.

Following the incubation period, the plates were equilibrated to room temperature for 15 minutes and to each well 50 µl of Bio-Glo reagent was added.

After an incubation for 5 min at room temperature, luminescence was measured with an integration time of 1.0 s per well using a plate reader.

The data was analysed in relation to the bioactivity of the 20 ng/ml VEGF-A calibration.

3.7.2. TIMP-3 bioactivity and IC_{50}

To determine the bioactivity of TIMP-3, an MMP-9 assay was used. MMP-9 uses a quenched substrate which is fluorescent after proteolysis. Therefore, the fluorescence is in proportion to the activity of MMP-9 [58].

Using the data gained from TIMP-3 release experiments (**3.6.**), the average uptake of TIMP-3 per gel was calculated as well as the expected release of TIMP-3. Following these calculations, the necessary volume for a release of TIMP-3 that is within the detection range (55 ng/ml – 100 ng/ml of TIMP-3) of the MMP-9 assay was determined. Lyophilized 50 µl GelMA, GelMA/HA-MAC and GelMA/sHA1-AC hydrogels (**3.2.1.**) were loaded with 400 µl of 500 ng/ml TIMP-3 solution in MMP-9 assay buffer (50 mM HEPES, 10 mM CaCl2, 0.05% Brij-35, pH 7.5) and incubated at 37°C overnight. The next day, supernatants were collected and 400 µl of assay buffer was added to each hydrogel and incubation at 37°C was continued. Samples were collected after 24, 168 and 336 h and were stored at -20°C.

The MMP-9 assay was prepared according to the manufacturer's instructions. A positive control (without inhibitor) and a negative control with 1.3 µM *N*-Isobutyl-*N*-(4-methoxyphenylsulfonyl)glycyl hydroxamic acid (NNGH, molecular weight 316.4 Da), a broad

spectrum MMP inhibitor, were prepared as instructed [3,163]. 70 µl of TIMP-3 samples (supernatants of the release assay) were added to the assay plate. To each well, 20 µl 0.134 U/µl of MMP-9's catalytic domain was added and incubated at 37°C according to protocol. In the next step, 10 µl of 40 µM substrate solution (OmniMMP^{TM} fluorogenic substrate peptide, molecular weight of 1093.2 Da) were added and the fluorescence was measured at excitation 328 nm and emission 420 nm every 45 s for 10 min using a Tecan plate reader.

The data was used to plot a graph of relative fluorescence units against time and to determine the linear range of the graph. Within the linear range, the slope was determined, and the slope of the positive control was set to equal 100%. The slope of every other replicate was set in relation to the positive control which resulted in the percentage of remaining MMP-9 activity compared to the positive control.

The IC_{50} of TIMP-3 for MMP-9 was determined using the MMP-9 assay as described above with a minor variation. Instead of release samples or a standard inhibitor, standard concentrations of TIMP-3 were used to inhibit MMP-9 and determine the IC_{50} of TIMP-3. The following concentrations of TIMP-3 were used: 825 ng/ml (37.5 nM), 550 ng/ml (25 nM), 220 ng/ml (10 nM), 110 ng/ml (5 nM), 66 ng/ml (3 nM), 55 ng/ml (2.5 nM), 5.5 ng/ml (0.25 nM) and 0 ng/ml (0 nM).

The MMP-9 activity was determined as described above and was blotted against the logarithmic concentrations of TIMP-3. For IC_{50}-determination, a non-linear fit model was used (log(inhibitor) vs. response -- Variable slope (four parameters), GraphPad Prism).

3.7.2.1. Matrix degradation assay

For the matrix degradation assay, a collagen coating was degraded using collagenase and TIMP-3 samples (**3.7.2.**) were used to inhibit the activity of collagenase. Sirius Red was used to stain the remaining collagen and afterwards the dye was washed out and the specific absorption of Sirius Red was used to quantify the remaining collagen [22,73].

48 well-plates were coated with collagen type I. For this 10 ml of 2 mg/ml collagen solution in 10 mM acetic acid was mixed on ice with 10 ml of a 60 mM phosphate buffer (50.15 mM Na_2HPO_4, 11.17 mM KH_2PO_4, pH 7.4), creating a 1 mg/ml collagen working solution. 200 µl of the collagen working solution was added to each well and then incubated at 37°C for 120 min for *in vitro* fibrillogenesis.

Afterwards, the coatings were dried, two times washed with water and then again dried.

To evaluate the influence of TIMP-3 on matrix degradation, 100 µl of released TIMP-3 (**3.7.2.**) for the following time points (24 and 168 h) was added each to one well on each plate and then

incubated at 37°C for 30 min. The addition of 100 µl of PBS instead of a TIMP-3 sample served as control.

Following the incubation period, 100 µl of 125 µg/ml collagenase in PBS which was warmed up to 37°C beforehand, was added to each well and incubated for 20 min for the 24 h samples and 60 min for the 168 h samples.

After the incubation period, the reaction was stopped using 400 µl of 0.2 M EDTA per well and the reaction supernatants were removed.

In a next step, the residual collagen coating was stained for 15 min using Sirius Red staining solution (**3.3.1.**) and afterwards, the coatings were washed using 0.01 M HCl until the staining was stable. In a next step, 300 µl 0.1 M NaOH was used to remove the Sirius Red staining from the collagen coatings and the supernatants were collected.

In a last step, the collected supernatants were added to a 96 well-plate and their absorption was measured at 540 nm using a Tecan plate reader.

3.8. Statistical analysis

For statistical analysis the software GraphPad Prism 8 (GraphPad Software, San Diego, USA) as well as Microsoft Excel (365 and LTSC Professional Plus licence) (Microsoft Corporation, Redmond, USA) were used.

For statistical analysis, the following tests were used:

- For tests with more than two groups and more than one time point of measurement: two-way ANOVA with Tukey's multiple comparisons test.
- For tests with more than two groups and one time point of measurement: one-way ANOVA with Tukey's multiple comparisons test.

The following representation was used to mark p-values in figures:

- * = $p<0.33$
- ** = $p<0.02$
- *** = $p<0.01$

The number of samples, if not specified otherwise, is three and the error bars represent the standard deviation.

4. Results

4.1. GAG-functionalization of GelMA hydrogels

First, a protocol for the preparation of newly developed, GAG-functionalized GelMA-based hydrogels as possible drug-releasing wound dressings was developed (Figure 4.1). To allow photopolymerization, photocrosslinkable HA and sHA derivatives were used. The approach of combining GelMA with different derivates of hyaluronan for hydrogel synthesis is depicted in Figure 4.1. Hydrogels with 2.5% GelMA were rather unstable and were puffy after lyophilization whereas 20% GelMA resulted in rigid hydrogels (Figure 4.2). Since the use of 10 % GelMA within the hydrogels resulted in form stable support-free hydrogels (Figure 4.2), this concentration was selected for all further hydrogel preparations.

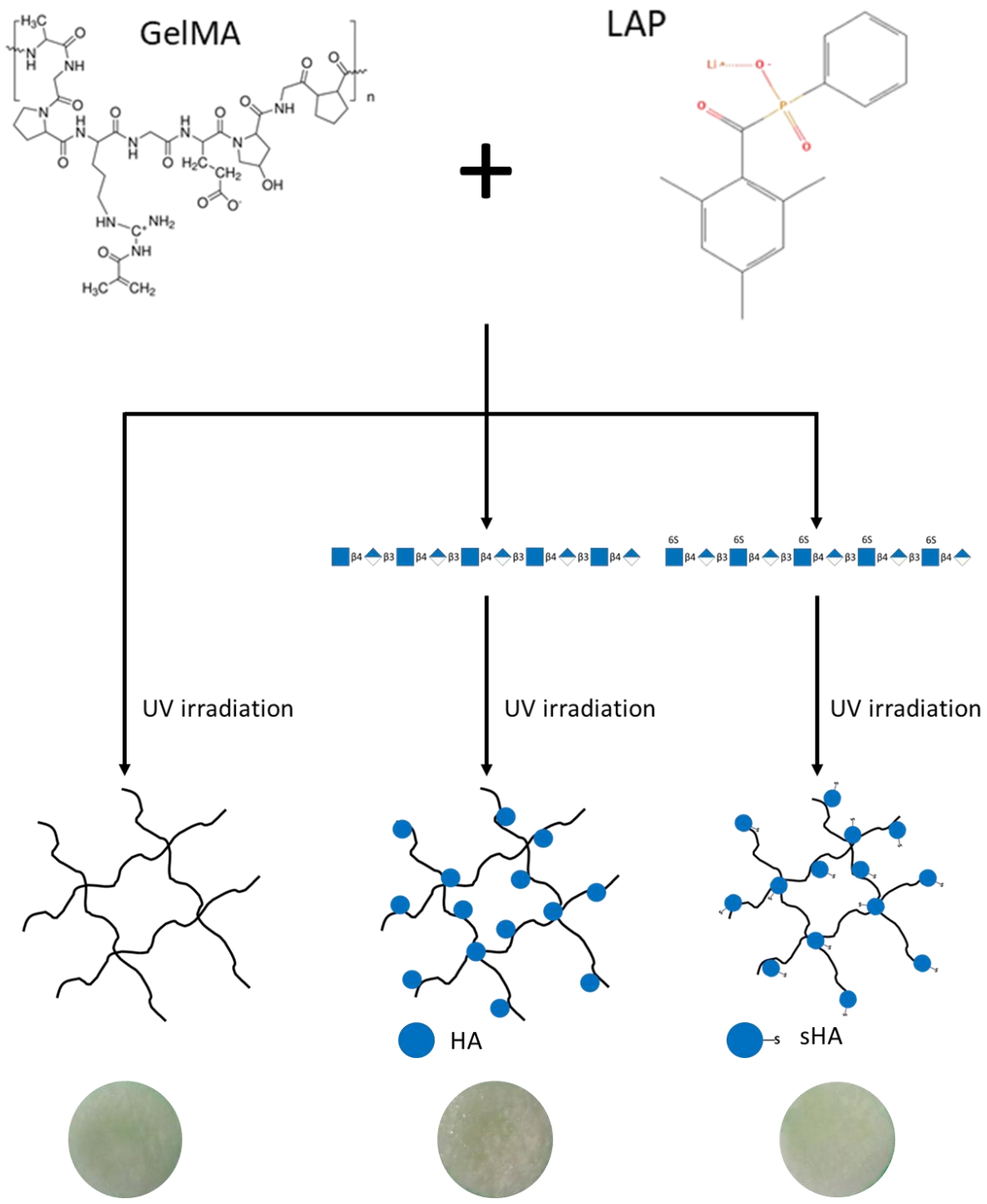

Figure 4.1 Simplified schematic explaining synthesis of GelMA-based hydrogels.

Figure 4.2 Lyophilized GelMA hydrogels of different concentrations. Concentrations of 2.5%, 10% and 20% GelMA are depicted.

Lyophilized hydrogels were stained using Sirius Red for collagen-derived molecules as well as Toluidine Blue for sHA. The stained hydrogels were visually examined for a homogenous distribution of the different components. As the Sirius Red shows, there is a homogenous distribution of GelMA within the different hydrogels (Figure 4.3). The Toluidine Blue staining shows that only GelMA/sHA1-AC hydrogels contain sGAG, in this case sHA1-AC. The sHA1-AC distribution appears to be homogenous (Figure 4.3). To summarize, the developed fabrication method for GelMA hydrogels is suitable for producing homogenous hydrogels.

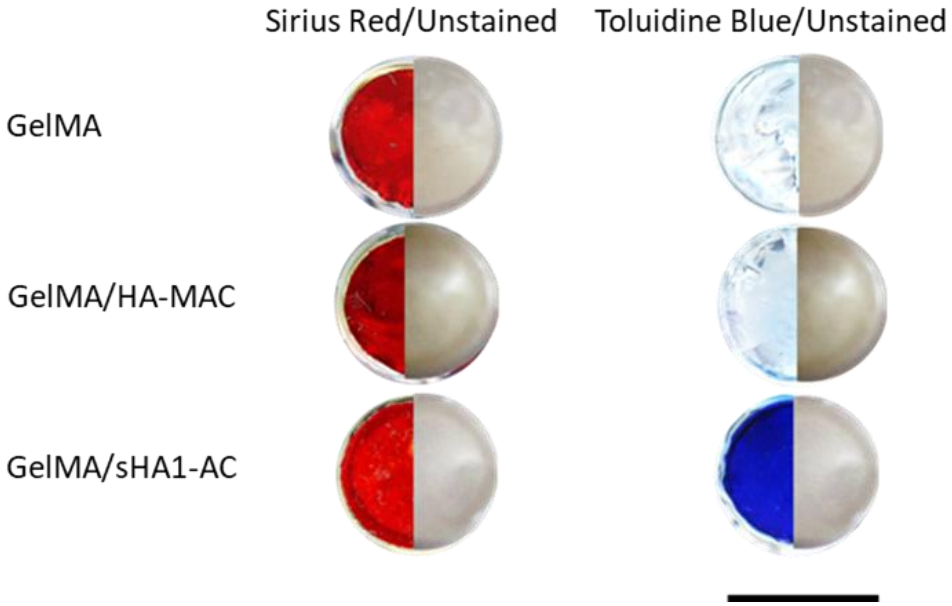

Figure 4.3 GelMA and sHA1 distribution in the hydrogels. GelMA, GelMA/HA-MAC and GelMA/sHA1-AC hydrogels are shown both unstained and stained with Sirius Red or Toluidine Blue. Scale bar 12 mm.

4.2. Characterization of GAG-functionalized GelMA hydrogels

The microstructure of the developed hydrogels was analysed using SEM imaging (Figure 4.4). GelMA hydrogels show a heterogeneous surface structure with many knob-like structures (Figure 4.4.A). However, the majority appears rather large in comparison to similar structures

on the surface of the GelMA/HA-MAC hydrogel (Figure 4.4.B). On the other hand, the GelMA/sHA1-AC hydrogel shows a different surface structure: its surface is porous and with a net-like structure. The pore size varies, some pores show a diameter between 50 – 75 µm whereas other pores have a diameter that is less than 10 µm. Apparently, there is a second layer of porous structure below the surface which is visible through the larger pores (Figure 4.4.C).

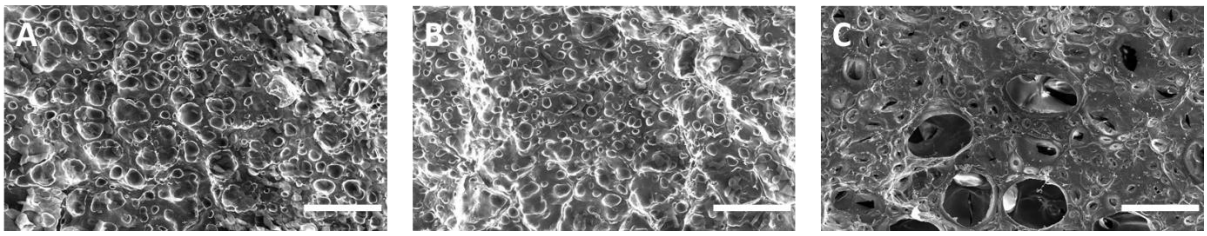

Figure 4.4 Microstructure of lyophilized GelMA, GelMA/HA-MAC and GelMA/sHA1-AC hydrogels. A: GelMA hydrogel. B: GelMA/HA-MAC hydrogel. C: GelMA/sHA1-AC. Scale bar: 100 µm. Images were taken by PD Dr. rer. nat. Wolfgang Metzger.

Additionally, the water binding capacity of the different hydrogels as well as their capability to swell was assessed. This is of particular importance because every wound dressing is exposed to moisture as well as different body fluids. Over the course of 96 h, all hydrogels increased their mass about 10 times equalling the quick absorption of an average of 47.3 mg (± 8.6%) of water per hydrogel. However, the hydrogels' swelling ratio of 7.5 (± 0.8%) only increased 1.2 times to an average of 9.1 (± 1.8%). Statistical testing did not reveal a significant difference in the swelling behaviour of the different hydrogels (Figure 4.5).

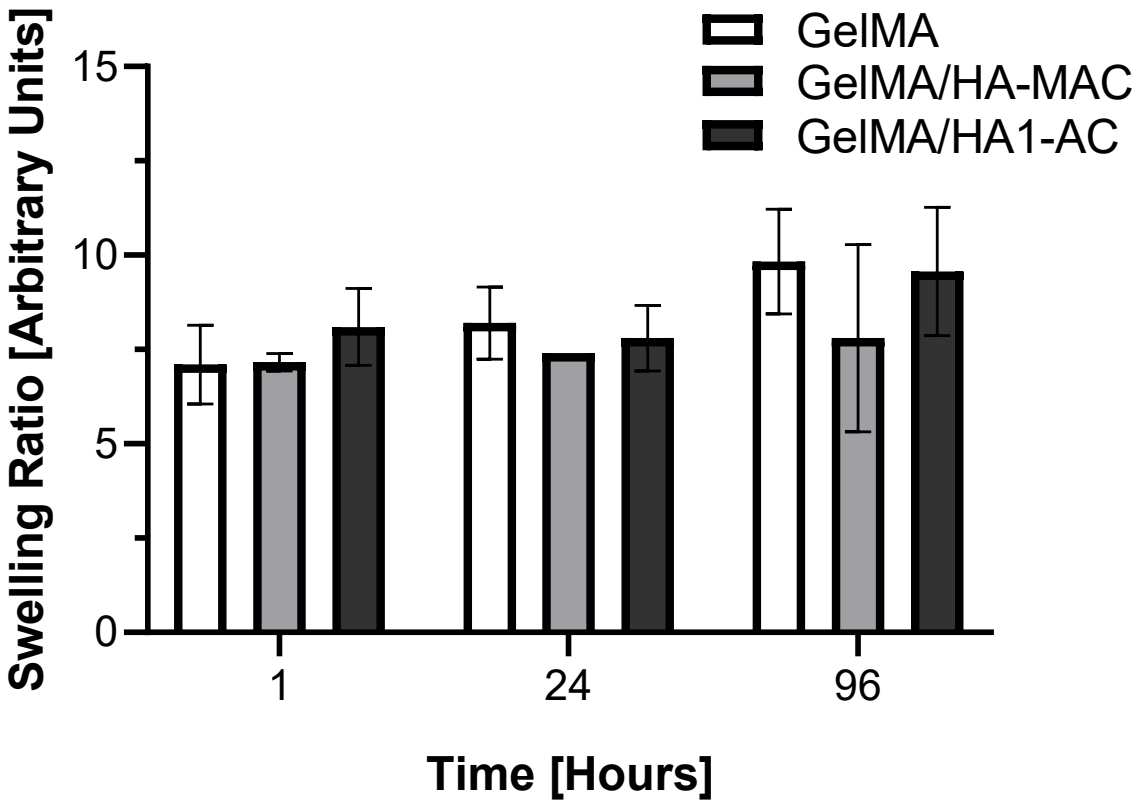

Figure 4.5 The swelling ratio of GelMA, GelMA/HA-MAC and GelMA/sHA1-AC hydrogels.

The stiffness of GelMA, GelMA/HA-MAC and GelMA/sHA1-AC hydrogels was evaluated using Young's modulus measurements (Figure 4.6). The Young's modulus of GelMA hydrogels (13.3 kPa ± 3.1%) was significantly less than the Young's modulus of GelMA/sHA1-AC hydrogels (95.0 kPa ± 18.9%). There was no significant difference in the Young's modulus between GelMA and GelMA/HA-MAC hydrogels (55.0 kPa ± 27.2%) as well as GelMA/HA-MAC and GelMA/sHA1-AC hydrogels (Figure 4.6).

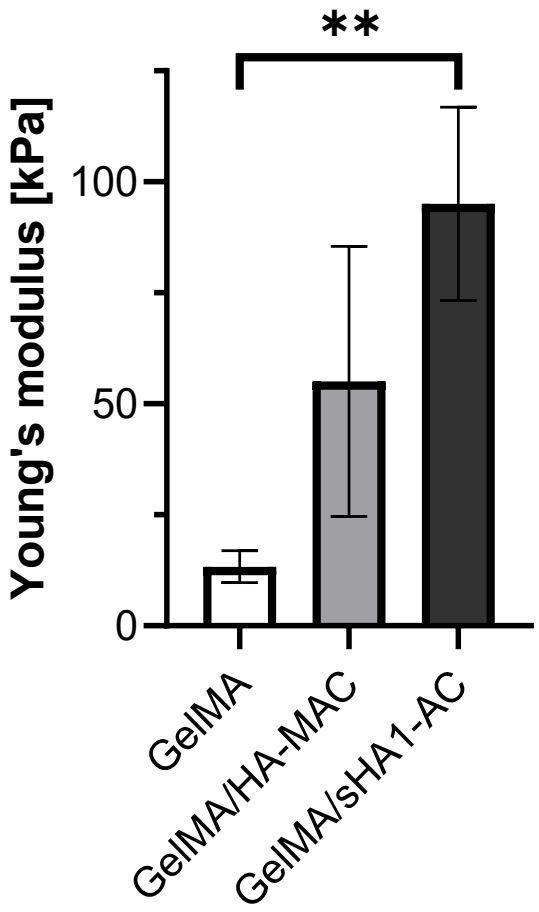

Figure 4.6 Young's modulus of GelMA-based hydrogels. GelMA (n=4), GelMA/HA-MAC (n=5), GelMA/sHA1-AC (n=4). Measurements were performed by Dr.-Ing. Poh Soo Lee.

The stability of the different hydrogels was analysed using the cumulative concentration of the release of GelMA and GAG over a period of 672 h (Figure 4.7). The hydrogels were incubated in PBS at 37°C and samples were collected at specific time points.

After 24 h of incubation, GelMA/sHA1-AC hydrogels released significantly less GelMA than GelMA or GelMA/HA-MAC hydrogels for the duration of the experiment (Figure 4.7.A). GelMA hydrogels released an average of 70.0% (± 8.5%), GelMA/HA-MAC hydrogels released 68.0% (± 8.8%) and GelMA/sHA1-AC hydrogels only released 18.5% (± 0.9%) of their initial amount of GelMA which is significantly less than the other two groups.

The release of HA-MAC and sHA1-AC out of the respective hydrogels was similar for the first 24 h and began to differ after 168 h leading to a constantly increasing cumulative release of HA-MAC whereas the cumulative sHA1-AC release remained on a constant level (Figure 4.7.B). The release of HA-MAC out of GelMA/HA-MAC hydrogels appeared to be more

heterogenous and scattered leading to an increased standard deviation whereas the release of sHA1-AC appeared to be more homogenous (Figure 4.7.B).

Over the course of 672 h, GelMA/HA-MAC hydrogels released an average of 60.3% (± 4.5%) of HA-MAC whereas GelMA/sHA1-AC hydrogels released an average of 70.0% (± 2.7%) of the initial sHA1-AC incorporated in the hydrogel. Both GelMA/HA-MAC and GelMA/sHA1-AC hydrogels showed no significant difference in their GAG release when compared to each other (Figure 4.7.B).

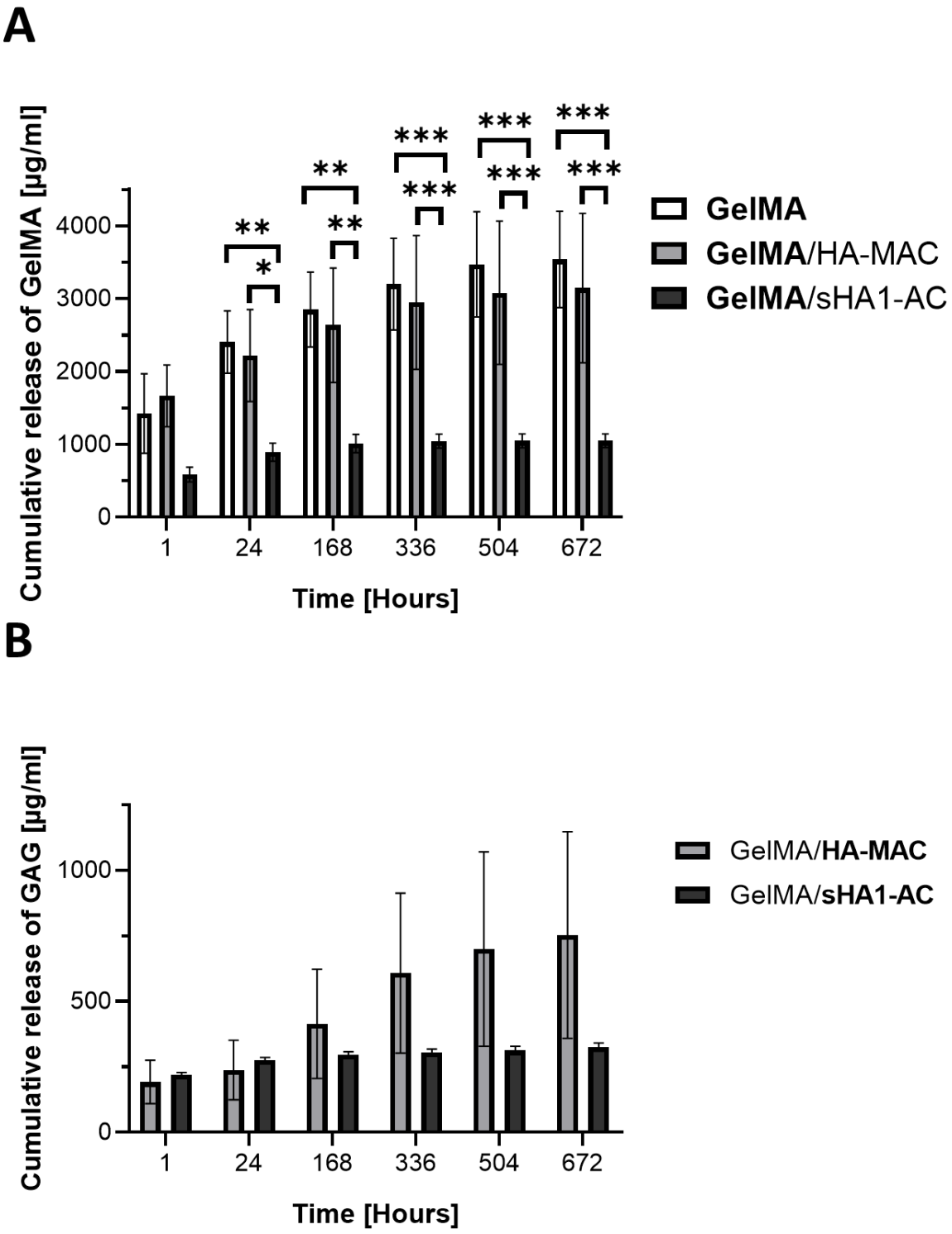

Figure 4.7 Evaluation of hydrogel stability. A: Cumulative GelMA release over 672 h. B: Cumulative GAG release over 672 h.

4.3. Binding and release profiles of GAG/GelMA hydrogels for VEGF-A and TIMP-3

4.3.1. Hydrogel loading and release profile of VEGF-A

To evaluate the VEGF-A binding capacity, the hydrogels were loaded with VEGF-A. Following this, they were incubated at 37°C and the release of VEGF-A was measured for a period of 504 h (Figure 4.8).

All hydrogels showed a significant binding of VEGF-A compared to the initial control concentration of 500 ng/ml VEGF-A (Figure 4.8.A). GelMA hydrogels showed an average VEGF-A uptake of 31.8% (± 3.0%), GelMA/HA-MAC hydrogels an uptake of 46.0% (± 1.7%) and GelMA/sHA1-AC hydrogels showed an average uptake of 35.5% (± 15.6%). There was no significant difference in the initially bound VEGF-A between GelMA, GelMA/HA-MAC and GelMA/sHA1-AC hydrogels.

In cumulation, GelMA and GelMA/HA-MAC hydrogels released significantly more VEGF-A compared to GelMA/sHA1-AC hydrogels after 504 h of VEGF-A release (Figure 4.8.B). However, there was no significant difference in the cumulative release of VEGF-A over 504 h between GelMA and GelMA/HA-MAC hydrogels (Figure 4.8.B). After 504 h, the cumulative release of VEGF-A was in average 15.7% (± 0.6%) of their initially bound VEGF-A for GelMA hydrogels, 10.6% (± 0.3%) for GelMA/HA-MAC hydrogels and GelMA/sHA1-AC hydrogels released 6.9% (± 0.9%) of their initially bound VEGF-A.

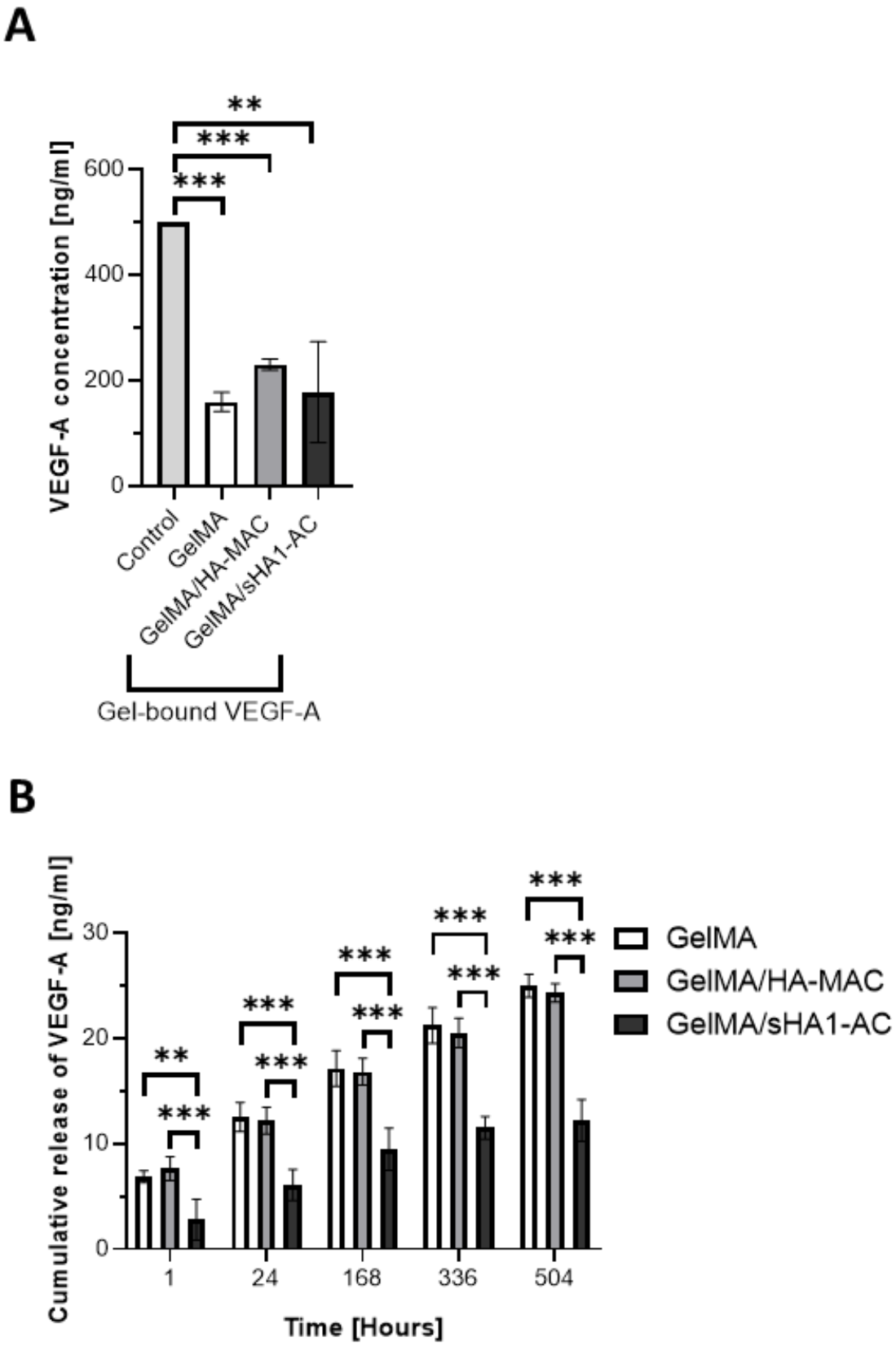

Figure 4.8 Hydrogel loading and VEGF-A release profile. A: VEGF-A control concentration and concentration of hydrogel bound VEGF-A. B: Cumulative release of VEGF-A over 504 h.

4.3.2. Hydrogel loading and release profile of TIMP-3

Moreover, hydrogels loaded with TIMP-3 were incubated at 37°C for 504 h (Figure 4.9). Following the incubation, the release was measured as well as the TIMP-3 uptake of the different hydrogels. Compared to the TIMP-3 control concentration, all hydrogels bound a significant TIMP-3 concentration (Figure 4.9.A). GelMA hydrogels showed an average TIMP-3 uptake of 48.8% (± 3.3%), GelMA/HA-MAC hydrogels had an uptake of 48.5% (± 4.6%) and GelMA/sHA1-AC hydrogels showed a TIMP-3 uptake of 49.8% (± 1.1%). There was no significant difference between the TIMP-3 uptake of the different hydrogels (Figure 4.9.A).

After 1 h of incubation of TIMP-3-loaded hydrogels, there was no significant difference in the release of TIMP-3 between the different hydrogels. After 24, 168, 336 and 504 h, GelMA/sHA1-AC hydrogels released significantly less TIMP-3 compared to GelMA and GelMA/HA-MAC hydrogels (Figure 4.9.B). GelMA hydrogels released a total of 37.7% (± 5.8%) of their initial uptake, GelMA/HA-MAC hydrogels released 31.2% (± 2.9%) and GelMA/sHA1-AC hydrogels released 14.7% (± 6.0%) of their initially bound TIMP-3 which was significantly less when compared to GelMA and GelMA/HA-MAC hydrogels (Figure 4.9.B).

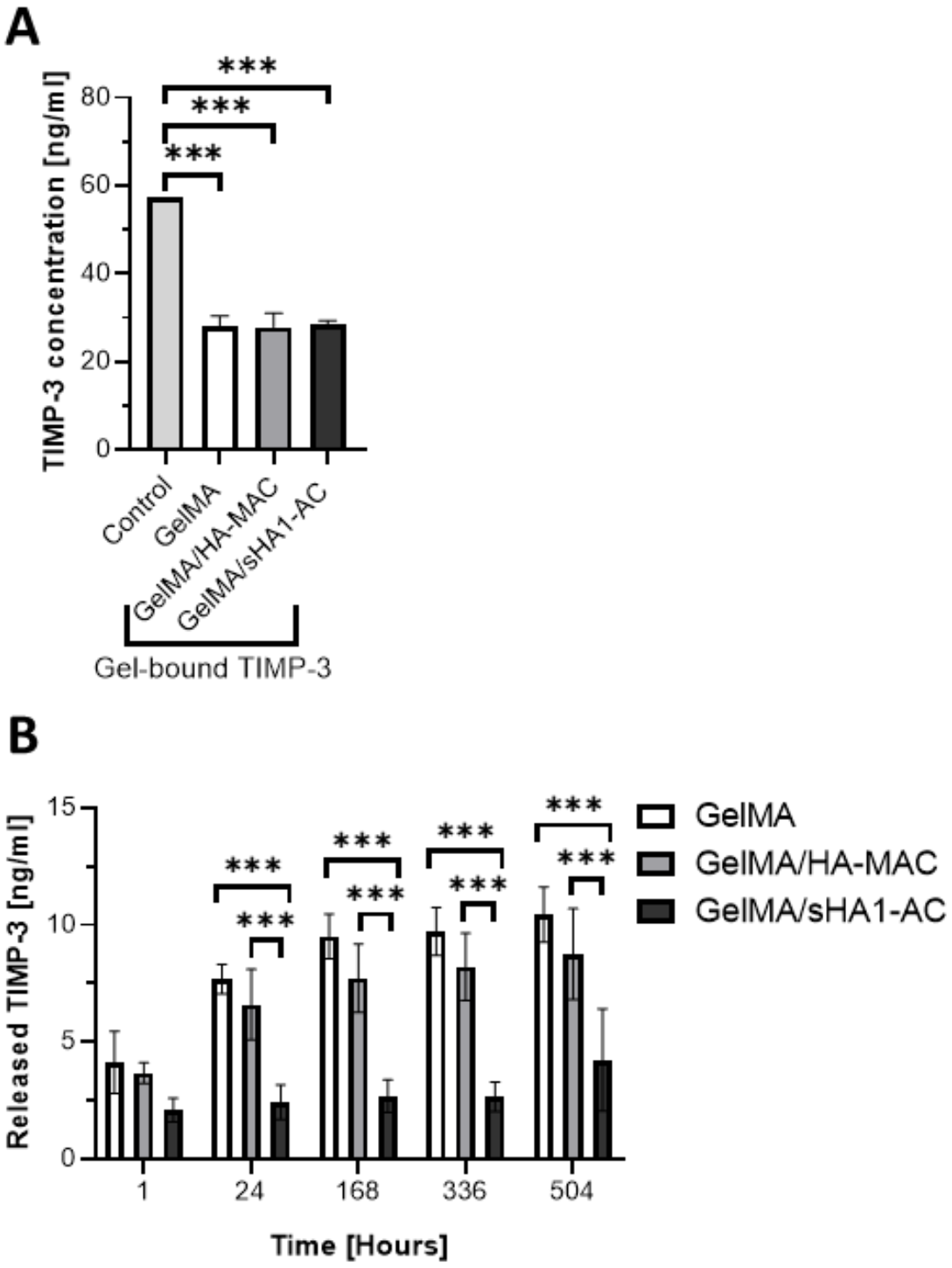

Figure 4.9 Hydrogel loading and TIMP-3 release profile. A: TIMP-3 output concentration in comparison to the input concentration of 57.4 ng/ml. B: Cumulative release of TIMP-3 over the time of 504 h. Measurements by M. Sc. Charlotte Berhorst.

4.3.3. Combined hydrogel loading and release profile of VEGF-A and TIMP-3

Following the evaluation of the individual VEGF-A and TIMP-3 binding capacities of the different hydrogels, a combined approach was used, and the hydrogels were loaded with both

VEGF-A and TIMP-3. They were incubated at 37°C for 504 h and the release as well as uptake of VEGF-A and TIMP-3 was measured (Figure 4.10).

All three types of hydrogels took up a significant amount of VEGF-A when compared to the initial concentration of 500 ng/ml (Figure 4.10.A). There was no significant difference in the VEGF-A uptake between the different hydrogels as GelMA hydrogels showed an average VEGF-A uptake of 58.6% (± 1.3%), GelMA/HA-MAC hydrogels had an average uptake of 57.9% (± 9.1%) and GelMA/sHA1-AC hydrogels showed an uptake of 74.8% (± 3.5%) (Figure 4.10.A).

Regarding the cumulative release of VEGF-A, there was no significant difference between the three hydrogel types after a period of 1 h and 24 h. After 168 h and 336 h, GelMA/sHA1-AC hydrogels released significantly less VEGF-A than GelMA hydrogels. Over the period of 504 h, GelMA/HA-MAC (5.8% ± 2.9%) and GelMA/sHA1-AC hydrogels (3.8% ± 0.1%) released significantly less VEGF-A compared to GelMA hydrogels (9.0% ± 0.1%) (Figure 4.10.B).

In the presence of VEGF-A, GelMA hydrogels bound 14.7% (± 8.1%) of TIMP-3, GelMA/HA-MAC hydrogels 14.8% (± 8.1%) and GelMA/sHA1-AC hydrogels 18.9% (± 12.9%) with no significant difference between the groups (Figure 4.10.C). The cumulative TIMP-3 release over 504 h of GelMA/sHA1-AC hydrogels (6.4% ± 1.2%) was significantly less than the cumulative TIMP-3 release of GelMA (29.3% ± 3.2%) and GelMA/HA-MAC (26.8% ± 2.2%) hydrogels (Figure 4.10.D).

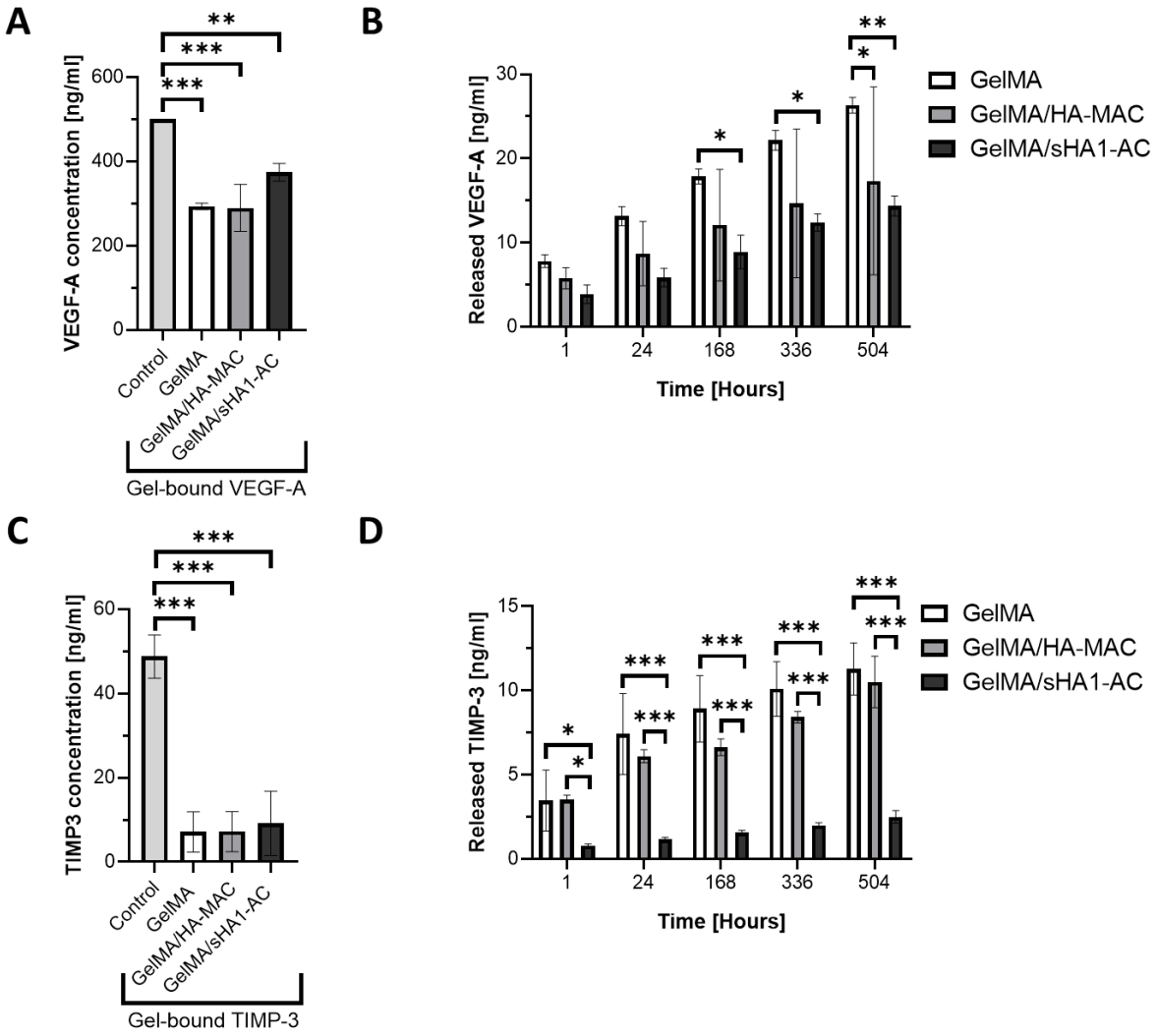

Figure 4.10 Combined evaluation of VEGF-A and TIMP-3 bioactivity. A: Output concentration of VEGF-A in comparison to input concentration. B: Output concentration of TIMP-3 in comparison to input concentration. C: Cumulative release of VEGF-A over 504 h. D: Cumulative release of TIMP-3 over the period of 504 h. TIMP-3 measurements by M. Sc. Charlotte Berhorst.

4.4. Bioactivity of hydrogel-released TIMP-3

For the evaluation of TIMP-3's inhibitory bioactivity after hydrogel release, an MMP-9 assay was performed (Figure 4.11).

Compared to a positive control (Control), over the period of 336 h released TIMP-3 significantly decreased the MMP-9 activity. However, when compared to the synthetic MMP inhibitor NNGH which served as negative control, the inhibitory activity of released TIMP-3 towards MMP-9 was significantly lower after 336 h of release (Figure 4.11).

After the incubation (0 h), TIMP-3 released from GelMA hydrogels reduced the MMP-9 activity significantly more compared to TIMP-3 released from GelMA/sHA1-AC hydrogels. The average MMP-9 activity after treatment with TIMP-3 released from GelMA hydrogels (0 h) was

12.9% (± 2.4%) compared to 27.3% (± 1.4%) for TIMP-3 released from GelMA/sHA1-AC hydrogels (Figure 4.11). The TIMP-3 released from GelMA hydrogels over 24 h inhibited MMP-9 significantly more efficiently compared to TIMP-3 from GelMA/HA-MAC and GelMA/sHA1-AC hydrogels (Figure 4.11). The MMP-9 activity after incubation with TIMP-3 released from GelMA hydrogels (24 h) was 33.3% (± 11.9%) compared to TIMP-3 from GelMA/HA-MAC with a remaining MMP-9 activity of 54.2% (± 8.2%) and TIMP-3 from GelMA/sHA1-AC with 59.0% remaining MMP-9 activity (± 1.0%) (Figure 4.11). There was no significant difference in the inhibitory activity of TIMP-3 released out of the different hydrogels, after 168 and 336 h towards MMP-9 (Figure 4.11).

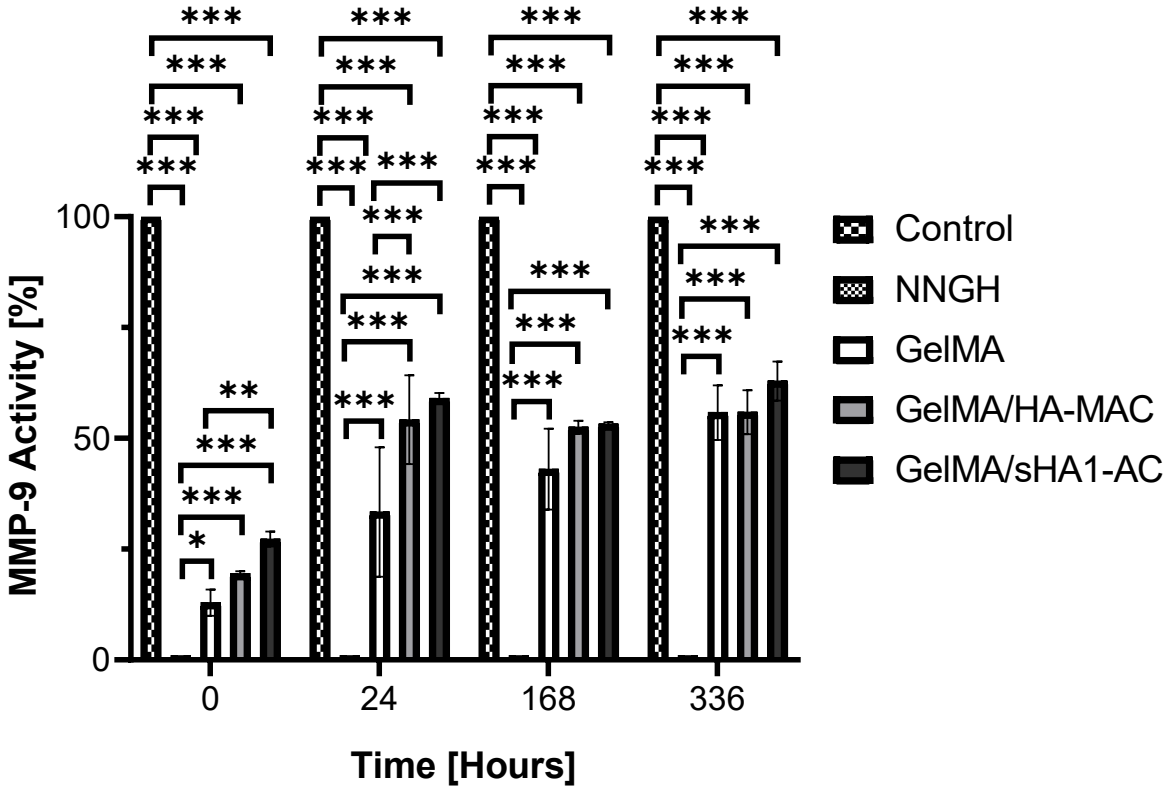

Figure 4.11 Evaluation of TIMP-3 bioactivity after release from hydrogels.

Different concentrations of TIMP-3 were used to determine its IC_{50} for MMP-9. There is a concentration dependency between TIMP-3 concentration and MMP-9 activity (Figure 4.12). The IC_{50} of TIMP-3 for MMP-9 was determined for a TIMP-3 concentration of 7.8 nM ± 3.0 nM (170.6 ng/ml) (Figure 4.12).

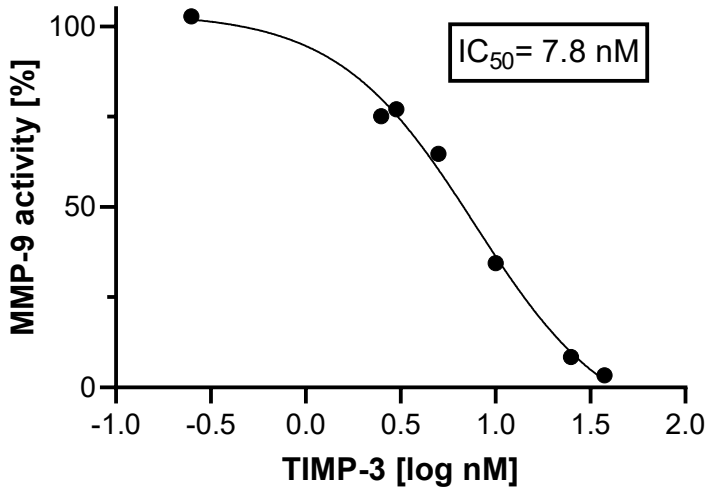

Figure 4.12 IC_{50}-determinatinon of TIMP-3 for MMP-9.

For further evaluation of the TIMP-3 bioactivity after release from the different hydrogels, an *in vitro*-matrix degradation assay of collagen coatings was performed (Figure 4.13). The inhibitory potential of released TIMP-3 on collagenase-mediated collagen degradation was evaluated.

TIMP-3 which was released over 24 h from GelMA and GelMA/sHA1-AC hydrogels, showed a significant inhibition of matrix degradation compared to the control (no inhibitor) after 20 min of incubation (Figure 4.13.A). The control led to a matrix degradation of 30.7% (± 1.0%) compared to TIMP-3 released from GelMA hydrogels with a matrix degradation of 19.3% (± 4.7%) and GelMA/sHA1-AC hydrogels with 18.7% (± 1.3%) (Figure 4.13.A). Compared to the control, TIMP-3 released from GelMA/HA-MAC hydrogels did not significantly inhibit matrix degradation (Figure 4.13.A).

TIMP-3 which was released over 168 h from GelMA/HA-MAC and GelMA/sHA1-AC hydrogels, showed a significant inhibition of matrix degradation compared to the control (no inhibitor) after 60 min of incubation (Figure 4.13.B). The control led to a matrix degradation of 78.1% (± 1.1%) compared to TIMP-3 released from GelMA/HA-MAC hydrogels with a matrix degradation of 53.6% (± 11.8%) and GelMA/sHA1-AC hydrogels with 53.0% (± 3.7%) (Figure 4.13.B) TIMP-3 released from GelMA hydrogels did not significantly inhibit matrix degradation (Figure 4.13.B).

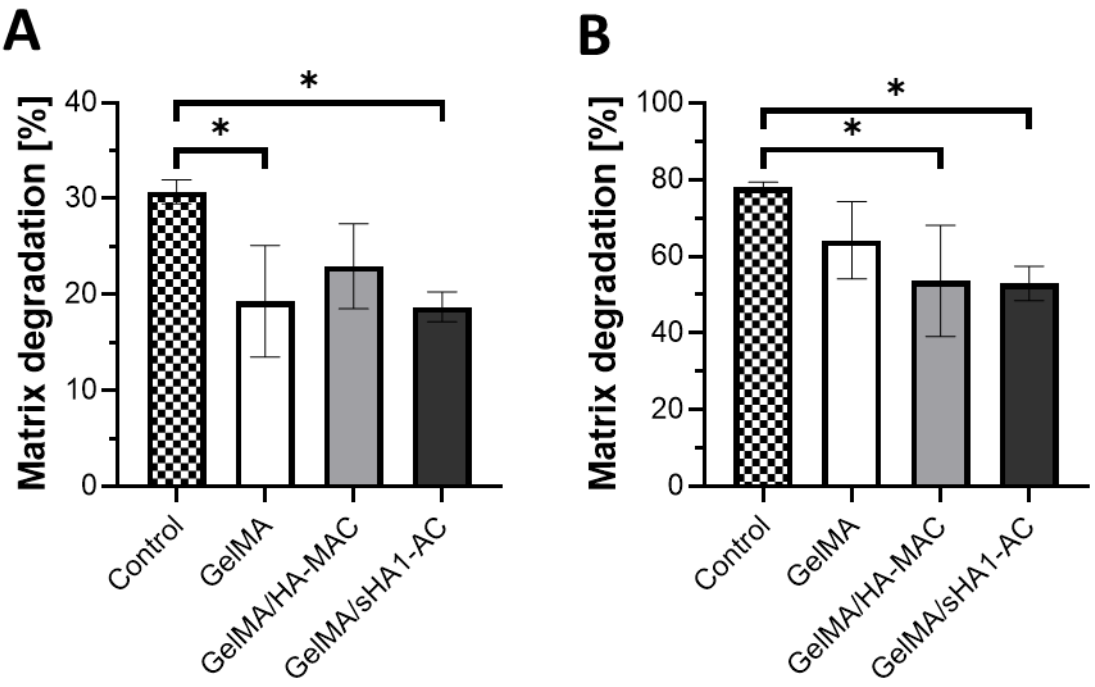

Figure 4.13 Matrix degradation. A: Matrix degradation after 20 min of incubation with TIMP-3 (24 h-release). B: Matrix degradation after 60 min of incubation with TIMP-3 (168 h-release).

4.5. Bioactivity of hydrogel-released VEGF-A

For the bioactivity evaluation of hydrogel-released VEGF-A was evaluated using a KDR/NF AT-RE HEK293 cell-based VEGF-A bioassay. Bioluminescence was used to evaluate VEGF-A/VEGFR interaction. Bioluminescence was interpreted as bioactivity and the lack of bioluminescence when VEGF-A was combined with TIMP-3 was interpreted as the inhibitory interaction between VEGFR and TIMP-3 (Figure 4.14).

VEGF-A released from hydrogels showed a significantly lower bioactivity compared to a 20 ng/ml VEGF-A solution which served as control with 100% bioactivity (Figure 4.14.A). After 24 h of release, the bioactivity of VEGF-A released from GelMA/sHA1-AC hydrogels was significantly higher compared to VEGF-A released from GelMA/HA-MAC hydrogels. The bioactivity of VEGF-A released from GelMA/sHA1-AC was on average 47.4% (± 5.9%) compared to VEGF-A from GelMA/HA-MAC hydrogels with an average of 29.4% (± 6.5%) (Figure 4.14.A). After 168 h of release, the VEGF-A released from GelMA/sHA1-AC hydrogels showed significantly more bioactivity compared to the VEGF-A released from GelMA and GelMA/HA-MAC hydrogels. The average bioactivity of VEGF-A released from GelMA/sHA1-AC was 20.3% (± 0.9%) compared to VEGF-A from GelMA/HA-MAC hydrogels with an average of 5.8% (± 0.8%) and VEGF-A from GelMA hydrogels with an average of 6.0% (± 0.7%) remaining VEGF-A bioactivity (Figure 4.14.A).

The released TIMP-3 of all groups significantly inhibited the VEGF-A/VEGFR interaction after 24 h leading to a remaining VEGF-A bioactivity after inhibition from hydrogel-released TIMP-3 of 68.3% (± 4.2%) for GelMA hydrogels, 71.9% (± 3.1%) for GelMA/HA-MAC and 73.6% (± 3.4%) for GelMA/sHA1-AC hydrogels (Figure 4.14.B). After 72 h (79.1% ± 4.7%) and 168 h (78.1% ± 6.0%) only TIMP-3 released from GelMA hydrogels significantly blocked the VEGF-A-mediated receptor activation (Figure 4.14.B).

After 168 h of release, VEGF-A released from GelMA/sHA1-AC hydrogels was significantly more bioactive compared to VEGF-A released from GelMA and GelMA/HA-MAC hydrogels (Figure 4.14.C). VEGF-A released from GelMA/sHA1-AC hydrogels showed an average bioactivity of 19.6% (± 8.9%) whereas VEGF-A released from GelMA hydrogels showed a bioactivity of 4.7% (± 0.3%) and VEGF-A released from GelMA/HA-MAC hydrogels 5.3% (± 0.8%) (Figure 4.14.C).

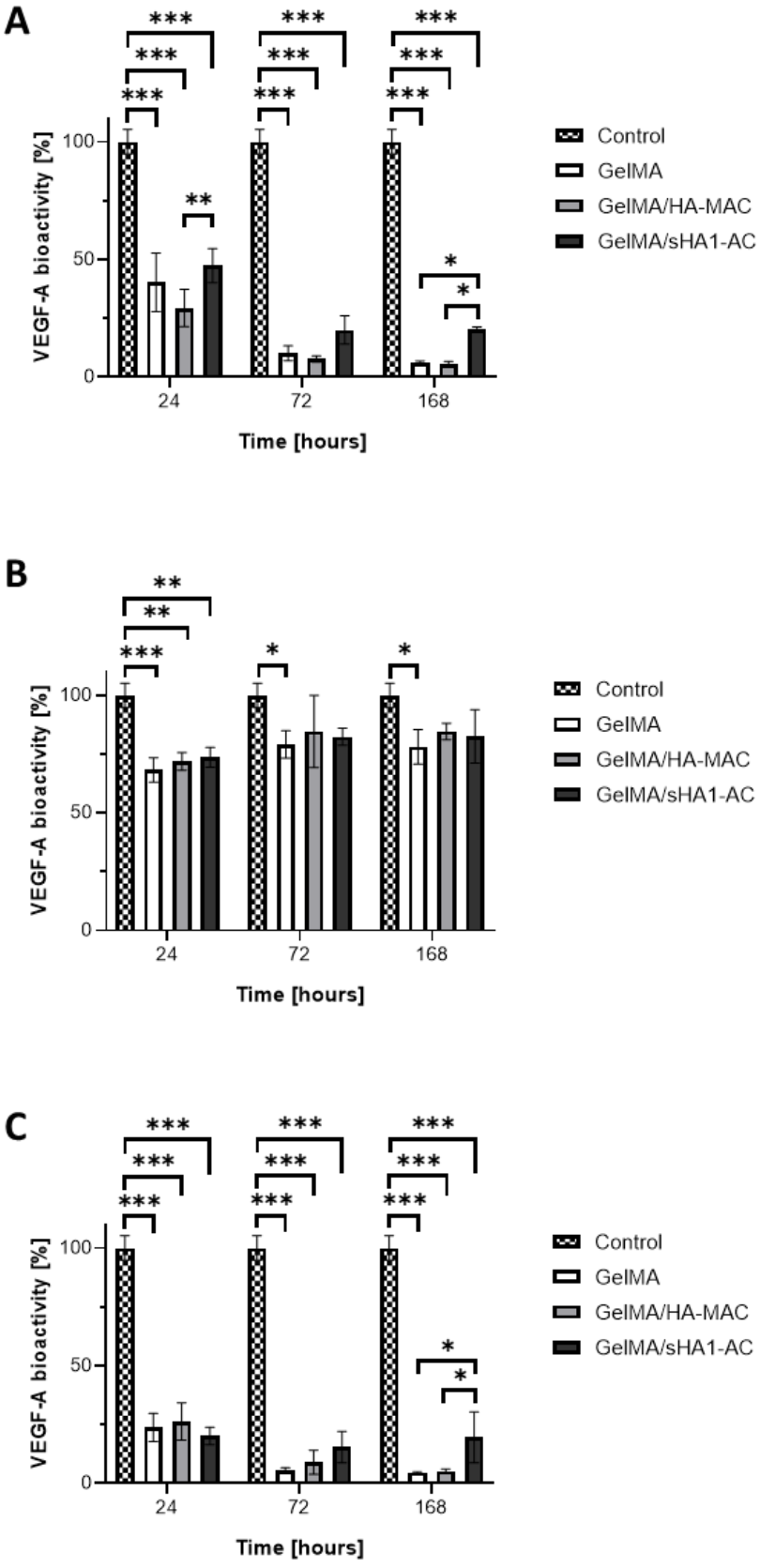

Figure 4.14 VEGF-A bioassay. A: VEGF-A bioactivity of VEGF-A only after 24, 72 and 168 h. B: Bioactivity of TIMP-3 interacting with VEGFR after a release of 24, 72 and 168 h. C: VEGF-A and TIMP-3 bioactivity after release of 24, 72 and 168 h. Measurements by Jun.-Prof. Dr. rer. nat. Sandra Rother.

5. Discussion

The goal of this thesis was to develop a GelMA-based GAG-functionalized hydrogel as a drug-delivery system for the pro- and anti-angiogenic factors VEGF-A and TIMP-3. The necessity for such systems arises as chronic wounds are an important cause of morbidity and health costs in European countries [94,100]. Hydrogels are suitable for the delivery of growth factors and as aECM they provide the necessary conditions for angiogenesis and other cellular processes [7,95,122].

As discussed earlier, GelMA still offers the necessary conditions for cells but its crosslinkability offers the possibility to develop different hydrogels for different applications [50,156]. Commonly used concentrations for GelMA range from 5% (w/v) to 15% (w/v) with 10% (w/v) being the GelMA concentration most commonly used for hydrogel synthesis showing promising results [65,66,86,105,151]. LAP as a photoinitiator for GelMA is non-toxic at low concentrations and only a short time of UV irradiation is necessary to initiate crosslinking [50,89,152]. LAP concentrations of less than 0.25% (w/w) showed no relevant cytotoxicity and therefore the chosen concentration of LAP in the developed hydrogel was 0.07% (w/v) [89]. Furthermore, the reported time of UV crosslinking ranged from 15 s to 15 min with good mechanical properties in the range between 15 s and 120 s [86,89,105]. Therefore 60 s of UV exposure were chosen as a compromise. sHA was shown to bind both VEGF-A and TIMP-3 and both acrylated HA and sHA are suitable for aECM synthesis [107–109,118,131]. Human skin has the highest content of HA but in absolute figures the concentration of HA is about 15.7 µg/ml or even lower [83,127,139]. For most GAG containing hydrogels supraphysiological concentrations of GAG are chosen and the here chosen concentration of 0.9% (w/v) of HA or sHA is no exception [65,109].

In summary, a hydrogel based on 10% GelMA with the addition of HA or sHA appeared to be a suitable candidate for further testing (Figures 4.1 and 4.2)

Sirius Red was found to be a suitable staining solution for different types of collagens and therefore was used to stain GelMA as a collagen derivative [73,136]. Hydrogel staining revealed a homogenous distribution of GelMA within all hydrogels (Figure 4.3). The qualitative staining with Toluidine Blue was used to reveal the homogenous distribution of sHA1-AC within GelMA/sHA1-AC hydrogels and it showed a lack of sGAG within the GelMA and GelMA/HA hydrogels (Figure 4.3) [140]. Similar results are found in the literature for sHA and collagen hydrogels [109].

Regarding the surface properties of GelMA hydrogels, the findings of an irregular knob-like surface (Figure 4.4) were consistent with previous findings using 15% GelMA hydrogels [101]. There was a discrepancy in the knob-like surface of GelMA/HA-MAC hydrogels (Figure 4.4)

compared to literature of HA-based hydrogels [23,86]. However, the surface was quite like the surface of GelMA hydrogels (Figure 4.4). The porous surface of GelMA/sHA1-AC hydrogels was consistent with the literature for sHA-based hydrogels and collagen-based hydrogels [109,123]. The possibility of controlling hydrogel morphology using sHA might be promising for further biomedical applications of GelMA. However, the shown surface properties might have been influenced by the lyophilization process which was necessary prior to SEM imaging.

The swelling ratio of all hydrogels remained the same over the course of 96 h without any significant change for all types of tested hydrogels (Figure 4.5). Current literature on GelMA-based hydrogels reported a swelling ratio between 10% and more than 3500% of swelling with the results of this thesis being within the previously reported range for the swelling ratio of GelMA-based hydrogels [64,86,90,101,105,142]. However, the swelling of GAG-functionalized GelMA-based hydrogels was less pronounced in comparison to similar collagen-based hydrogels [109]. This property might be advantageous in a wound dressing as the swelling enables the hydrogel to close the wound and absorb moisture and other fluids but without the disadvantage of a continuous swelling which e.g., could impact microcirculation in the wound due to the pressure applied by the continued hydrogel-swelling.

The addition of GAG to a GelMA-based hydrogel led to an increase in the Young's modulus of the hydrogels (Figure 4.6). Previous findings showed that the Young's modulus of sHA hydrogels was increased compared to HA hydrogels [123]. Furthermore, the Young's modulus depended on the GelMA concentration used for hydrogel synthesis and the Young's modulus for 10% GelMA measured in this study was like the Young's modulus found in literature for hydrogels based on 10% GelMA [90,142]. However, the reported Young's modulus for GAG-functionalized GelMA-based hydrogels was rather heterogenous even when compared to 10% GelMA hydrogels [64,86]. This could have been the result of the different GAG and different GAG concentrations used in these studies. However, the current findings were supported by evidence suggesting that the addition of HA to GelMA hydrogels leads to an increase in its Young's modulus [65].

The combined findings of SEM imaging, swelling ratio and Young's modulus suggested that these factors were determined by the hydrogel composition as much as the ratio of the different components. Interestingly, *Sturabotti et al.* proposed that the hydrogel surface may depend on the Young's modulus and that an increased Young's modulus would lead to more stable pores [123]. The findings of this thesis were consistent with their theory as only GelMA/sHA1-AC hydrogels showed pores whereas the others did not (Figure 4.4). GelMA/sHA1-AC hydrogels showed a significantly increased Young's modulus when compared to GelMA hydrogels (Figure 4.6). As for the swelling ratio, there was no evidence that it was either influenced by the hydrogel's surface or its Young's modulus, but it might have been largely influenced by the

hydrogel's main component, GelMA, as the Young's modulus and therefore most likely the hydrogel's surface seemed to be mainly influenced by sHA1-AC. As found by *Nichol et al.* and others, an increase in the degree of methacrylation led to an increase in the Young's modulus and an increase in the degree of methacrylation and GelMA mass fraction led to a reduction of the swelling ratio [10,90]. This might be a further reason for the previously mentioned heterogeneity in the reported swelling ratio and Young's modulus.

Over the course of 672 h, 10% GelMA hydrogels showed a GelMA release of up to 70% (Figure 4.7.A). In the current literature, the actual release of GelMA is often substituted using the loss of mass and weight in ratio to the initial mass or weight which showed for 10% and 15% GelMA hydrogels, that the degradation was 70% or more after at least 20 days [66,105,151]. The literature also suggested that the addition of crosslinkable molecules e.g., sodium alginate-dopamine or the here used sHA1-AC (Figure 4.7.A) reduced the hydrogel's degradation after more than 20 days [109,151]. The comparison is of course limited due to the differences in determining the hydrogel degradation as well as the differences in added molecules. However, the available literature supported the findings of this study. The increased stability of GelMA/sHA1-AC hydrogels might be a result of an increased stability due to sHA as hydrogels composed of collagen and sHA showed an increased stability compared to other collagen-based hydrogels [109].

Regarding the release of GAG, there was no significant difference in the release between HA-MAC and sHA1-AC (Figure 4.7.B). The release kinetic for both HA and sHA with an initial increased and then steady release seems to be characteristic for GelMA-based hydrogels as it can be found with GAG as well as non-organic components like nanoclusters based on Molybdenum polyoxometalate [68,86]. Previous data showed that similar to the release of collagen from collagen-based hydrogels, collagen and HA-based hydrogels released less HA compared to HA/sHA1-AC/collagen hydrogels which could be the result of an increased stability of GelMA hydrogels as there was no significant difference in the release of HA-MAC or sHA1-AC [109].

Biodegradation is advantageous for a drug-delivery system as it enables a controlled release of the incorporated substances [146]. As the hydrogels designed and characterized in this study can release both GelMA and GAG in a controlled manner (Figure 4.7.B), they show potential as a drug-delivery system. Furthermore, GelMA hydrogels are reported to not only show controlled degradation *in vitro* in absence of proteinases but also when degradation is aided by MMP [10].

The ability of the hydrogels to function as a drug-delivery system for pro-angiogenic factors was evaluated for VEGF-A because of its importance for angiogenesis in wound healing [41].

In surface plasmon resonance experiments, $VEGF_{165}$ showed an increased binding capacity to sHA1-AC compared to HA [111].

It is well established that heparin and desulphated derivatives of it, can be used to modulate the release of VEGF-A out of hydrogels [35,159]. Heparin is commonly used as an anticoagulant with its anticoagulant potencies depending on the degree of sulphation [35,51,157]. However, the ability to bind VEGF-A and achieve a controlled release is not impacted by selective desulphation [35]. In contrast, sHA was shown not to have anticoagulative abilities [75]. Most experiments with GAG and VEGF-A, including this study (Figure 4.8.B), showed an accelerated release in the beginning of the release which decelerated after some time and sometimes led to a plateau phase in the release pattern [35,159,160]. This is not only the case for VEGF-A but for other growth factors as well [110,114]. Regarding the usage of sHA1-AC as sGAG and GelMA as a basis for the hydrogels, a VEGF-A uptake (Figure 4.8.A) of a similar scale (GelMA-based about 40%, collagen-based about 25%) was observed for collagen-based sHA1-AC hydrogels [111]. Coherent with the findings of this study, collagen/sHA1-AC hydrogels released less VEGF-A compared to collagen/HA hydrogels with a release kinetic like GelMA, GelMA/HA-MAC and GelMA/sHA1-AC hydrogels (Figure 4.8.B) [111].

TIMP-3 as anti-angiogenic factor and key regulator of matrix turnover plays a role in the regulation of angiogenesis and was shown to bind to natural occurring sGAG as well as sHA1-AC [107,108,115,154]. Therefore, TIMP-3 release from GelMA, GelMA/HA-MAC and GelMA/sHA1-AC hydrogels was investigated as well. For hydrogels based on different materials and without the addition of sGAG, the release kinetic for TIMP-3 was similar to the one found in this study for GelMA and GelMA/HA hydrogels (Figure 4.9.B) with an initial fast release which then decreased over time, sometimes reaching a plateau phase with differences in total release probably depending on the initial TIMP-3 concentration as well as the specific components of the different hydrogels [6,25,97]. *Purcell et al.* found that the addition of sulphate groups to a HA-based hydrogel decreased TIMP-3 release to about 30% of the bound TIMP-3 which is similar to the release found in this study for GelMA/sHA1-AC hydrogels (Figure 4.9.B) [97]. Interestingly, the release kinetic of a synthetic, protein-based MMP-inhibitor was influenced by sGAG as well [29]. The TIMP-3 uptake of about 50% of the input concentration (Figure 4.9.A) might be explained by the fact of TIMP-3 binding to the aECM [115].

As GAG, sGAG, VEGF-A and TIMP-3 all show an influence on VEGFR-mediated cell activation, the different approaches were combined into one experiment [108]. For the combined release of VEGF-A and TIMP-3, the release profile of each substance was comparable to the profile for the release of either VEGF-A or TIMP-3 (Figures 4.10.B, 4.10.D,

4.8.B and 4.9.B). However, the reduced TIMP-3 release from GelMA/sHA1-AC hydrogels compared to the single-protein release (Figures 4.10.D and 4.9.B), after similar TIMP-3 uptake of all hydrogels (Figure 4.10.C) and the differences in TIMP-3 uptake (VEGF-A/TIMP-3 co-incubation: TIMP-3 ca. 15 to 20%) (Figure 4.10.C) compared to the uptake of TIMP-3 only (TIMP-3: about 50%) (Figure 4.9.A) might indicate a displacement of TIMP-3 by VEGF-A. Therefore, it is hypothesized that VEGF-A shows a stronger binding affinity and therefore might be able to replace TIMP-3 when co-incubated together. Previously reported findings showed that TIMP-3 recovery after interaction with a GAG coating seemed to depend on the used GAG as well as whether TIMP-3 was co-incubated with VEGF-A. However, similar to the results of this study, the co-incubation with TIMP-3 did not influence VEGF-A recovery [108].

Both the release of VEGF-A and TIMP-3 from GelMA/sHA1-AC hydrogels was reduced over time compared to GelMA and GelMA/HA-MAC hydrogels even though the initial uptake was similar. These findings suggest that GelMA/sHA1-AC can be used to control the release of either VEGF-A, TIMP-3 or both as it would be necessary for a drug-delivery system whereas GelMA/HA-MAC hydrogels do not influence the release of VEGF-A and/or TIMP-3 compared to GelMA hydrogels which suggests an uncontrolled release.

As it is necessary for a drug-delivery system to deliver, in this case, proteins with remaining bioactivity to influence the pathophysiological conditions, the here developed system was tested regarding its ability to deliver pro- and anti-angiogenic factors with remaining bioactivity.

Over the complete duration of the release assay, hydrogel-released TIMP-3 was still able to inhibit MMP-9 (Figure 4.11) but to a different extent. Similar findings were reported for a synthetic, protein-based MMP inhibitor [29]. The differences between the reduction in MMP-9 activity in different groups might be a result of the different amounts of released TIMP-3 as GelMA/sHA1-AC hydrogels released significantly less TIMP-3 compared to GelMA and GelMA/HA-MAC hydrogels (Figure 4.9.B). Only after 0 h and 24 h, TIMP-3 released from GelMA and GelMA/HA-MAC hydrogels inhibited MMP-9 activity significantly more than TIMP-3 released from GelMA/sHA1-AC hydrogels (Figure 4.11) which could be caused by the increased TIMP-3 release of those two groups compared to TIMP-3 released from GelMA/sHA1-AC hydrogels (Figure 4.9.B). After 168 h and 336 h, there was no difference in the bioactivity of the released TIMP-3 between the different groups (Figure 4.11) even though GelMA/sHA1-AC hydrogels released significantly less TIMP-3 when compared to GelMA and GelMA/HA-MAC hydrogels (Figure 4.9.B). This is suggestive of the fact that TIMP-3 released out of GelMA/sHA1-AC hydrogels maintained an increased ability to inhibit MMP-9 compared to the two other groups (Figure 4.11) and therefore GelMA/sHA1-AC-released TIMP-3 maintained a higher degree of bioactivity. Furthermore, this process could have been aided by the fact that HA and sHA1 were shown to inhibit MMP as well [107,112]. The IC_{50} of TIMP-3

for MMP-9 was determined (Figure 4.12) to evaluate the inhibition efficiency and it was found to be within the ranges set by the current literature for TIMP-3 and metalloproteinase interactions [46,103].

Not only MMP-9 was inhibited by the hydrogel-released TIMP-3. Collagenase was inhibited by the released TIMP-3 as well. GelMA/sHA1-AC hydrogel-released TIMP-3 showed a significant decrease in matrix degradation compared to a control group without inhibitors (Figure 4.13). This finding is consistent with the known fact that TIMP can inhibit different types of collagenases [57,128]. This again suggests that TIMP-3 released from GelMA/sHA1-AC hydrogels has an increased bioactivity after hydrogel-release compared to GelMA and GelMA/HA-MAC hydrogels (Figure 4.13). A further addition to the inhibitory potential might be the reported fact that certain sGAG not only inhibit hyaluronidase but are also involved in inhibiting collagenases [67,109].

When combining the findings of MMP-9 and collagenase-based matrix degradation inhibition of released TIMP-3, there is evidence that TIMP-3 from GelMA/sHA1-AC hydrogels retained its bioactivity and therefore its inhibitory potential to a larger degree (Figure 4.11 and Figure 4.13) even though the released concentration of TIMP-3 was decreased compared to GelMA and GelMA/HA-MAC hydrogels (Figure 4.9.B). Furthermore, the inhibitory potential could have been increased by the interaction of sGAG and MMP-9 or collagenase.

As was shown for a different heparin-binding growth factor, epidermal growth factor-like growth factor, the growth factor was still bioactive after the release from collagen/HA/sHA1-AC hydrogels [132]. This study found similar results for VEGF-A. After 24 h of VEGF-A release, VEGF-A/VEGFR interaction is decreased compared to a VEGF-A standard (Figure 4.14.A) as was to be expected by the amount of released VEGF-A (Figure 4.8.B) (about 50% of the used standard). Contrary to the current literature, the experiment did not find an increased binding response of VEGF-A/VEGFR after VEGF-A interaction with HA, instead there was evidence of an increased binding response after VEGF-A interaction with sHA1-AC (Figure 4.14.C) [108]. However, as this trend continued for the duration of the experiment, it might be evidence of a decreased VEGF-A bioactivity (Figure 4.14.A). Interestingly, as with the bioactivity of TIMP-3 (Figure 4.9.B, 4.11 and 4.13) VEGF-A released from GelMA/sHA1-AC hydrogels showed an increased bioactivity after 168 h of release (Figure 4.14.A) even though there was less released VEGF-A compared to GelMA and GelMA/HA-MAC hydrogels (Figure 4.8.B). This might be an indicator that VEGF-A released from GelMA/sHA1-AC hydrogels has an increased remaining bioactivity compared to VEGF-A released from GelMA and GelMA/HA-MAC hydrogels.

As the interaction between TIMP-3 and VEGFR is influenced by sGAG as well, released TIMP-3 was used to evaluate its potential to interact with VEGFR compared to a standard VEGF-A

concentration [108]. Only after 24 h of hydrogel-release, there was a significant influence of the released TIMP-3 on VEGFR activity but there was no significant difference between the different hydrogels (Figure 4.14.B). This pronounced difference between these results (Figure 4.14.B) and the effects of released TIMP-3 on proteolytic enzymes (Figure 4.11 and 4.13) might be caused by a difference in the necessary TIMP-3 concentrations to effect either MMP or VEGFR, as in previous experiments with GAG, TIMP-3 and MMP, much lower concentrations of TIMP-3 were used than for experiments regarding the interaction of TIMP-3, GAG and VEGFR [107,108]. However, TIMP-3 is still able to influence VEGFR response after 24 h of release.

As for the interaction between GAG, VEGF-A, TIMP-3 and their respective response on VEGFR, the co-release of VEGF-A and TIMP-3 was studied for VEGF-A bioactivity. The VEGF-A bioactivity in this experiment was like the VEGF-A bioactivity determined in the previous experiment which only investigated VEGF-A released from hydrogels. However, there was no difference in VEGF-A bioactivity of VEGF-A released from GelMA/HA-MAC and GelMA/sHA1-AC after 24 h (Figure 4.14.A and 4.14.C) even though the concentration of released VEGF-A differed between both hydrogels. VEGF-A released from GelMA/sHA1-AC hydrogels showed an increased bioactivity after 168 h compared to GelMA and GelMA/HA-MAC hydrogels (Figure 4.14.C). The underlying reasons for this fact are explained above as they are probably the same. However, most of the interaction between VEGF-A/VEGFR in the presence of TIMP-3 seems to be tuned down in comparison to the experiment only using VEGF-A with an excerpt of VEGF-A/VEGFR interaction of VEGF-A released from GelMA/sHA1-AC hydrogels after 168 h (Figure 4.14.A and 4.14.C). TIMP-3 recovery and therefore its ability to bind to VEGFR was reported to be increased in the presence of both sHA and VEGF-A which would explain the findings of the present study showing a decreased VEGF-A bioactivity in the presence of TIMP-3 [108].

To conclude these last findings, the VEGF-A bioactivity seemed to show an improved preservation after prolonged release from GelMA/sHA1-AC hydrogels whereas it was decreased in comparison after the prolonged release from GelMA and GelMA/HA-MAC hydrogels. Even though there was no difference in how released TIMP-3 interacted with VEGF-A/VEGFR, it is evident that after a prolonged period of release, TIMP-3 still influenced VEGF-A/VEGFR interaction which was interpreted as a further sign of bioactivity.

5.1. Limitations of this study

This study's aim was to develop a GAG-functionalized GelMA-based hydrogel as a perspective drug-delivery system for chronic wounds and possibly other conditions as well. However, there are aspects of these hydrogels which still require further study. The proposed preparation of

these hydrogels was limited to a simple geometric form and therefore the investigation of further geometric configurations might be necessary. However, the hydrogels proposed in this thesis are suitable for bioprinting [156]. Furthermore, it might be of interest to further investigate the influence of temperature on pore size and what implications this might have on the release of VEGF-A and/or TIMP-3 [126]. Another aspect which might need further investigation is the influence of GelMA concentration and degree of methacrylation on the mechanical properties of GelMA/sHA1-AC hydrogels which influences e.g. the hydrogel's ability to swell and therefore properties which are necessary for a drug-delivery system which acts as wound dressing as well [88,126].

When it comes to VEGF-A and/or TIMP-3 release as well as their bioactivity, this study is limited as only *in vitro* conditions were studied whereas *in vivo* conditions are more complex and therefore might have an influence on the here found properties of GelMA/sHA1-AC hydrogels. However, previous studies have shown that sHA, TIMP-3 and VEGF-A influenced the migration of endothelial cells [108].

5.2. Outlook and future clinical implications of GelMA/sHA1-AC hydrogels

To further investigate the interaction between the proposed system of GelMA/sHA1-AC hydrogels and living cells, cell culture assays based on endothelial cells e.g., a scratch assay, should be the next step because of the known effects of sHA, VEGF-A and TIMP-3 [108]. A further way to investigate the possibilities of GelMA/sHA1-AC hydrogels would be to attempt the formation of a microvascular network, similar to *Limasale et al.*, either within a hydrogel or in the vicinity of one [70]. A similar, tissue-engineering-based approach would be to use microvascular fragments (MVF), which are derived from adipose tissue. MVF secrete pro-angiogenic factors like VEGF-A and offer a more physiologic cell environment than a single-cell system. Implanted and perfused MVF can evolve into mature vessels [59]. MVF can rapidly integrate themselves into an intact microvasculature [59,150]. The cultivation and implantation into mice of MVFs in a collagen-based scaffold together with GAG with or without growth factor stimulation led to promising results which could be translated for GelMA/sHA1-AC hydrogels [60]. MFV could be used for tissue vascularization e.g., pancreatic islets, scaffold vascularization or for the treatment of ischaemic heart disease and pre-vascularized scaffolds could be used as "vessel units" for tissue engineering because of their rapid development into a perfused microvasculature [59,150]. Inevitably, the necessity of an animal model would arise.

GelMA/sHA1-AC hydrogels loaded with TIMP-3 could be evaluated and used in post-myocardial infarction care as a drug-delivery system based on a HA hydrogel and loaded with TIMP-3 showed improved recovery in a porcine animal model [133].

When it comes to the use of GelMA/sHA1-AC hydrogels as a drug-delivering wound dressing, gelatine-based hydrogels offer necessary properties including the retention of body fluids, the protection of the wound as well as a low antigenicity, and in the case of gelatine cost effectiveness as well as further properties necessary for an “ideal” wound dressing [88].

To summarize, the here developed GelMA/sHA1-AC hydrogel-based drug-delivery systems for VEGF-A and/or TIMP-3 show a promising potential for a variety of both biomedical and research applications. They could not only be used for the application of VEGF-A and/or TIMP-3 but also for the application of other biological-active agents binding to sHA1-AC like TGF-β.

6. Conclusions

In this thesis, a drug-delivery system for pro- and anti-angiogenic factors was developed for the potential use in the treatment of chronic wounds. The results showed that GelMA/sHA1-AC hydrogels are promising candidates for the delivery of VEGF-A and/or TIMP-3 which can be used to study the influence on wound healing. It was shown in the present study that GelMA/sHA1-AC hydrogels released VEGF-A and/or TIMP-3 but also that the proteins kept their bioactivity after they were released over an extended time period. Due to the release from sHA1-AC out of the hydrogels not only the proteins loaded into the hydrogel can influence cellular signalling, but the hydrogel itself is able to act as a mediator. Furthermore, the basic principle of this study can be applied not only to wound healing but also to other applications.

To conclude, the development of GelMA/sHA1-AC hydrogels can be seen as an advance in biomaterial design both for biomedical application as well as medical research.

7. References

1. Aird WC (2015) Endothelium and haemostasis. Hamostaseologie 35:11–16
2. Aisenbrey EA, Murphy WL (2020) Synthetic alternatives to Matrigel. Nat Rev Mater 5:539
3. Albelwi FF, Teleb M, Abu-Serie MM, Al Moaty MNA, Alsubaie MS, Zakaria MA, Kilany Y El, Aouad MR, Hagar M, Rezki N (2021) Halting tumor progression via novel non-hydroxamate triazole-based mannich bases mmp-2/9 inhibitors; design, microwave-assisted synthesis, and biological evaluation. Int J Mol Sci 22:10324
4. Anand-Apte B, Pepper MS, Voest E, Montesano R, Olsen B, Murphy G, Apte SS, Zetter B (1997) Inhibition of angiogenesis by tissue inhibitor of metalloproteinase-3. Invest Ophthalmol Vis Sci 38:817–823
5. Apte RS, Chen DS, Ferrara N (2019) VEGF in Signaling and Disease: Beyond Discovery and Development. Cell 176:1248–1264
6. Awada HK, Long DW, Wang Z, Hwang MP, Kim K, Wang Y (2017) A single injection of protein-loaded coacervate-gel significantly improves cardiac function post infarction. Biomaterials 125:65–80
7. Badylak SF, Freytes DO, Gilbert TW (2009) Extracellular matrix as a biological scaffold material: Structure and function. Acta Biomater 5:1–13
8. Bayer IS (2020) Hyaluronic Acid and Controlled Release: A Review. Molecules 25:2649
9. Bonnans C, Chou J, Werb Z (2014) Remodelling the extracellular matrix in development and disease. Nature Reviews Molecular Cell Biology 2014 15:12 15:786–801
10. Bose S, Phan C-M, Rizwan M, Tse JW, Yim E, Jones L (2023) Fabrication and Characterization of an Enzyme-Triggered, Therapeutic-Releasing Hydrogel Bandage Contact Lens Material. Pharmaceutics 16:26
11. Bowers S, Franco E (2020) Chronic Wounds: Evaluation and Management. Am Fam Physician 101:159–166
12. Burdick JA, Prestwich GD (2011) Hyaluronic Acid Hydrogels for Biomedical Applications. Adv Mater 23:H41

13. Cabral-Pacheco GA, Garza-Veloz I, Rosa CCD La, Ramirez-Acuña JM, Perez-Romero BA, Guerrero-Rodriguez JF, Martinez-Avila N, Martinez-Fierro ML (2020) The Roles of Matrix Metalloproteinases and Their Inhibitors in Human Diseases. Int J Mol Sci 21:1–53

14. Cai C, Zhang X, Li Y, Liu X, Wang S, Lu M, Yan X, Deng L, Liu S, Wang F, Fan C (2022) Self-Healing Hydrogel Embodied with Macrophage-Regulation and Responsive-Gene-Silencing Properties for Synergistic Prevention of Peritendinous Adhesion. Advanced Materials 34:e2106564

15. Chakroborty D, Goswami S, Basu S, Sarkar C (2020) Catecholamines in the regulation of angiogenesis in cutaneous wound healing. The FASEB Journal 34:14093–14102

16. Chang KH, Liao HT, Chen JP (2013) Preparation and characterization of gelatin/hyaluronic acid cryogels for adipose tissue engineering: in vitro and in vivo studies. Acta Biomater 9:9012–9026

17. Chang M, Nguyen TT (2021) Strategy for Treatment of Infected Diabetic Foot Ulcers. Acc Chem Res 54:1080–1093

18. Chen YC, Lin RZ, Qi H, Yang Y, Bae H, Melero-Martin JM, Khademhosseini A (2012) Functional Human Vascular Network Generated in Photocrosslinkable Gelatin Methacrylate Hydrogels. Adv Funct Mater 22:2027

19. Coulon S, Heindryckx F, Geerts A, Van Steenkiste C, Colle I, Van Vlierberghe H (2011) Angiogenesis in chronic liver disease and its complications. Liver International 31:146–162

20. Coulson-Thomas V, Gesteira T (2014) Dimethylmethylene Blue Assay (DMMB). Bio Protoc 4:e1236

21. Cruz-Munoz W, Sanchez OH, Di Grappa M, English JL, Hill RP, Khokha R (2006) Enhanced metastatic dissemination to multiple organs by melanoma and lymphoma cells in timp-3−/− mice. Oncogene 2006 25:49 25:6489–6496

22. Dapson RW, Fagan C, Kiernan JA, Wickersham TW (2011) Certification procedures for sirius red F3B (CI 35780, Direct red 80). Biotech Histochem 86:133–139

23. Andrade del Olmo J, Pérez-Álvarez L, Sáez Martínez V, Benito Cid S, Pérez González R, Vilas-Vilela JL, Alonso JM (2022) Drug Delivery from Hyaluronic Acid–BDDE Injectable Hydrogels for Antibacterial and Anti-Inflammatory Applications. Gels 8:223

24. Díaz-Flores L, Gutiérrez R, Gayoso S, García MP, González-Gómez M, Díaz-Flores L, Sánchez R, Carrasco JL, Madrid JF (2020) Intussusceptive angiogenesis and its counterpart intussusceptive lymphangiogenesis. Histol Histopathol 35:1083–1103

25. Eckhouse SR, Purcell BP, McGarvey JR, Lobb D, Logdon CB, Doviak H, O'Neill JW, Shuman JA, Novack CP, Zellars KN, Pettaway S, Black RA, Khakoo A, Lee TW, Mukherjee R, Gorman JH, Gorman RC, Burdick JA, Spinale FG (2014) Local Hydrogel Release of Recombinant TIMP-3 Attenuates Adverse Left Ventricular Remodeling After Experimental Myocardial Infarction. Sci Transl Med 6:223ra21

26. Eming SA (2004) Increased Levels of the Soluble Variant of the Vascular Endothelial Growth Factor Receptor VEGFR-1 Are Associated with a Poor Prognosis in Wound Healing. Journal of Investigative Dermatology 123:799–802

27. Evans I (2015) An Overview of VEGF-Mediated Signal Transduction. Humana Press, New York. URL: https://link.springer.com/10.1007/978-1-4939-2917-7_7

28. Fadel PJ (2017) Nitric Oxide and Cardiovascular Regulation: Beyond the Endothelium. Hypertension 69:778–779

29. Fan Z, Fu M, Xu Z, Zhang B, Li Z, Li H, Zhou X, Liu X, Duan Y, Lin PH, Duann P, Xie X, Ma J, Liu Z, Guan J (2017) Sustained Release of a Peptide-Based Matrix Metalloproteinase-2 Inhibitor to Attenuate Adverse Cardiac Remodeling and Improve Cardiac Function Following Myocardial Infarction. Biomacromolecules 18:2820–2829

30. Fearnley GW, Wheatcroft SB, Ponnambalam S (2015) Detection and Quantification of Vascular Endothelial Growth Factor Receptor Tyrosine Kinases in Primary Human Endothelial Cells. URL: https://link.springer.com/10.1007/978-1-4939-2917-7_4

31. Fischer I, Gagner J-P, Law M, Newcomb EW, Zagzag D (2005) Angiogenesis in Gliomas: Biology and Molecular Pathophysiology. Brain pathology 15:297–310

32. Fletcher B, Gulanick M, Lamendola C (2002) Risk factors for type 2 diabetes mellitus. J Cardiovasc Nurs 16:486

33. Fowlkes JL, Winkler MK (2002) Exploring the interface between metallo-proteinase activity and growth factor and cytokine bioavailability. Cytokine Growth Factor Rev 13:277–287

34. Frantz C, Stewart KM, Weaver VM (2010) The extracellular matrix at a glance. J Cell Sci 123:4195–4200

35. Freudenberg U, Zieris A, Chwalek K, Tsurkan M V., Maitz MF, Atallah P, Levental KR, Eming SA, Werner C (2015) Heparin desulfation modulates VEGF release and angiogenesis in diabetic wounds. Journal of Controlled Release 220:79–88

36. Garantziotis S, Savani RC (2019) Hyaluronan biology: A complex balancing act of structure, function, location and context. Matrix Biology 78–79:1–10

37. Gardeazabal L, Izeta A (2024) Elastin and collagen fibres in cutaneous wound healing. Exp Dermatol 33:e15052

38. Georges S, Heymann D, Padrines M (2012) Modulatory effects of proteoglycans on proteinase activities. Methods Mol Biol 836:307–322

39. Ghimire K, Altmann HM, Straub AC, Isenberg JS (2017) Gaso-Transmitters: Nitric oxide: what's new to NO? Am J Physiol Cell Physiol 312:C254

40. Guo A, Zhang S, Yang R, Sui C (2024) Enhancing the mechanical strength of 3D printed GelMA for soft tissue engineering applications. Mater Today Bio 24:100939

41. Guo S, DiPietro LA (2010) Factors Affecting Wound Healing. J Dent Res 89:219

42. Guyot M, Pagès G (2015) VEGF Splicing and the Role of VEGF Splice Variants: From Physiological-Pathological Conditions to Specific Pre-mRNA Splicing. URL: https://link.springer.com/10.1007/978-1-4939-2917-7_1

43. Haalboom M (2018) Chronic Wounds: Innovations in Diagnostics and Therapeutics. Curr Med Chem 25:5772–5781

44. Hamburg NM, Creager MA (2017) Pathophysiology of Intermittent Claudication in Peripheral Artery Disease. Circulation Journal 81:281–289

45. Han Y, Yang J, Zhao W, Wang H, Sun Y, Chen Y, Luo J, Deng L, Xu X, Cui W, Zhang H (2021) Biomimetic injectable hydrogel microspheres with enhanced lubrication and controllable drug release for the treatment of osteoarthritis. Bioact Mater 6:3596–3607

46. Hashimoto G, Aoki T, Nakamura H, Tanzawa K, Okada Y (2001) Inhibition of ADAMTS4 (aggrecanase-1) by tissue inhibitors of metalloproteinases (TIMP-1, 2, 3 and 4). FEBS Lett 494:192–195

47. Heyer K, Herberger K, Protz K, Glaeske G, Augustin M (2016) Epidemiology of chronic wounds in Germany: Analysis of statutory health insurance data. Wound Repair Regen 24:434–442

48. Hintze V, Schnabelrauch M, Rother S (2022) Chemical Modification of Hyaluronan and Their Biomedical Applications. Front Chem 10:830671

49. Hynes RO (2009) Extracellular matrix: not just pretty fibrils. Science 326:1216

50. Im G-B, Lin R-Z (2022) Bioengineering for vascularization: Trends and directions of photocrosslinkable gelatin methacrylate hydrogels. Front Bioeng Biotechnol 10:1053491

51. Jones GR, Hashim R, Power DM (1986) A comparison of the strength of binding of antithrombin III, protamine and poly(l-lysine) to heparin samples of different anicoagulant activities. Biochimica et Biophysica Acta (BBA) - General Subjects 883:69–76

52. Kang MG, Lee MY, Cha JM, Lee JK, Lee SC, Kim J, Hwang Y-S, Bae H (2019) Nanogels Derived from Fish Gelatin: Application to Drug Delivery System. Mar Drugs 17:246

53. Karamanos NK, Theocharis AD, Piperigkou Z, Manou D, Passi A, Skandalis SS, Vynios DH, Orian-Rousseau V, Ricard-Blum S, Schmelzer CEH, Duca L, Durbeej M, Afratis NA, Troeberg L, Franchi M, Masola V, Onisto M (2021) A guide to the composition and functions of the extracellular matrix. FEBS J 288:6850–6912

54. Khayat A, Monteiro N, Smith EE, Pagni S, Zhang W, Khademhosseini A, Yelick PC (2017) GelMA-Encapsulated hDPSCs and HUVECs for Dental Pulp Regeneration. J Dent Res 96:192–199

55. Kikuchi R, Nakamura K, MacLauchlan S, Ngo DTM, Shimizu I, Fuster JJ, Katanasaka Y, Yoshida S, Qiu Y, Yamaguchi TP, Matsushita T, Murohara T, Gokce N, Bates DO, Hamburg NM, Walsh K (2014) An anti-angiogenic isoform of VEGF-A contributes to impaired vascularization in peripheral artery disease. Nat Med 20:1464

56. Kline KA, Bowdish DME (2016) Infection in an aging population. Curr Opin Microbiol 29:63–67

57. Knäuper V, López-Otin C, Smith B, Knight G, Murphy G (1996) Biochemical characterization of human collagenase-3. J Biol Chem 271:1544–1550

58. Knight CG, Willenbrock F, Murphy G (1992) A novel coumarin-labelled peptide for sensitive continuous assays of the matrix metalloproteinases. FEBS Lett 296:263–266

59. Laschke MW, Menger MD (2015) Adipose tissue-derived microvascular fragments: Natural vascularization units for regenerative medicine. Trends Biotechnol 33:442–448

60. Laschke MW, Kontaxi E, Scheuer C, Heß A, Karschnia P, Menger MD (2019) Insulin-like growth factor 1 stimulates the angiogenic activity of adipose tissue-derived microvascular fragments. J Tissue Eng 10:2041731419879837

61. Lauer G, Sollberg S, Cole M, Flamme I, Stürzebecher J, Mann K, Krieg T, Eming SA (2000) Expression and proteolysis of vascular endothelial growth factor is increased in chronic wounds. J Invest Dermatol 115:12–18

62. Lee K, Silva EA, Mooney DJ (2011) Growth factor delivery-based tissue engineering: general approaches and a review of recent developments. J R Soc Interface 8:153

63. Lee MH, Atkinson S, Murphy G (2007) Identification of the extracellular matrix (ECM) binding motifs of tissue inhibitor of metalloproteinases (TIMP)-3 and effective transfer to TIMP-1. J Biol Chem 282:6887–6898

64. Lei T, Tong Z, Zhai X, Zhao Y, Zhu H, Wang L, Wen Z, Song B (2023) Chondroitin Sulfate Improves Mechanical Properties of Gelatin Hydrogel for Cartilage Regeneration in Rats. Adv Biol 7:e2300249

65. Levett PA, Melchels FPW, Schrobback K, Hutmacher DW, Malda J, Klein TJ (2014) A biomimetic extracellular matrix for cartilage tissue engineering centered on photocurable gelatin, hyaluronic acid and chondroitin sulfate. Acta Biomater 10:214–223

66. Li S, Sun J, Yang J, Yang Y, Ding H, Yu B, Ma K, Chen M (2023) Gelatin methacryloyl (GelMA) loaded with concentrated hypoxic pretreated adipose-derived mesenchymal stem cells(ADSCs) conditioned medium promotes wound healing and vascular regeneration in aged skin. Biomater Res 27:11

67. Li Z, Yasuda Y, Li W, Bogyo M, Katz N, Gordon RE, Fields GB, Brömme D (2004) Regulation of collagenase activities of human cathepsins by glycosaminoglycans. J Biol Chem 279:5470–5479

68. Liao X, Shen M, Li T, Feng L, Lin Z, Shi G, Pei G, Cai X (2023) Combined Molybdenum Gelatine Methacrylate Injectable Nano-Hydrogel Effective Against Diabetic Bone Regeneration. Int J Nanomedicine 18:5925

69. Lim DK, Wylie RG, Langer R, Kohane DS (2016) Selective binding of C-6 OH sulfated hyaluronic acid to the angiogenic isoform of VEGF165. Biomaterials 77:130

70. Limasale YDP, Fusenig M, Samulowitz M, Atallah P, Sievers J, Dennison N, Freudenberg U, Friedrichs J, Werner C (2024) Glycosaminoglycan Concentration and Sulfation Patterns of Biohybrid Polymer Matrices Direct Microvascular Network Formation and Stability. Adv Funct Mater 34:2411475

71. Lin W, Lin S, Zhou X, Yang F, Lin Z, Li S, Zhang H, Ouyang Y, Zhu J, Sun W, Huang D, Liao B, Zhu J (2023) Biodegradable double-network GelMA-ACNM hydrogel microneedles for transdermal drug delivery. Front Bioeng Biotechnol 11:1110604

72. Loessner D, Meinert C, Kaemmerer E, Martine LC, Yue K, Levett PA, Klein TJ, Melchels FPW, Khademhosseini A, Hutmacher DW (2016) Functionalization, preparation and use of cell-laden gelatin methacryloyl–based hydrogels as modular tissue culture platforms. Nature Protocols 2016 11:4 11:727–746

73. López De Padilla CM, Coenen MJ, Tovar A, De la Vega RE, Evans CH, Müller SA (2021) Picrosirius Red Staining: Revisiting Its Application to the Qualitative and Quantitative Assessment of Collagen Type I and Type III in Tendon. Journal of Histochemistry and Cytochemistry 69:633–643

74. Lu P, Takai K, Weaver VM, Werb Z (2011) Extracellular matrix degradation and remodeling in development and disease. Cold Spring Harb Perspect Biol 3:a005058

75. Magnani A, Lamponi S, Rappuoli R, Barbucci R (1998) Sulfated hyaluronic acids: a chemical and biological characterization. Polym Int 46:225–240

76. Malchesky PS (2010) Do We Need to Wait for Organ Transplants? Artif Organs 34:177–178

77. Maloney FP, Kuklewicz J, Corey RA, Bi Y, Ho R, Mateusiak L, Pardon E, Steyaert J, Stansfeld PJ, Zimmer J (2022) Structure, substrate-recognition, and initiation of hyaluronan synthase. Nature 604:195

78. Martinengo L, Olsson M, Bajpai R, Soljak M, Upton Z, Schmidtchen A, Car J, Järbrink K (2019) Prevalence of chronic wounds in the general population: systematic review and meta-analysis of observational studies. Ann Epidemiol 29:8–15

79. Martínez-Pérez D, Guarch-Pérez C, Purbayanto MAK, Choińska E, Riool M, Zaat SAJ, Święszkowski W (2023) 3D-printed dual drug delivery nanoparticle- loaded hydrogels to combat antibiotic-resistant bacteria. Int J Bioprint 9:64–79

80. Masola V, Zaza G, Secchi MF, Gambaro G, Lupo A, Onisto M (2014) Heparanase is a key player in renal fibrosis by regulating TGF-β expression and activity. Biochimica et Biophysica Acta (BBA) - Molecular Cell Research 1843:2122–2128

81. Mayfosh AJ, Nguyen TK, Hulett MD (2021) The Heparanase Regulatory Network in Health and Disease. Int J Mol Sci 22:11096

82. Mendoza-Cerezo L, Rodríguez-Rego JM, Macías-García A, Callejas-Marín A, Sánchez-Guardado L, Marcos-Romero AC (2024) Three-Dimensional Bioprinting of

GelMA Hydrogels with Culture Medium: Balancing Printability, Rheology and Cell Viability for Tissue Regeneration. Polymers (Basel) 16:1437

83. Meyer LJM, Stern R (1994) Age-Dependent Changes of Hyaluronan in Human Skin. Journal of Investigative Dermatology 102:385–389

84. Mirza R, Koh TJ (2011) Dysregulation of monocyte/macrophage phenotype in wounds of diabetic mice. Cytokine 56:256–264

85. Möller S, Theiß J, Deinert TIL, Golat K, Heinze J, Niemeyer D, Wyrwa R, Schnabelrauch M, Bogner E (2022) High-Sulfated Glycosaminoglycans Prevent Coronavirus Replication. Viruses 14:413

86. Murphy CA, Serafin A, Collins MN (2024) Development of 3D Printable Gelatin Methacryloyl/Chondroitin Sulfate/Hyaluronic Acid Hydrogels as Implantable Scaffolds. Polymers (Basel) 16:1958

87. Naito H, Iba T, Takakura N (2020) Mechanisms of new blood-vessel formation and proliferative heterogeneity of endothelial cells. Int Immunol 32:295–305

88. Ndlovu SP, Ngece K, Alven S, Aderibigbe BA (2021) Gelatin-Based Hybrid Scaffolds: Promising Wound Dressings. Polymers (Basel) 13:2959

89. Nguyen AK, Goering PL, Reipa V, Narayan RJ (2019) Toxicity and photosensitizing assessment of gelatin methacryloyl-based hydrogels photoinitiated with lithium phenyl-2,4,6-trimethylbenzoylphosphinate in human primary renal proximal tubule epithelial cells. Biointerphases 14:021007

90. Nichol JW, Koshy ST, Bae H, Hwang CM, Yamanlar S, Khademhosseini A (2010) Cell-laden microengineered gelatin methacrylate hydrogels. Biomaterials 31:5536–5544

91. Nowak-Sliwinska P, Alitalo K, Allen E, Anisimov A, Aplin AC, Auerbach R, Augustin HG, Bates DO, van Beijnum JR, Bender RHF, Bergers G, Bikfalvi A, Bischoff J, Böck BC, Brooks PC, Bussolino F, Cakir B, Carmeliet P, Castranova D, Cimpean AM, Cleaver O, Coukos G, Davis GE, de Palma M, Dimberg A, Dings RPM, Djonov V, Dudley AC, Dufton NP, Fendt SM, Ferrara N, Fruttiger M, Fukumura D, Ghesquière B, Gong Y, Griffin RJ, Harris AL, Hughes CCW, Hultgren NW, Iruela-Arispe ML, Irving M, Jain RK, Kalluri R, Kalucka J, Kerbel RS, Kitajewski J, Klaassen I, Kleinmann HK, Koolwijk P, Kuczynski E, Kwak BR, Marien K, Melero-Martin JM, Munn LL, Nicosia RF, Noel A, Nurro J, Olsson AK, Petrova T v., Pietras K, Pili R, Pollard JW, Post MJ, Quax PHA, Rabinovich GA, Raica M, Randi AM, Ribatti D, Ruegg C, Schlingemann RO, Schulte-Merker S, Smith LEH, Song JW, Stacker SA, Stalin J, Stratman AN, van de Velde M,

van Hinsbergh VWM, Vermeulen PB, Waltenberger J, Weinstein BM, Xin H, Yetkin-Arik B, Yla-Herttuala S, Yoder MC, Griffioen AW (2018) Consensus guidelines for the use and interpretation of angiogenesis assays. Angiogenesis 21:425

92. Okonkwo U, DiPietro L (2017) Diabetes and Wound Angiogenesis. Int J Mol Sci 18:1419

93. Pasut A, Becker LM, Cuypers A, Carmeliet P (2021) Endothelial cell plasticity at the single-cell level. Angiogenesis 24:311

94. Phillips CJ, Humphreys I, Fletcher J, Harding K, Chamberlain G, Macey S (2016) Estimating the costs associated with the management of patients with chronic wounds using linked routine data. Int Wound J 13:1193–1197

95. Prestwich GD (2008) Engineering a clinically-useful matrix for cell therapy. Organogenesis 4:42–47

96. Pugsley MK, Tabrizchi R (2000) The vascular system: An overview of structure and function. J Pharmacol Toxicol Methods 44:333–340

97. Purcell BP, Lobb D, Charati MB, Dorsey SM, Wade RJ, Zellars KN, Doviak H, Pettaway S, Logdon CB, Shuman JA, Freels PD, Gorman JH, Gorman RC, Spinale FG, Burdick JA (2014) Injectable and bioresponsive hydrogels for on-demand matrix metalloproteinase inhibition. Nat Mater 13:653

98. Purcell BP, Barlow SC, Perreault PE, Freeburg L, Doviak H, Jacobs J, Hoenes A, Zellars KN, Khakoo AY, Lee T, Burdick JA, Spinale FG (2018) Delivery of a matrix metalloproteinase-responsive hydrogel releasing TIMP-3 after myocardial infarction: effects on left ventricular remodeling. Am J Physiol Heart Circ Physiol 315:H814–H825

99. Qi JH, Ebrahem Q, Moore N, Murphy G, Claesson-Welsh L, Bond M, Baker A, Anand-Apte B (2003) A novel function for tissue inhibitor of metalloproteinases-3 (TIMP3): inhibition of angiogenesis by blockage of VEGF binding to VEGF receptor-2. Nature Medicine 2003 9:4 9:407–415

100. Raeder K, Jachan DE, Müller-Werdan U, Lahmann NA (2020) Prevalence and risk factors of chronic wounds in nursing homes in Germany: A Cross-Sectional Study. Int Wound J 17:1128–1134

101. Rahali K, Ben Messaoud G, Kahn C, Sanchez-Gonzalez L, Kaci M, Cleymand F, Fleutot S, Linder M, Desobry S, Arab-Tehrany E (2017) Synthesis and Characterization of Nanofunctionalized Gelatin Methacrylate Hydrogels. Int J Mol Sci 18:2675

102. Randi AM, Smith KE, Castaman G (2018) von Willebrand factor regulation of blood vessel formation. Blood 132:132

103. R&D Systems (2022) Recombinant Human TIMP-3, Catalog Number: 973-TM. URL: https://www.rndsystems.com/products/recombinant-human-timp-3-protein-cf_973-tm#product-citations

104. Ribatti D, Crivellato E (2012) “Sprouting angiogenesis”, a reappraisal. Dev Biol 372:157–165

105. Ribeiro JS, Sanz CK, Münchow EA, Kalra N, Dubey N, Suárez CEC, Fenno JC, Lund RG, Bottino MC (2022) Photocrosslinkable methacrylated gelatin hydrogel as a cell-friendly injectable delivery system for chlorhexidine in regenerative endodontics. Dental Materials 38:1507–1517

106. Robbins JL, Schuyler Jones W, Duscha BD, Allen JD, Kraus WE, Regensteiner JG, Hiatt WR, Annex BH (2011) Relationship between leg muscle capillary density and peak hyperemic blood flow with endurance capacity in peripheral artery disease. J Appl Physiol (1985) 111:81–86

107. Rother S, Samsonov SA, Hofmann T, Blaszkiewicz J, Köhling S, Moeller S, Schnabelrauch M, Rademann J, Kalkhof S, von Bergen M, Pisabarro MT, Scharnweber D, Hintze V (2016) Structural and functional insights into the interaction of sulfated glycosaminoglycans with tissue inhibitor of metalloproteinase-3 - A possible regulatory role on extracellular matrix homeostasis. Acta Biomater 45:143–154

108. Rother S, Samsonov SA, Moeller S, Schnabelrauch M, Rademann J, Blaszkiewicz J, Köhling S, Waltenberger J, Pisabarro MT, Scharnweber D, Hintze V (2017) Sulfated Hyaluronan Alters Endothelial Cell Activation in Vitro by Controlling the Biological Activity of the Angiogenic Factors Vascular Endothelial Growth Factor-A and Tissue Inhibitor of Metalloproteinase-3. ACS Appl Mater Interfaces 9:9539–9550

109. Rother S, Galiazzo VD, Kilian D, Fiebig KM, Becher J, Moeller S, Hempel U, Schnabelrauch M, Waltenberger J, Scharnweber D, Hintze V (2017) Hyaluronan/Collagen Hydrogels with Sulfated Hyaluronan for Improved Repair of Vascularized Tissue Tune the Binding of Proteins and Promote Endothelial Cell Growth. Macromol Biosci 17:1700154

110. Rother S, Krönert V, Hauck N, Berg A, Moeller S, Schnabelrauch M, Thiele J, Scharnweber D, Hintze V (2019) Hyaluronan/collagen hydrogel matrices containing high-sulfated hyaluronan microgels for regulating transforming growth factor-β1. J Mater Sci Mater Med 30:65

111. Rother S, Ruiz-Gómez G, Balamurugan K, Koehler L, Fiebig KM, Galiazzo VD, Hempel U, Moeller S, Schnabelrauch M, Waltenberger J, Pisabarro MT, Scharnweber D, Hintze V (2021) Hyaluronan/Collagen Hydrogels with Sulfated Glycosaminoglycans Maintain VEGF $_{165}$ Activity and Fine-Tune Endothelial Cell Response. ACS Appl Bio Mater 4:494–506

112. Ruiz-Gómez G, Vogel S, Möller S, Pisabarro MT, Hempel U (2019) Glycosaminoglycans influence enzyme activity of MMP2 and MMP2/TIMP3 complex formation - Insights at cellular and molecular level. Sci Rep 9:4905

113. Sajib S, Zahra FT, Lionakis MS, German NA, Mikelis CM (2017) Mechanisms of angiogenesis in microbe-regulated inflammatory and neoplastic conditions. Angiogenesis 2017 21:1 21:1–14

114. Sakiyama-Elbert SE, Hubbell JA (2000) Controlled release of nerve growth factor from a heparin-containing fibrin-based cell ingrowth matrix. Journal of Controlled Release 69:149–158

115. Sang QXA (1998) Complex role of matrix metalloproteinases in angiogenesis. Cell Research 1998 8:3 8:171–177

116. Scharnweber D, Hübner L, Rother S, Hempel U, Anderegg U, Samsonov SA, Pisabarro MT, Hofbauer L, Schnabelrauch M, Franz S, Simon J, Hintze V (2015) Glycosaminoglycan derivatives: promising candidates for the design of functional biomaterials. J Mater Sci Mater Med 26:1–10

117. Schmaus A, Rothley M, Schreiber C, Möller S, Roßwag S, Franz S, Garvalov BK, Thiele W, Spataro S, Herskind C, Prunotto M, Anderegg U, Schnabelrauch M, Sleeman J (2022) Sulfated hyaluronic acid inhibits the hyaluronidase CEMIP and regulates the HA metabolism, proliferation and differentiation of fibroblasts. Matrix Biol 109:173–191

118. Schnabelrauch M, Schiller J, Möller S, Scharnweber D, Hintze V (2021) Chemically modified glycosaminoglycan derivatives as building blocks for biomaterial coatings and hydrogels. Biol Chem 402:1385–1395

119. Schneider-Barthold C, Baganz S, Wilhelmi M, Scheper T, Pepelanova I (2016) Hydrogels based on collagen and fibrin - Frontiers and applications. BioNanoMaterials 17:3–12

120. Seitz O, Schürmann C, Hermes N, Müller E, Pfeilschifter J, Frank S, Goren I (2010) Wound Healing in Mice with High-Fat Diet- or *ob* Gene-Induced Diabetes-Obesity Syndromes: A Comparative Study. Exp Diabetes Res 2010:1–15

121. Sigen A, Xu Q, McMichael P, Gao Y, Li X, Wang X, Greiser U, Zhou D, Wang W (2018) A facile one-pot synthesis of acrylated hyaluronic acid. Chemical Communications 54:1081–1084

122. Slaughter B V., Khurshid SS, Fisher OZ, Khademhosseini A, Peppas NA (2009) Hydrogels in Regenerative Medicine. Adv Mater 21:3307

123. Sturabotti E, Consalvi S, Tucciarone L, Macrì E, Di Lisio V, Francolini I, Minichiello C, Piozzi A, Vuotto C, Martinelli A (2022) Synthesis of Novel Hyaluronic Acid Sulfonated Hydrogels Using Safe Reactants: A Chemical and Biological Characterization. Gels 8:480

124. Su C-W, Lin C-W, Yang W-E, Yang S-F (2019) TIMP-3 as a therapeutic target for cancer. Ther Adv Med Oncol 11:1758835919864247

125. Sun L, Xu Y, Han Y, Cui J, Jing Z, Li D, Liu J, Xiao C, Li D, Cai B (2023) Collagen-Based Hydrogels for Cartilage Regeneration. Orthop Surg 15:3026–3045

126. Sun M, Sun X, Wang Z, Guo S, Yu G, Yang H (2018) Synthesis and Properties of Gelatin Methacryloyl (GelMA) Hydrogels and Their Recent Applications in Load-Bearing Tissue. Polymers (Basel) 10:1290

127. Tammi R, Ågren UM, Tuhkanen AL, Tammi M (1994) Hyaluronan Metabolism in Skin. Prog Histochem Cytochem 29:III–77

128. Taylor KB, Jack Windsor L, Caterina NCM, Kirby Bodden M, Engler JA (1996) The mechanism of inhibition of collagenase by TIMP-1. J Biol Chem 271:23938–23945

129. Theocharis AD, Skandalis SS, Gialeli C, Karamanos NK (2016) Extracellular matrix structure. Adv Drug Deliv Rev 97:4–27

130. Theocharis AD, Manou D, Karamanos NK (2019) The extracellular matrix as a multitasking player in disease. FEBS J 286:2830–2869

131. Thönes S, Kutz LM, Oehmichen S, Becher J, Heymann K, Saalbach A, Knolle W, Schnabelrauch M, Reichelt S, Anderegg U (2017) New E-beam-initiated hyaluronan acrylate cryogels support growth and matrix deposition by dermal fibroblasts. Int J Biol Macromol 94:611–620

132. Thönes S, Rother S, Wippold T, Blaszkiewicz J, Balamurugan K, Moeller S, Ruiz-Gómez G, Schnabelrauch M, Scharnweber D, Saalbach A, Rademann J, Pisabarro MT, Hintze V, Anderegg U (2019) Hyaluronan/collagen hydrogels containing sulfated hyaluronan improve wound healing by sustained release of heparin-binding EGF-like growth factor. Acta Biomater 86:135–147

133. Thorn SL, Shuman JA, Stacy MR, Purcell BP, Doviak H, Burdick JA, Spinale FG, Sinusas AJ (2023) Matrix Metalloproteinase-Targeted SPECT/CT Imaging for Evaluation of Therapeutic Hydrogels for the Early Modulation of Post-Infarct Myocardial Remodeling. J Cardiovasc Transl Res 16:155–165

134. Ucuzian AA, Greisler HP (2007) In vitro models of angiogenesis. World J Surg 31:654–663

135. Ulfig † N (2019) Kurzlehrbuch Histologie. 5th edition. Georg Thieme Verlag, Stuttgart

136. Van Den Bulcke AI, Bogdanov B, De Rooze N, Schacht EH, Cornelissen M, Berghmans H (2000) Structural and rheological properties of methacrylamide modified gelatin hydrogels. Biomacromolecules 1:31–38

137. Varki A, Cummings RD, Aebi M, Packer NH, Seeberger PH, Esko JD, Stanley P, Hart G, Darvill A, Kinoshita T, Prestegard JJ, Schnaar RL, Freeze HH, Marth JD, Bertozzi CR, Etzler ME, Frank M, Vliegenthart JF, Lütteke T, Perez S, Bolton E, Rudd P, Paulson J, Kanehisa M, Toukach P, Aoki-Kinoshita KF, Dell A, Narimatsu H, York W, Taniguchi N, Kornfeld S (2015) Symbol Nomenclature for Graphical Representations of Glycans. Glycobiology 25:1323–4

138. Veith AP, Henderson K, Spencer A, Sligar AD, Baker AB (2019) Therapeutic Strategies for Enhancing Angiogenesis in Wound Healing. Adv Drug Deliv Rev 146:97

139. Verdier-Sévrain S, Bonté F (2007) Skin hydration: a review on its molecular mechanisms. J Cosmet Dermatol 6:75–82

140. Volpi N, Maccari F, Titze J (2005) Simultaneous detection of submicrogram quantities of hyaluronic acid and dermatan sulfate on agarose-gel by sequential staining with toluidine blue and Stains-All. Journal of Chromatography B 820:131–135

141. Wan J, He Z, Peng R, Wu X, Zhu Z, Cui J, Hao X, Chen A, Zhang J, Cheng P (2023) Injectable photocrosslinking spherical hydrogel-encapsulated targeting peptide-modified engineered exosomes for osteoarthritis therapy. J Nanobiotechnology 21:284

142. Wang J, Wang X, Liang Z, Lan W, Wei Y, Hu Y, Wang L, Lei Q, Huang D (2023) Injectable antibacterial Ag-HA/ GelMA hydrogel for bone tissue engineering. Front Bioeng Biotechnol 11:1219460

143. Wang L, Xu G ling, Gao K, Wilkinson J, Zhang F, Yu L, Liu C yu, Yu C fei, Wang W bo, Li M, Chen W, Fan F, Cong M, Wang JZ (2016) Development of a robust reporter-based assay for the bioactivity determination of anti-VEGF therapeutic antibodies. J Pharm Biomed Anal 125:212–218

144. Wang LX, Amin MN (2014) Chemical and Chemoenzymatic Synthesis of Glycoproteins for Deciphering Functions. Chem Biol 21:51

145. Wang W, Lo ACY (2018) Diabetic Retinopathy: Pathophysiology and Treatments. Int J Mol Sci 19:1816

146. Wang W, Lu KJ, Yu CH, Huang QL, Du YZ (2019) Nano-drug delivery systems in wound treatment and skin regeneration. J Nanobiotechnology 17:82

147. Wang Y, Nagase S, Koyama A (2004) Stimulatory effect of IGF-I and VEGF on eNOS message, protein expression, eNOS phosphorylation and nitric oxide production in rat glomeruli, and the involvement of PI3-K signaling pathway. Nitric Oxide 10:25–35

148. Werdin F, Tennenhaus M, Schaller H-E, Rennekampff H-O (2009) Evidence-based Management Strategies for Treatment of Chronic Wounds. Eplasty 9:e19

149. Wilkinson J, Robers M, Fan F, Cong M (2018) A Novel MOA-Based Bioluminescent Bioassay for Quantitative Measurement of Anti-VEGF Antibody Potency and Stability Poster PS348. 2800 Woods Hollow Rd, Madison, WI 53711. URL: www.promega.com

150. Wrublewsky S, Weinzierl A, Hornung I, Prates-Roma L, Menger MD, Laschke MW, Ampofo E (2022) Co-transplantation of pancreatic islets and microvascular fragments effectively restores normoglycemia in diabetic mice. NPJ Regen Med 7:67

151. Xia W, Lai G, Li Y, Zeng C, Sun C, Zhang P, Zhu G, Li L, Wu L (2023) Photo-crosslinked adhesive hydrogel loaded with extracellular vesicles promoting hemostasis and liver regeneration. Front Bioeng Biotechnol 11:1170212

152. Xu H, Casillas J, Krishnamoorthy S, Xu C (2020) Effects of Irgacure 2959 and lithium phenyl-2,4,6-trimethylbenzoylphosphinate on cell viability, physical properties, and microstructure in 3D bioprinting of vascular-like constructs. Biomedical Materials 15:055021

153. Yang TT, Hawkes SP (1992) Role of the 21-kDa protein TIMP-3 in oncogenic transformation of cultured chicken embryo fibroblasts. Proc Natl Acad Sci U S A 89:10676–10680

154. Yu WH, Yu SSC, Meng Q, Brew K, Woessner JF (2000) TIMP-3 binds to sulfated glycosaminoglycans of the extracellular matrix. J Biol Chem 275:31226–31232

155. Yue K, Trujillo-de Santiago G, Alvarez MM, Tamayol A, Annabi N, Khademhosseini A (2015) Synthesis, properties, and biomedical applications of gelatin methacryloyl (GelMA) hydrogels. Biomaterials 73:254

156. Yue K, Trujillo-de Santiago G, Alvarez MM, Tamayol A, Annabi N, Khademhosseini A (2015) Synthesis, properties, and biomedical applications of gelatin methacryloyl (GelMA) hydrogels. Biomaterials 73:254–271

157. Zang L, Zhu H, Wang K, Liu Y, Yu F, Zhao W (2022) Not Just Anticoagulation—New and Old Applications of Heparin. Molecules 27:6968

158. Zetser A, Bashenko Y, Edovitsky E, Levy-Adam F, Vlodavsky I, Ilan N (2006) Heparanase induces vascular endothelial growth factor expression: correlation with p38 phosphorylation levels and Src activation. Cancer Res 66:1455–1463

159. Zieris A, Prokoph S, Levental KR, Welzel PB, Grimmer M, Freudenberg U, Werner C (2010) FGF-2 and VEGF functionalization of starPEG–heparin hydrogels to modulate biomolecular and physical cues of angiogenesis. Biomaterials 31:7985–7994

160. Zieris A, Dockhorn R, Röhrich A, Zimmermann R, Müller M, Welzel PB, Tsurkan M V., Sommer JU, Freudenberg U, Werner C (2014) Biohybrid networks of selectively desulfated glycosaminoglycans for tunable growth factor delivery. Biomacromolecules 15:4439–4446

161. Zou L, Liu R, Hashem S, Lo JF (2018) Stain-free LED scanning lifetime imaging system for diabetes modified tissue matrices. Rev Sci Instrum 89:125116

162. Lithium Phenyl(2,4,6-trimethylbenzoyl)phosphinate | C16H16LiO3P| CID 68384915 - PubChem. URL: https://pubchem.ncbi.nlm.nih.gov/compound/68384915

163. N-isobutyl-N-(4-methoxyphenylsulfonyl)glycyl hydroxamic acid | C13H20N2O5S | CID 448002 - PubChem. URL: https://pubchem.ncbi.nlm.nih.gov/compound/nngh

III. Publications and Presentations

III.1. Contributions to conferences

III.1.1. Oral presentations

Fabian Junker, Charlotte Berhorst, Annika Clemenz, Poh Soo Lee, Wolfgang Metzger and Sandra Rother (2024) Decreasing extracellular matrix degradation with TIMP-3-releasing biomaterials. Annual Meeting of the German Society for Biomaterials (DGBM). Abstract-ID: 75; Programme-ID: O-67.

Lena Beuck, **Fabian Junker**, Dunya Arabi, Sandra Rother (2024) Die süße und saure Seite der Knorpelregeneration – Rolle von Glykosaminoglykanen. Verband der Diätassistenten (VDD) Bundeskongress 2024.

III.1.2. Poster presentations

Fabian Junker, Toni Radanovic, Emmanuel Ampofo, Matthias W. Laschke, Wolfgang Metzger and Sandra Rother (2023) Glycosaminoglycan-Functionalized Hydrogels as Tools to Modulate Angiogenesis. European Society for Biomaterials (ESB) 2023. PoA.10.11.

Toni Radanovic, **Fabian Junker**, Wolfgang Metzger and Sandra Rother (2023) Glycosaminoglycan-gelatin hydrogels to promote fibroblast proliferation, migration and angiogenesis. European Society for Biomaterials (ESB) 2023. PoA.10.41.

III.2. Publications

Fabian Junker, Stefan Rupf, Charlotte Berhorst, Gloria Ruiz-Gómez, M. Teresa Pisabarro, Poh Soo Lee, Stephanie Moeller, Albrecht Berg, Bergita Ganse, Emmanuel Ampofo, Matthias W. Laschke, Wolfgang Metzger, Matthias Hannig, Sandra Rother Glycosaminoglycan-functionalized hydrogels for sustained delivery of tissue inhibitor of metalloproteinase-3 mediating matrix metalloprotease inhibition and extracellular matrix stabilization. Bioactive Materials. Manuscript Number: BIOACTMAT-D-25-00258. Currently under review.

IV. Acknowledgements

First of all, I would like to convey my gratitude to **Jun.-Prof. Dr. rer. nat. Sandra Rother**. Without her and her continuing support, none of this would have been possible. Her expertise and passion for this subject inspired me and encouraged me to give my very best. Her support (and baking) kept me focused on my work and helped me to achieve my goals. Therefore, I would like to conclude this paragraph with a heartfelt “Thank you, Sandra!”.

This work was financially supported by the start-up funding program (Anschubfinanzierung) of Saarland University.

I am thankful for the technical support which Ms. **M. Sc. Charlotte Berhorst** and Mrs. **Daniela Sossong** offered me whenever it was necessary. In the case of Charlotte, I am very thankful to her as she performed the TIMP-3 ELISA measurements.

Furthermore, I would like to thank **PD Dr. rer. nat. Wolfgang Metzger** for the support he offered and provided. Wolfgang was supportive throughout the SEM experiments and provided me with assistance when needed. I appreciate his time for taking the SEM images in my thesis.

Without **Dr.-Ing. Poh Soo Lee** (Max-Bergmann Centre for Biomaterials, Technical University Dresden) it would not have been possible to perform measurements of Young’s modulus and therefore, I am very thankful for his contribution.

I would like to thank my dear cousin Ms. **M. Ed. Christina Sauer** for helping me to review my thesis.

Last but not least, I would like to thank **Prof. Dr. rer. nat. Robert Ernst**, **Prof. Dr. rer. nat. Martin Jung** and **PD Dr. rer. nat. Emmanuel Ampofo** and their respective groups as they were all willing to provide technical support or equipment if necessary.

At the end, I would like to thank my friends and family as they supported me during my work. I am very grateful for their support as it would have been impossible for me to complete this work without them.

V. Curriculum vitae

For reasons of data protection, the curriculum vitae is not published in the online version of this dissertation.